UNIVERSITY OF OKLAHOMA

GRADUATE COLLEGE

ANATOMICAL AND FUNCTIONAL NEUROIMAGING BIOMARKERS FOR SPINAL CORD ALTERATIONS IN DEGENERATIVE CERVICAL MYELOPATHY

A DISSERTATION

SUBMITTED TO THE GRADUATE FACULTY

in partial fulfillment of the requirements for the

Degree of

DOCTOR OF PHILOSOPHY

By

GRACE HAYNES

Norman, Oklahoma

2025

ANATOMICAL AND FUNCTIONAL NEUROIMAGING BIOMARKERS FOR SPINAL CORD ALTERATIONS IN DEGENERATIVE CERVICAL MYELOPATHY

A DISSERTATION APPROVED FOR THE

STEPHENSON SCHOOL OF BIOMEDICAL ENGINEERING

BY THE COMMITTEE CONSISTING OF

Dr. Lei Ding, Chair

Dr. Zachary Smith, Co-Chair

Dr. Ari Berkowitz

Dr. David Sherry

Dr. Qinggong Tang

Dr. Han Yuan

ABSTRACT

Degenerative cervical myelopathy (DCM) is a common form of age-related, non-traumatic cervical cord compression that can lead to sensory or motor symptoms like loss of balance, loss of hand coordination, and pain. Previous investigations into DCM have found evidence of structural changes in both the white matter (WM) and gray matter (GM) that are associated with subjective clinical measurements and imply that they are the source of this impediment. However, whether the damage to these tissues can reflect clinical severity and impact spinal cord functionality is undetermined. Establishing these relationships and alterations can not only further our understanding of DCM's pathophysiology but also help to create biomarkers that inform surgical decision making and reduce permanent neurological damage. Therefore, in my dissertation studies, I applied three different imaging methodologies to investigate changes in the structure and function of the DCM spinal cord. In my first study to indirectly measure the change in WM content between conservative and surgical treatment groups, I categorized DCM patients based on their modified Japanese Orthopaedic Association (mJOA) score (mild: 15-17; moderate/severe: 0-14). Comparisons between healthy controls (HCs) and the moderate/severe DCM groups revealed significant decreases in magnetization transfer ratio (MTR) in the ventral regional of the spinal cord, as well as several ventral cord tracts (e.g., ventral corticospinal and reticulospinal). Significant correlations were also found between the MTR values of the ventral reticulospinal tract and both upper and lower limb motor mJOA scores. To determine whether DCM impacts GM volume, I extracted overall and regional GM volumes from the level of maximum compression (MCL). When compared to HCs, the GM volume in DCM patients was significantly decreased in all GM regions. However, the GM of the

spinal cord plays a key role in neuronal interconnectivity because it houses cell bodies that help form reflex arcs capable of responding to stimuli without input from the brain. To quantify any impairment to the GM spinal cord reflex arcs, an electrical stimulation paradigm aimed at activating these reflex arcs by inducing a minimal motor response was applied to the median nerve. This threshold was found to significantly increase in DCM subjects. Furthermore, the GM volume in the ventral region of DCM patients was also found to correlate to WM MTR in the ventral cord. Together, these first two structural MRI studies demonstrate a ventral region injury pattern that impacts motor performance and worsens as the myelopathy progresses. Not only can establishing this severity-sensitive injury pattern help to give insight into the progressive development of DCM, but it could also be applied as an objective indicator of structural damage by clinicians looking to prevent permanent neurological damage in patients. However, what this injury pattern cannot demonstrate is how these structural changes affect functional activity in the spinal cord. In my final study, subjects underwent two task-based fMRI sessions (sub-motor and motor) with electrical stimulation to the median nerve. The amount of blood oxygenation-level dependent (BOLD) activated voxels in HCs increased from the sub-motor stimulation condition to the motor stimulation condition and peaked at the C7 segment in both conditions. HC activations were bilaterally distributed and primarily located within the GM. Conversely in DCM patients, BOLD activations decreased from sub-motor and motor conditions, peaked at C6 during sub-motor activation, and were more distributed to the ipsilateral side of stimulation. The DCM sub-motor condition also had significant spikes in deactivation at C6, especially when compared to the HC sub-motor at C6. This task-based fMRI study represents the first effort to demonstrate a disruption to the overall, segmental, and lateralized functional activation and deactivation patterns in DCM spinal cords, which could indicate compensatory spinal cord mechanisms

helping to retain partial motor and sensory functions in the wake of compressive structural damage. Combined, these studies establish a ventral cord injury pattern in DCM that could serve as structural biomarkers indicating severity-associated damage and alterations in functional patterns that could help to pave the way for the development of fMRI as a clinical biomarker.

ACKNOWLEDGEMENTS

I would first like to thank my co-advisors, Drs Zachary Smith and Lei Ding, for their support, guidance, and expertise that made the works included in this dissertation possible. Throughout my PhD studies, you both have helped me grow as a young professional and I greatly appreciate all of the effort you have put into your continued mentorship. Your insights have been truly indispensable and the knowledge that you have instilled will be something that I will carry with me into my future endeavors. Additionally, I want to thank Drs Ari Berkowitz, Qinggong Tang, David Sherry, and Han Yuan for taking the time to serve on my committee and deliver their constructive feedback during this process. I also would like to thank my lab members – Drs Fauziyya Muhammad, Sanaa Hameed, and Ali Khan – who have become trusted colleagues and helped contribute to my training as a researcher. I have learned a great amount from each of you and look forward to all of our continued collaborations.

Furthermore, I would like to extend a thank you to our collaborators – Drs Kenneth Weber 2nd (Stanford School of Medicine) and Michael Rohan (Laureate Institute of Brain Research) – and funding sources – the National Institutes of Health (R01:NS129852-01A1), the National Institute of Neurological Disorders and Stroke (K23:NS091430), the Presbyterian Health Foundation, and the Oklahoma Shared Clinical and Translational Resources – without whom these projects would not have been possible.

Finally, I would like to thank all of my family and friends. Your unwavering support, love, and encouragement has given me the strength and determination to complete my studies, and I simply could not have done it without any of you. I hope I have made you all proud.

TABLE OF CONTENTS

LIST OF ABBREVIATIONS

ALFF: Amplitude of Low Frequency Fluctuation

BOLD: Blood Oxygenated Level Dependent

CSF: Cerebrospinal Fluid

DCM: Degenerative Cervical Myelopathy

EPI: Echo-Planar Imaging

FEAT: FMRIB Expert Analysis Tool

fMRI: functional MRI

FMRIB: Functional Magnetic Resonance Imaging of the Brain

FSL: FMRIB Software Library

FWHM: Full Width at Half Maximum

GE: General Electric

GLM: General Linear Model

GM: Gray Matter

HC: Healthy Control

IRB: Institutional Review Board

LIBR: Laureate Institute of Brain Research

mJOA: modified Japanese Orthopaedic Association

MRI: Magnetic Resonance Imaging

MTR: Magnetization Transfer Ratio

NDI: Neck Disability Index

OUHSC: Oklahoma Health Sciences Center

RETROICOR: Retrospective Image Correction

SCT: Spinal Cord Toolbox

SEEP: Signal Enhancement by Extravascular Protons

WM: White Matter

LIST OF FIGURES

LIST OF TABLES

Chapter 1: Overview of Investigating Structural and Functional Biomarkers in DCM

1.1. Objectives

Degenerative cervical myelopathy (DCM) is an age-related compressive disease that can result in patients experiencing significant motor (Muhammad et al., 2023) and sensory (Hameed et al., 2024) symptoms that heavily impact their quality of life. Explanations for symptom manifestation include the damage occurring to the white (Cloney et al., 2018; Hopkins et al., 2018) and gray (Smith et al., 2020) matters, which have both been associated with clinical deficits (Cloney et al., 2018; Smith et al., 2020). However, little is known about how this structural damage relates to worsening DCM severity and impacts the functional activation of the spinal cord. Therefore, the objective of this project was to identify gray and white matter biomarkers indicative of structural DCM damage and investigate how this damage contributes to the manifestation of motor symptoms and functional impairment in DCM patients.

1.2. Aims and Hypotheses

1.2.1. Aim 1: Utilize improved spinal cord analysis methodologies to demonstrate MTR's ability to quantify white matter damage in DCM

As a means to interrogate the relationship between white matter damage and DCM severity, I separated the DCM cohort into two groups to mimic the type of treatment patients are likely to receive based on their severity (i.e. mild and moderate/severe). I then utilize the MT imaging methodology – which is capable of indirectly quantifying the presence of myelin – and an advanced spinal cord analysis pipeline to indirectly measure the white matter content in the different regions and tracts of the spinal cord. To determine whether MTR is able to quantify the

severity of white matter damage, the MTR values of HCs, mild DCM patients, and moderate/severe DCM patients were compared. Because increasing compressive damage will cause demyelination (Dohle et al., 2023), a significant decrease in MTR scores is expected to occur as the myelopathy worsens in this study, which reflects a decrease in myelin macromolecules.

1.2.2. Aim 2: Test the relationship between DCM damage and the impediment of spinal cord reflex arcs

In order to establish what impact white and gray matter damage has on the functional reflex arcs of the spinal cord, I applied electrical stimulation to the median nerve at the minimum level needed to evoke an involuntary motor response. I also utilized MT and T2* imaging to extract indirectly measure white and gray matter, respectively, at the regional level. This aim interrogates the impact that damage has on the spinal cord reflex arcs, the relationship between the gray matter volumes, region MTR measures, and the threshold amplitude required to evoke an involuntary motor response in participants.

1.2.3. Aim 3: Interrogate changes in functional activation with an electrical stimulation paradigm capable of inducing an involuntary motor reaction

In the past, functional MRI (fMRI) has been applied to study changes in resting state and task-based functional activation patterns of spinal cords experiencing pathologies like multiple sclerosis, fibromyalgia, and spinal cord injury (Haynes et al., 2023) to provide deeper insight into functional impediment and the compensatory mechanisms responding to neuronal damage. However, while resting state fMRI has been applied in DCM (Liu et al., 2016), there are currently no task-based functional imaging studies that interrogate DCM compression. This lack of task-based fMRI leaves a large gap in the pathophysiological understanding of DCM, as

alterations to the sensorimotor pathways remain unknown. Therefore, the final aim is to apply a task-based fMRI paradigm to interrogate how the structural damage previously investigated impacts the sensorimotor pathways of DCM spinal cords. However, it has been established that DCM patients have a decrease in motor performance, which could cause consistency and reliability issues when applying a task-based motor paradigm. To help mitigate this, I applied a normalized median nerve stimulation to evoke an involuntary motor response in controls and patients during functional MRI runs. The compressive damage present in DCM spinal cords is expected to alter functional patterns in response to the applied stimulation.

1.3. Contributions

Each study investigating the aims described above includes the application of improved analysis methods and several scientific discoveries. For example, in all three aims, an updated MRI processing technique using an automated, deep learning algorithm to segment the spinal cord was applied. This segmentation processing methodology helped to limit error/bias, improve registration to a normalized space (i.e. PAM50 template), and allowed for more accurate data extraction from both the white and gray matter regions and tracts of interest. Furthermore, my findings can contribute to the clinical treatment of DCM. For example, in aim 1, I compared MTR values between DCM treatment groups (mild vs moderate/severe) to give a more complete picture of DCM and showed that the ventral region MTR is capable of displaying significant white matter damage in moderate/severe patients (Haynes et al., 2024). I also showed in aim 2 that ventral horn GM loss correlates to this decrease in MTR (Haynes, Muhammad, Weber, Khan, Hameed, Ding, et al., 2025). This damage to the ventral region also potentially explains the appearance of motor symptoms in DCM.

To further quantify the association between structural damage and functional impairment, a task-based paradigm capable of inducing a motor response that was unaffected by the DCM motor symptoms impairing performance had to be developed. For this task, direct electrical stimulation to the median nerve was chosen for its ability to induce an involuntary reaction that mimics the spinal cord reflex arcs passing through the gray matter. In aim 2, a minimum stimulation needed to evoke an involuntary reaction was applied and demonstrated that DCM patients do experience functional impairment, as they required a higher stimulus amplitude (Haynes, Muhammad, Weber, Khan, Hameed, Ding, et al., 2025). This paradigm was also applied in aim 3, where it induced functional sub-motor and motor responses that aligned with known neuroanatomy in HCs and revealed changes in the functional patterns of DCM patients (Haynes, Muhammad, Weber, Khan, Hameed, Shakir, et al., 2025).

Together, the studies provide a significant contribution to the current understanding of injury and compensatory mechanisms affecting DCM patients. The structural analyses in aims 1 and 2 reveal a pattern of injury to the ventral region (Haynes, Muhammad, Weber, Khan, Hameed, Ding, et al., 2025; Haynes et al., 2024), aligning reports of ventral region injury (Cloney et al., 2018; Dohle et al., 2023; Filimonova, Abdaev, et al., 2024a) and reduction of motor performance (Hameed et al., 2024; Muhammad et al., 2023; Muhammad, Weber, Haynes, et al., 2025). However, aim 1 revealed that these structural changes specifically appear in patients with moderate/severe myelopathy (Haynes et al., 2024), which helps to define mechanisms of structural injury as the myelopathy progresses into a more severe form. Despite this damage having no significant correlation to a required involuntary motor threshold increase (Haynes, Muhammad, Weber, Khan, Hameed, Ding, et al., 2025), though, alterations in overall, segmental, and lateralized functional patterns were present (Haynes, Muhammad, Weber, Khan,

Hameed, Shakir, et al., 2025) when stimulation was applied. Aim 3 gives insight into how the function of the spinal cord changes as it undergoes degenerative chronic compression. It also represents the first task-based fMRI paradigm to be applied in a DCM cohort and demonstrates that spinal cord fMRI could be used to establish functional, clinical biomarkers in the future.

Chapter 2: Background of Degenerative Cervical Myelopathy

2.1. Degenerative Cervical Myelopathy

Degenerative cervical myelopathy (DCM) is an age-related, non-traumatic compression of the cervical spinal cord that primarily impacts those over 55 years old (Davies et al., 2022; Fehlings et al., 2015; Grodzinski et al., 2021; L. Tetreault et al., 2015). Symptoms of DCM commonly include clumsiness, upper and lower extremity muscle weakness, gait instability, upper extremity/neck pain, bowel/bladder dysfunction, and paresthesia (Bakhsheshian et al., 2017; Balmaceno-Criss et al., 2024; Lannon & Kachur, 2021; Tetreault et al., 2014), some of which can be associated with radiological measures of compression (Nouri, Tetreault, et al., 2017) and clinical scores (Kalsi-Ryan et al., 2020). Motor performance in DCM patients – like dexterity, grip strength, balance, and gait speed – has also been noted to decrease compared to healthy controls (Muhammad et al., 2023).

2.1.1. Diagnosis of DCM

There are several different methodologies that clinicians can employ to properly diagnose DCM and gain a better understanding of its severity. Clinical surveys like the modified Japanese Orthopaedic Association (mJOA) score, the Nurick scale for cervical myelopathy, and the Neck Disability Index (NDI) (Bakhsheshian et al., 2017; Balmaceno-Criss et al., 2024; Lannon & Kachur, 2021; Soufi et al., 2022) can be used to record patient-reported measures of symptom severity. The primary survey that is used is the mJOA score, which was modified from the original Japanese Orthopaedic Association (JOA) score (Yonenobu et al., 1986), and has proven to have good inter- and intra-observer reliability (Yonenobu et al., 2001). It is based on four individual measures (upper limb motor, lower limb motor, upper limb sensory, and bladder dysfunction) that add up to 18 total (Benzel et al., 1991). The mJOA score has also been shown

to correlate with its unmodified counterpart, JOA, (Kato et al., 2015). The mJOA score can be used to categorize patients into mild (15-17), moderate (12-14), and severe (≤11) categories (Tetreault et al., 2017), and can reflect performance in gait (Fu et al., 2024; Muhammad et al., 2023; Yoo et al., 2021), dexterity, balance, and grip strength (Muhammad et al., 2023). Similar to mJOA's lower limb motor score, the Nurick scale for cervical myelopathy (Nurick, 1972) relies on six grades (0-5) solely based on the patient's gait abilities. Both gait and balance performances correlate with Nurick grades (Fu et al., 2024; Muhammad et al., 2023; Yoo et al., 2021). The final clinical survey that is commonly used is the NDI, which is comprised of 10 items that interrogate the patient's pain and motor performance. It was developed from the Oswestry Low Back Pain Index (Vernon & Mior, 1991), with a higher score indicating greater dysfunction, and has been shown to correlate to symptom duration of more than twelve months (Muhammad et al., 2023) and poorer gait performance (Smith et al., 2019).

Furthermore, reflex testing can also be applied in the clinic to diagnose DCM. Some common reflexes that clinicians can test include the Hoffman's sign, Babinski's sign, and the pathological clonus (Bakhsheshian et al., 2017; Balmaceno-Criss et al., 2024; Lannon & Kachur, 2021; Tu et al., 2021). The Hoffman's sign is a reflex test performed by flicking the nail of the middle finger to see if flexion occurs in the index finger and thumb (Tu et al., 2021), and has been seen to associate with DCM compression (Chikuda et al., 2010; Harrop et al., 2010; Nouri, Tetreault, et al., 2017; Tejus et al., 2015), signal change ratio (e.g. an indicator of how much a hyperintense signal differed from other baseline signals in the same image) (Nouri, Tetreault, et al., 2017), and the narrowing of the spinal canal (Denno & Meadows, 1991; Nouri, Tetreault, et al., 2017; Tuchman et al., 2019). Additionally, the prevalence of Hoffman's sign has also been seen to increase in patients with a more severe mJOA score (Chikuda et al., 2010; Funaba et al.,

2021; Houten & Noce, 2008). The second sign commonly used, the Babinski's sign, is a reflex test performed by running an object along the outer sole of the foot to see if extension of the big toe occurs (Tu et al., 2021). It has been found in the majority of DCM patients with compression (Funaba et al., 2021; Tejus et al., 2015), and has been associated with a greater signal change ratio (Nouri, Tetreault, et al., 2017) and a lower mJOA (Chikuda et al., 2010; Funaba et al., 2021). Finally, the pathological clonus is a reflex test performed by maintaining an ankle flex and pressure on the sole of the foot to see if involuntary muscle contractions occur (Tu et al., 2021). The clonus is significantly associated with lower mJOA (Chikuda et al., 2010) and higher specificity for DCM diagnosis, along with the Babinski sign (Jiang et al., 2024; Sharma et al., 2025). However, despite the prevalent use of reflex tests in clinical diagnostics, several studies have concluded that reflex testing alone is not sensitive enough to detect DCM and that clinicians should not rely solely on them for diagnosis (Glaser et al., 2001; Hirai et al., 2021; Rhee et al., 2009; Wong et al., 2004).

The final tool commonly used by clinicians to diagnose DCM is structural MRI (Bakhsheshian et al., 2017; Balmaceno-Criss et al., 2024). Not only is compression commonly visible to the naked eye, but hypo- and hyperintense signals on T1-weighted (T1W) and T2-weighted (T2W) images are common MRI findings (Bakhsheshian et al., 2017; Khan et al., 2023; Lannon & Kachur, 2021; Nouri, Martin, et al., 2017; Nouri et al., 2016) that can give insight into cord damage and possible surgical outcomes. This is because T1W images reflect how long it takes for protons to realign with the magnetic field after a radiofrequency (RF) pulse has been applied. Protons contained within larger macromolecules like fat have less range of motion and realign faster, which will yield a brighter signal due to a shorter re-alignment time. As an example, myelin, a key component in the nervous system that insulates axons to help

increase conduction, is made up of approximately 70-80% lipids (Poitelon et al., 2020). Demyelination of white matter axons due to damage would result in a decrease in myelin levels that would appear as a hypointense (i.e. decreased) signal in T1W images. T2W images are nearly the exact opposite of T1W images and instead measure how long it takes for the protons to become out of phase and lose signal. In this instance, smaller molecules like water yield a brighter signal because they allow for more movement and can maintain their phases for longer. Therefore, demyelination would appear as a hyperintense (i.e. increased) signal on a T2W image because of the resulting release of excess water in the area. The reliance on the microstructural makeup of the tissues means that T1W (Baucher et al., 2021; Farah et al., 2025; Filimonova, Letyagin, et al., 2024; Maier et al., 2020) and T2W (Filimonova, Letyagin, et al., 2024; Lebret et al., 2023; Martin et al., 2017; Muhammad, Weber, Bedard, et al., 2024; Vallotton et al., 2021) MR images can reflect structural alterations and morphometric changes in DCM patients (Khan et al., 2023; Nouri et al., 2016). T1W hypointensities have been associated with a greater signal change ratio at the region of compression (Nouri, Tetreault, et al., 2017). T2W hyperintensities have been found to correlate to lower mJOA scores compared to those without (Martin et al., 2017) and have been associated with greater spinal cord compression, canal compromise, and signal change ratio (Nouri, Tetreault, et al., 2017). The appearance of T2W hyperintensity is also considered to be the most important post-operative recovery predictor amongst spine surgeons (Tetreault et al., 2014), as specific patterns of T2W hyperintensities can act as post-operative predictors of clinical recovery (Mummaneni et al., 2009; Soda et al., 2022).

2.1.2. Treatment of DCM

A common treatment for DCM is surgical intervention, which is primarily reserved for moderate and severe cases and done at the surgeon's discretion. Surgical intervention has

reportedly resulted in improvements in mJOA, Nurick, and NDI scores (Badhiwala et al., 2019; Fehlings et al., 2017; Kopjar et al., 2018), indicating a general decrease in impairment after surgery. However, an issue with surgical intervention being reserved for moderate and severe cases is the possibility of compression causing permanent neurological damage. Symptom duration has been found to associate with poorer surgical outcomes (i.e. less neurological recovery) (Kopjar et al., 2018; L. A. Tetreault et al., 2015), with severe myelopathy patients often retaining symptoms after surgery (Kopjar et al., 2018). On the other hand, however, patients with less than four months of symptoms have had better mJOA outcomes post-surgery (Tetreault et al., 2019).

For mild DCM patients, an alternative to surgery can be offered in the form of more conservative treatment methods like neck immobilization, pharmacological treatment, lifestyle modifications, physical therapy, bed rest, and avoidance of high-risk activities (Bakhsheshian et al., 2017; Rao et al., 2007). However, for conservative treatments involving pharmaceuticals, physical therapy, and psychological management, evidence is scarce (Balmaceno-Criss et al., 2024; Rhee et al., 2013) and results vary (Kato & Fehlings, 2016; Lannon & Kachur, 2021). It is unknown as to why these conservative treatment outcomes vary, but one possibility is that it could be a result on DCM heterogeneous nature. Defining these differences and establishing biomarkers that can distinguish between mild, moderate, and severe disease is critical in this regard, as severity can alter the treatment recommendations and result in different effectiveness. For example, a study focusing on patients with mild/moderate DCM concluded that non-operative treatments were equivalent to surgical treatment (Holly, 2009) and another focusing on moderate/severe groups concluded that non-operative treatments were inferior to surgical ones (Bakhsheshian et al., 2017). Furthermore, developing predictive biomarkers that can determine

the risk of mild myelopathy progressing into more severe versions would also help to improve treatment decisions, prevent permanent neurological damage, and improve quality of life for DCM patients.

2.2. Impact of DCM on the structural integrity of the spinal cord

2.2.1. Structural MRI Methodologies for Studying the Spinal Cord

As previously mentioned, hypo- and hyper-intense signals are a common DCM finding on T1W and T2W scans, respectively. However, another common anatomical MRI method is T2* (Grabher et al., 2017; Hopkins et al., 2018; Lebret et al., 2023; Martin et al., 2017; Smith et al., 2020; Vallotton et al., 2021), which is similar to T2W but instead takes into account the inhomogeneities in the magnetic field and results in a faster decaying signal. T2* images are commonly used to depict the contrast between white and gray matter, which can be separated more easily due to different relaxation times.

In addition to these three anatomical imaging methods, there are several advanced MRI methods that can be applied to study microstructural changes, like demyelination, in DCM patients (Khan et al., 2023; Martin et al., 2016; Nouri et al., 2016; Zhang et al., 2014). These advanced imaging methods can provide more structural details by increasing the strength of the MRI magnet (i.e. 3T vs 1.5T) and provide information that is normally unavailable through standard clinical scans. For example, diffusion tensor imaging (DTI) (Atchut et al., 2023; Chen et al., 2022; Grabher et al., 2017; Vallotton et al., 2021) applies magnetic field gradients that can cancel out signal from stationary water molecules, causing phase shift and signal loss in those diffusing (O'Donnell & Westin, 2011). Another advanced MRI method that can indirectly measure white matter content is magnetization transfer (MT) (Al-Shawwa et al., 2025; Cloney et al., 2018; Filimonova, Abdaev, et al., 2024a; Haynes et al., 2024; Paliwal et al., 2020; Suleiman

et al., 2018), which applies a saturation pulse that energizes hydrogen atoms bound to macromolecules (e.g., primarily the proteins and lipids that are highly present in myelin) and then transfers the excess to those in the extracellular water. The final advanced methodology used to indirectly measure white matter content is myelin water fraction (MWF) (Liu et al., 2017), which compares the T2W relaxation times of the myelin and intra-/extra-cellular water to estimate a ratio between myelin- and nonmyelin-bound protons.

Furthermore, not all advanced MRI techniques are used to define structural spinal cord changes. Magnetic resonance spectroscopy (MRS) (Ali & Badawy, 2013; Holly et al., 2009; Horak et al., 2021; Salamon et al., 2013) is a method that applies a weak magnetic field to help atomic nuclei achieve resonance, which are then energized by an RF pulse and allowed to return to equilibrium. Different signal decay rates then make it possible to distinguish between different nuclei to create a biochemical spectrum of the target tissue (Tognarelli et al., 2015).

These advanced structural and chemical MRI methods can be extremely useful, especially in providing more information about the development and pathobiology of DCM. The most common advanced techniques can be used to detect changes in water diffusion, myelination, and biochemicals, which helps to provide more detailed alterations in DCM spinal cords that would be overlooked on normal clinical MRI scans. These advanced scans can also easily be implemented on clinically available MRIs, giving clinicians easy access to biomarker information available through these scans and allowing them to more easily make medical decisions.

2.2.2. Using Structural MRI to Study DCM Changes in the Spinal Cord

Thanks to the application of these MRI methodologies, the structural impact that DCM has on the spinal cord can be studied. For example, T1W, T2W, and T2* images have

established that DCM patients have a significantly smaller cross-sectional area (CSA) of their spinal cords (Farah et al., 2025; Filimonova, Letyagin, et al., 2024; Martin et al., 2017; Muhammad, Weber, Bedard, et al., 2024) and canal space (Salamon et al., 2013) than healthy controls. Furthermore, these structural methodologies have helped to establish that white matter tract volume (Hopkins et al., 2018), gray matter volume (Smith et al., 2020), and the CSA above the level of compression (Lebret et al., 2023; Vallotton et al., 2021) are decreased compared to healthy controls. T1 mapping of the spinal cord has shown that relaxation values increase in the whole cord, specifically in the anterior and intermediate GM, and have negative correlations to mJOA scores (Baucher et al., 2021; Farah et al., 2025). Furthermore, multiple types of structural imaging, like T1W and T2*, can reveal signs of microstructural changes to spinal cord levels above and below the region of compression, including changes in signal intensity and diffusion metrics (Baucher et al., 2021; Martin et al., 2017; Muhammad, Weber, Haynes, et al., 2025; Vallotton et al., 2021).

Advanced methodologies have also been put to good use in identifying structural spinal cord changes due to DCM. DTI, for example, has established that fractional anisotropy (i.e. the directionality of diffusion) is decreased in DCM patients (Atchut et al., 2023; Martin et al., 2017; Vallotton et al., 2021), especially in the lateral corticospinal tract and dorsal fasciculi (i.e. fasciculus gracilis and fasciculus cuneatus) (Chen et al., 2022; Valosek et al., 2021). DTI has also provided evidence of an increased apparent diffusion coefficient (i.e. mobility of water molecules) (Atchut et al., 2023) in the lateral corticospinal tract of patients with hyperintensities (Chen et al., 2022). Mean diffusivity (i.e. overall water diffusion) and radial diffusivity (i.e. diffusion perpendicular to the white matter tracts) have also been noted to increase (Vallotton et al., 2021; Valosek et al., 2021). Furthermore, MT is decreased in DCM patients (Cloney et al.,

2018; Filimonova, Abdaev, et al., 2024a; Haynes et al., 2024; Suleiman et al., 2018), especially above and at the level of compression (Martin et al., 2017). MTR is also associated with clinical mJOA/JOA scores (Filimonova, Abdaev, et al., 2024a; Haynes et al., 2024) and their post-operative recovery (Paliwal et al., 2020). The measurements in the dorsal and ventral funiculi above the level of compression have even been able to predict the deterioration of mild patients (Al-Shawwa et al., 2025). The final indirect white matter measure, MWF, has not been used as frequently as DTI or MT, but it has been found to decrease in DCM patients with pathological somatosensory evoked potentials (SSEPs) (Liu et al., 2017).

The final advanced methodology, MRS, is also not used as commonly as DTI or MT, but it can give more insight into biochemical changes in the spinal cord. For example, MRS has been used to identify a decrease in the N-acetylaspartate (NAA) found in axons of the spinal cord (Ali & Badawy, 2013; Holly et al., 2009; Horak et al., 2021) and motor cortex (Kowalczyk et al., 2012) of DCM patients, indicating an increase of damaged axons and neuronal damage. Another finding from MRS is an increased choline levels in patients with T2W hyperintensities (Salamon et al., 2013). Choline plays a significant role in maintaining the structural integrity of cell membranes, which can help provide insight into the biochemical changes occurring as DCM progresses from asymptomatic to symptomatic.

2.3. The current state of spinal cord fMRI and its application in clinical research

* The following section has been adapted from the article (Haynes et al., 2023) (© 2023 American Society of Neuroimaging) and has been included with permission of John Wiley and Sons via a reuse license (Supplemental Material C).

The MRI techniques previously mentioned have played a key role in developing a more comprehensive knowledge of DCM injury mechanisms and the impact they have on the structural tissues of the spinal cord. They can be used by clinicians and surgeons for initial diagnosis and can help to predict the surgical recovery of DCM patients. One thing that these structural MRI techniques cannot give insight into, however, is function. The following section is a narrative review on the state of spinal cord fMRI research and how it has been applied to pathological conditions like DCM.

2.3.1. Introduction

While more widely applied to study the brain, the use of functional magnetic resonance imaging (fMRI) by clinicians and researchers to study the spinal cord has increased in the past decade (Stroman, Tomanek, et al., 2002; Yoshizawa et al., 1996). Functional MRI relies on blood oxygen consumption and blood flow changes in response to neuronal activation (Ogawa et al., 1992), which all contribute to regional oxygenated/deoxygenated hemoglobin concentration changes in creating the so-called Blood Oxygenation Level Dependent (BOLD) signal detectable in an MRI scanner (Glover, 2011).

Although the fundamental mechanisms of BOLD imaging are common to both the brain and spinal cord, technical challenges specific to spinal cord fMRI include small size, boney surroundings, and proximity to involuntary physiological motions (i.e., heartbeat, cerebrospinal fluid pulsations, and breathing) of the spinal cord (Harrison et al., 2021). Novel or alternative imaging parameters, sequences, field strength, and other technical aspects have been developed to enhance spinal cord fMRI and optimize its imaging quality. As an example, Barry et al. (2018) (Barry, Vannesjo, et al., 2018) reviewed the current state of ultra-high field for spinal cord imaging. Moreover, functional studies further rely on spinal cord-specific neurophysiology to

design stimulation protocols that can interrogate motor and sensory functionality. Evolution of the novel imaging methodologies and stimulation protocols has, therefore, allowed for the promotion of spinal cord fMRI as a research tool in assessing the role of healthy spinal cords in sensory and motor pathways (see (Landelle et al., 2021) for a detailed review). The most recent functional studies of the spinal cord using fMRI have also gone beyond these "signal highways" of the brain and into more complicated functional mechanisms, e.g., resting-state functional connectivity (RSFC, see the review by (Harrison et al., 2021)), driven by significant discoveries of characteristic RSFC in the brain (Harrison et al., 2021; Heine et al., 2012; Seitzman et al., 2019).

More importantly, fMRI can be applied to more than a healthy state nervous system. Within the brain, researchers and clinicians use BOLD fMRI to study abnormal conditions, e.g., major depressive disorder (Fitzgerald et al., 2008), post-traumatic stress disorder (Bryant et al., 2021), and concussions (Churchill et al., 2019), as an ongoing effort to advance it for clinical applications, e.g., searching biological markers of diseases. Now, with the establishment of fMRI as a powerful tool to investigate the healthy spinal cord, spinal cord fMRI has paved its way into clinical research (Agosta, Valsasina, Caputo, et al., 2008; Bosma et al., 2016; Stroman, Tomanek, et al., 2002), though at a relatively slower pace than brain fMRI. Propelled by the improvement of imaging methodologies and stimulation protocols in healthy populations, spinal cord fMRI has been used to map altered functional activity and connectivity within disease and injury conditions impacting the spinal cord (Agosta, Valsasina, Caputo, et al., 2008; Bosma et al., 2016; Stroman, Tomanek, et al., 2002). Insights resulting from these investigations could lead to the discovery of root causes of devastating degenerative diseases and their corresponding chronic symptoms. Additionally, these results could further inform the development of

breakthrough medical innovations and treatments for patients who are experiencing spinal cord impairment.

While various aspects of spinal cord fMRI, e.g., ultra-high field (Barry, Vannesjo, et al., 2018), sensorimotor pathways (Landelle et al., 2021), RSFC (Harrison et al., 2021), and a new contrast signal (Figley et al., 2010) have been reviewed recently in literature and a more recent review (Kinany et al., 2022) has further covered wide aspects of spinal cord fMRI including methodologies, basic and clinical studies. The goal of our review is to provide a comprehensive coverage with the focus on reported clinical applications and potential future clinical studies enabled by its current methodological advancements and knowledge gained from healthy populations. Furthermore, we conducted and reported a comprehensive search protocol beyond what narrative reviews typically do to include as many spinal cord fMRI papers as possible since its inception in 1996. Briefly, we performed a comprehensive search on spinal cord fMRI literature with appropriately defined keywords using PubMed and an additional exhaustive approach on cited literatures in the papers identified from the PubMed search. After applying inclusion and exclusion criteria, a total of 90 peer-reviewed journal papers were examined and reviewed in the following three aspects. Firstly, we summarized the current state of spinal cord fMRI technology and the most common stimulation protocols being used in spinal cord fMRI. Secondly, we reviewed the application of these methodologies in studying the functionality of the healthy spinal cord. Thirdly, we discussed the current state of spinal cord fMRI used in studying diseased or injured spinal cords. At the end, we envisioned the future of spinal cord fMRI in clinical research and practice and discussed how it could be further improved to allow for more utilization in diagnosing and treating diseased and injured spinal cords.

2.3.2. Literature Search

For this review, papers utilizing spinal cord fMRI since the first one in 1996 (Yoshizawa et al., 1996) were found by inputting three blocks of keywords into PubMed. These keywords included: ('spinal cord', 'cervical cord') AND ('functional magnetic resonance imaging', 'fMRI', 'functional MRI', 'MRI', 'BOLD', 'functional imaging', 'resting state') AND ('cervical myelopathy', 'cervical spondylotic myelopathy', 'degenerative cervical myelopathy', DCM, spondylosis, CSM, 'tactile stimulation', 'functional activity', 'resting state functional connectivity', 'plasticity', 'functional connectivity', 'pain modulation', 'intrinsic functional network', 'interneuronal systems'). Keywords in the first block (i.e., 'spinal cord' or 'cervical spine') were used to find research papers covering the spinal cord, and the keywords within the second block (i.e., 'functional magnetic resonance imaging', or 'fMRI', or 'functional MRI', etc.) were applied to further narrow down spinal cord research papers utilizing fMRI. After a preliminary search using the combination of the keywords from the first and second blocks, it resulted in too many irrelevant papers. The third block of keywords (i.e., 'cervical myelopathy', or 'resting state functional connectivity', etc.) were then used to narrow the search further to papers pertaining to prevailing relevant research topics of spinal cord fMRI. The papers that included non-human participants or ones that were not available in English were excluded. This search resulted in 1135 papers.

After the initial search, the abstract of each paper was screened by one of three co-authors (Ms. Grace Haynes, Dr. Ali Khan, and Dr. Esmaeil Mohammadi) utilizing an AI powered tool, i.e., Rayyan (Ouzzani et al., 2016). Exclusion criteria included 'Non-Peer-Reviewed Journal Article', 'Non-fMRI Focused', 'Non-Spinal Cord Focused', and 'Others'. Papers that were not peer-reviewed research articles (e.g., case reports, letters to the editor) were excluded. This

'Non-fMRI Focused' category typically included papers that mainly utilized diffusion weighted MR imaging or CT imaging, but only mentioned fMRI for the purpose of comparisons. Papers that mainly imaged the brain or other parts of the body without imaging the spinal cord were categorized into the 'Non-Spinal Cord Focused' group, while studies that imaged the spinal cord and brain at the same time were kept. Finally, the papers were not good fits for this review for other reasons, e.g., focusing on testing image processing methods and machine learning algorithms, were classified into the 'Others' category. After applying these exclusion criteria, 50 papers remained and, after applying the same exclusion criteria on the full papers, a total of 34 remained.

An additional search, termed as the "completion search", on the reference sections of the papers from the above PubMed search was performed, which allowed papers from other search engines, like Google Scholar, to be included. The same exclusion criteria for both abstracts and full papers were applied as the papers from the PubMed search. As a result, a total of additional 56 papers were found.

In total, 90 peer-reviewed journal articles were included in this review (Figure 1.1).

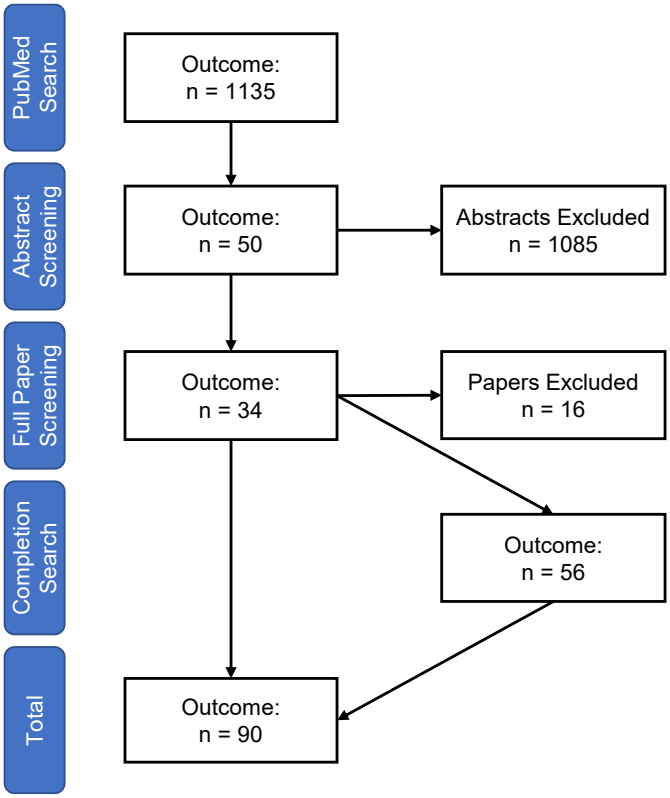

Figure 1.1: Numbers of papers (*n*) from PubMed and completion search before and after applying exclusion criteria.

2.3.3. fMRI Methodologies for Studying the Spinal Cord

The spinal cord has historically been considered as a simple signal highway for the incoming and outgoing brain signals, while recent research indicates that its functions are much more complex than that (Bosma et al., 2016; Kong et al., 2014; Sprenger et al., 2015). Therefore, functional MRI's (fMRI) ability to map spinal cord's functional activations was firstly reliably demonstrated amongst researchers (Barry et al., 2016; Govers et al., 2007; Madi et al., 2001; San Emeterio Nateras et al., 2016; Stroman et al., 1999; Yoshizawa et al., 1996) together with appropriate stimulation protocols in evoking sensory and motor nerve fibers. From the technical aspects, similar to brain fMRI, factors that impact image quality of spinal cord fMRI images include magnetic field strength, imaging sequence, and functional contrast signals (Stroman,

Krause, et al., 2002a). Additionally, spinal cord studies rely heavily on stimulation protocols being implemented as different protocols can be designed targeting specific parts and processes of the spinal cord. Below we discuss the MRI mechanisms for acquiring spinal cord fMRI data and various established stimulation protocols for studying spinal cord functions from the selected papers in this review.

2.3.3.1. The BOLD effect and other functional signals

During the onset of neuronal activity, localized concentrations of oxygenated and deoxygenated hemoglobins (HbO and HbR) are altered in the area of activity, which gives rise to the well-known BOLD effect because of the paramagnetic property of HbR (Sparacia et al., 2019). BOLD contrast signals have been popularly used in studying human brains since 1992 (Ogawa et al., 1992), and their usage in spinal cord could be traced back to as early as 1996 (Yoshizawa et al., 1996). Yoshizawa et al.'s study was the first to prove that BOLD fMRI is feasible in imaging the spinal cord, thanks to the same oxygen supply system to the spinal cord as in the brain (Barry et al., 2016; Govers et al., 2007; Madi et al., 2001; San Emeterio Nateras et al., 2016; Stroman et al., 1999). BOLD signals have shown both feasibility and reliability at all scanner fields in imaging human spinal cords (Barry et al., 2016; Govers et al., 2007; Madi et al., 2001; San Emeterio Nateras et al., 2016; Stroman et al., 1999).

In spinal cord fMRI, not all contrast signals stem from changes associated with blood flow and oxygenation. In several studies performed by Stroman, et al. (2001), changes in the T2 signal intensities were observed to occur in conjunction with neuronal activity that could not be attributed to the BOLD effect (Stroman, Krause, Malisza, et al., 2001; Stroman & Ryner, 2001). A follow-up study proposed the concept of "signal enhancement by extravascular protons" (SEEP), which alters the proton density (PD) at the site of neural activations due to proton

motions in surrounding extravascular fluids (Stroman, Krause, et al., 2002a). Therefore, the imaging mechanisms are different between BOLD (susceptibility-weighted mechanism) and SEEP (PD-weighted mechanism) (Figure 1.2). As compared to BOLD, it has been suggested that SEEP might have the advantages of its relative insensitivity to magnetic field distortions due to, e.g., static field inhomogeneities, metal implants, or fast spatial tissue property changes (a case in the transverse plane of spinal cord), its insensitivity to field strength (could be used in low field), and evidence for better spatial localization to the actual sites of neuronal activations. Detailed information about the SEEP contrast and its differences from BOLD can be found in the review paper by Figley, et al. (2010) (Figley et al., 2010).

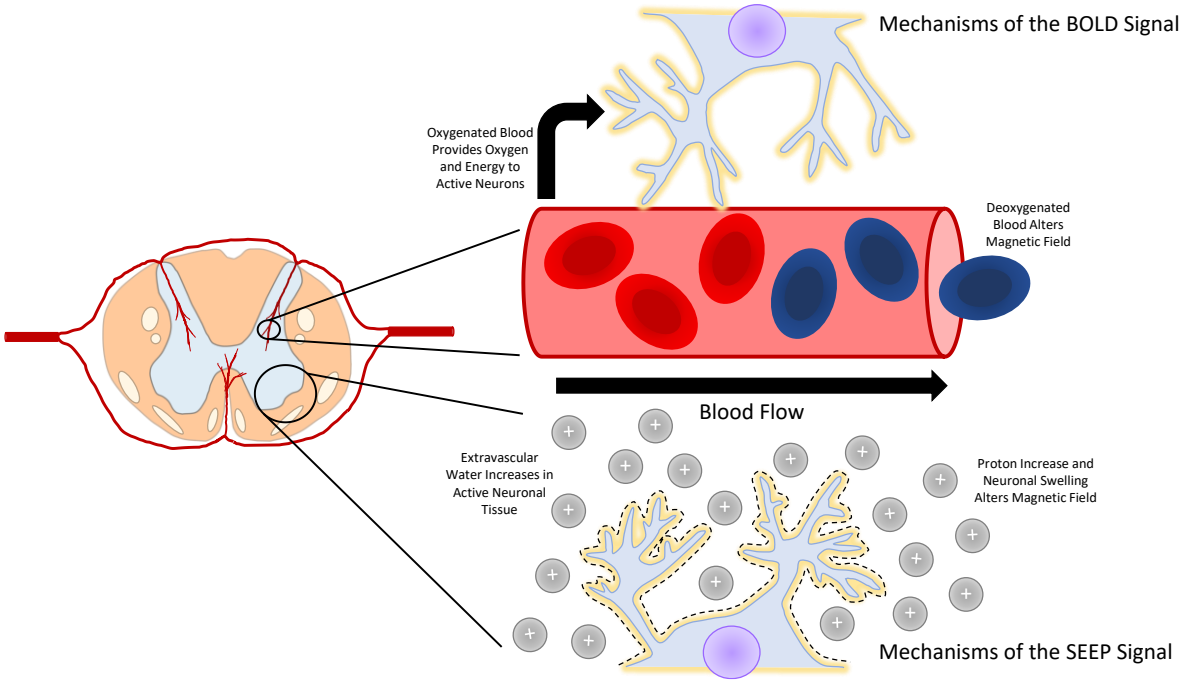

Figure 1.2: The mechanistic differences between a Blood Oxygenation Level Dependent (BOLD) signal, which depends on oxygenated hemoglobin (HbO) and deoxygenated hemoglobin (HbR) concentration changes, and a Signal Enhancement by Extravascular Protons (SEEP) signal, which relies on extravascular proton density changes.

Speculation about whether the SEEP effect is a viable functional signal is still being debated. While some studies have reported the successful use of SEEP signals for functional imaging or to enhance the detectability of BOLD signals by boosting resting-state functional

signals (Stroman, Krause, Malisza, et al., 2001; Stroman & Ryner, 2001), others have claimed to see little to no evidence of a SEEP signal (Giulietti et al., 2008; Govers et al., 2007; Stracke et al., 2005). It should also be noted that, though SEEP has been detected within the brain, its presence is greater in the spinal cord (Figley et al., 2010; Stroman, Krause, Frankenstein, et al., 2001; Stroman, Krause, Malisza, et al., 2001). SEEP detection relies heavily on imaging sequences, as its effect is more prominent in SE scans with shorter TEs (Stroman, Krause, Frankenstein, et al., 2001; Stroman, Krause, Malisza, et al., 2001; Stroman & Ryner, 2001). SEEP signals are more detectable in T2-weighted SE sequences (e.g., SE-EPI and TSE) than the T2*-weighted GRE sequences (e.g., GE-EPI and GRE) (Stroman, Krause, Frankenstein, et al., 2001; Stroman & Ryner, 2001) that usually maximize the BOLD effect. While some studies have reported detecting only SEEP signals, most T2-weighted studies that claim to detect SEEP signals have also reported an equal or greater contributions from BOLD (Rempe et al., 2014, 2015; Stroman, Krause, Malisza, et al., 2001; Stroman & Ryner, 2001).

2.3.3.2. Technical challenges in spinal cord fMRI

Although spinal cord fMRI has been thoroughly validated and deemed reliable in many studies, it is unavoidably challenged by technical factors not present in brain fMRI. One major challenge is caused by physiological motions, which have been found to be higher within the spinal cord than the brain and are at least partially responsible for signal loss (Barry et al., 2016; Bosma & Stroman, 2014; Bouwman et al., 2008; Cohen-Adad et al., 2010; Harita & Stroman, 2017; Stroman, 2006; Wei et al., 2010; Xie et al., 2012). Since these motions, including heart and cerebrospinal fluid pulsations, breathing, and swallowing, can cause the spinal cord to shift during imaging and thus degrade image quality, they are now being addressed by minimizing

subject motion within imaging sequences (Moffitt et al., 2005) and regressing movement out during the image post-processing stage (Cohen-Adad et al., 2010; Stroman, 2006).

The second challenge of the spinal cord fMRI is related to the anatomy of the spinal cord, which is notoriously small and surrounded by bony vertebrae in comparison to the brain. Though cord measurements can vary due to demographic factors like age, race, and gender, the cervical spinal cord, for example, ranges from 11 millimeters (mm) to 14 mm in the transverse plane and from 7 mm to 9 mm in the sagittal plane depending on the vertebral level (Sherman et al., 1990). Because of its small area, the cord requires a higher resolution than the brain in anatomical and functional imaging to provide accurate and valuable information (Barry, Conrad, et al., 2018; Islam et al., 2019). The bony vertebrae surrounding the cord are also another source of signal distortion, which is known to cause field inhomogeneities due to the difference in bone-tissue magnetic susceptibility (Barry et al., 2016; Stroman et al., 2014).

2.3.3.3. Prevailing fMRI stimulation protocols for the healthy spinal cord

From the selected papers included in this review, various rich stimulation protocols targeting both sensory and motor pathways have been introduced, developed, and demonstrated with spinal cord fMRI. These stimulations include a variety of types, e.g., thermal, tactile, visual, and auditory forms for sensory stimulations; tapping, flexing, and squeezing forms for motor stimulations; and electrical stimulations for both sensory and motor responses. These stimulations have been well demonstrated in controlling the magnitude of responses, e.g., painful and painless sensations, and a few studies have also studied the attentional and emotional dimensions in their responses. Furthermore, precisely targeted activations within the spinal cord gray matter could be achieved with the use of electrical stimulations or specialized task designs, e.g., a pedaling task targeting the lumber section (Kornelsen & Stroman, 2004, 2007). Finally,

the ‘resting-state’ protocol, where no explicit stimulations and/or tasks present, have been demonstrated in spinal cord fMRI as well.

The establishment of these stimulation protocols in spinal cord fMRI demonstrates that spinal cord functions can be similarly interrogated as the brain with neuroimaging technologies (Smith & Kornelsen, 2011; Stroman & Ryner, 2001; Yoshizawa et al., 1996). Such a correspondence between spinal cord fMRI and brain fMRI in healthy populations suggest the potential of spinal cord fMRI being used in diseased/injured conditions as brain fMRI has been successfully used in various brain disorders with exact same simulation protocols. It is noted that some of these stimulation protocols have been used when both brain and spinal cord are imaged simultaneously by fMRI (Bosma et al., 2015; Bosma et al., 2016; Cahill & Stroman, 2011; Khatibi et al., 2022; Kinany, Khatibi, et al., 2023; Leung & Stroman, 2016; Oliva et al., 2022; Rempe et al., 2014; Staud et al., 2021; Stroman, 2009; Tinnermann et al., 2022). Scientific knowledge gained in healthy populations can therefore be used to build the distribution of certain image metrics for specific functionality of the healthy spinal cord, which acts as the reference to be compared with diseased/injured populations. The specificity and controllable responses of each stimulation protocol can further knowledge and understanding of disease and injury mechanisms within the spinal cord. The possibility of using the same stimulation protocols to interrogate both brain and spinal cord simultaneously also presents the opportunity to understand the impacts of a particular disease/condition on these two important components of the central nervous system.

2.3.4. Studying Spinal Cord Pathologies with fMRI

In the selected papers for this review, it seems obvious that the studies of healthy spinal cords are the key cornerstone steps before applying the same stimulation protocols to particular

clinical populations together with spinal cord functional MRI (fMRI). For example, Bosma, et al. (2015) utilized spinal cord fMRI to validate the cord's response to thermal stimulation (Bosma & Stroman, 2015) and to characterize spinal cord and brainstem pain pathways (Bosma et al., 2015) in healthy controls first. Shortly after, the Bosma, et al. team applied the same thermal stimulation to study the origin of pain in fibromyalgia (FM) patients (Bosma et al., 2016). Similarly, tactile stimulation was firstly applied to healthy controls (Agosta et al., 2009; Valsasina et al., 2008) before it was applied to populations of multiple sclerosis (MS) patients (Agosta, Valsasina, Caputo, et al., 2008; Valsasina et al., 2010; Valsasina et al., 2012). Kornelsen, et al. tested their passive (i.e., involuntary) vs active ankle flex movement protocol for the lumbar spine of healthy controls (Kornelsen & Stroman, 2004) before moving this protocol onto those with spinal cord injury (SCI) conditions (Kornelsen & Stroman, 2007), as did Stroman, et al. with their thermal stimulation methodology (Stroman et al., 2004; Stroman, Krause, et al., 2002b; Stroman, Tomanek, et al., 2002). Furthermore, several studies, including Stroman, et al., worked to validate the detection of spinal cord neuronal signals with fMRI in healthy controls (Eippert et al., 2017; Govers et al., 2007; Kornelsen et al., 2013; Madi et al., 2001; Stracke et al., 2005; Stroman et al., 1999; Weber et al., 2016a; Yoshizawa et al., 1996) and improve the performance of imaging and processing methods (Barry, Conrad, et al., 2018; Bosma & Stroman, 2014; Bouwman et al., 2008; Brooks et al., 2008; Harita & Stroman, 2017; Kinany et al., 2020; Stroman, 2006; Xie et al., 2012), before its application to clinical populations. In general, as compared with the number of spinal cord fMRI papers on healthy spinal cords, the use of fMRI in diseased spinal cords is still at its infant stage. However, a steadily increasing number of works over the past decade has begun to apply spinal cord fMRI protocols tested in healthy controls to populations with clinical conditions (Kinany et al., 2022;

Landelle et al., 2021), which have made significant clinical discoveries and contributions. It is also important to note that many of these clinical discoveries are obtained using the knowledge gained from healthy populations as the reference points (see below for detailed discussions), which attests the importance of studying healthy spinal cords as discussed in the above section.

One such clinical condition is fibromyalgia. FM is a chronic condition of an unknown etiology that is characterized by muscle pain and fatigue, of which a cure does not exist (Bhargava & Hurley, 2023). In the first paper to study FM with spinal cord fMRI, Bosma, et al. used a thermal stimulation temporal summation of second pain (TSSP) paradigm, designed to deliver stimuli at a frequency high enough to cause pain established from their early healthy control study (Bosma et al., 2015), to investigate how a spinal cord with FM processes pain (Bosma et al., 2016). As compared with healthy controls, the study resulted in two major findings: the activation of TSSP at low stimulus frequencies and heightened activations in the dorsal horn that perpetuates after stimulus delivery in FM patients (Bosma et al., 2016). More importantly, understanding the mechanism of pain modulations in the healthy spinal cord acts as a critical piece in discovering the origin and impact that FM has on patients. Specifically, areas of functional changes along the established descending pain processing pathways in healthy controls, i.e., the dorsal and ventral horns, RVM, locus coeruleus, and PAG, lead to the first evidence of pain pathway alterations in FM patients (Bosma et al., 2016). Similar functional connectivity alterations in descending pain pathways in FM patients are observed later and reported by another research lab (Staud et al., 2021). In 2019, a resting-state spinal cord fMRI study from a different lab reported a higher amplitude of low frequency fluctuations (ALFF) score, which measures Blood Oxygenation Level Dependent (BOLD) signal fluctuations during resting state, within the ventral horn than the dorsal horn, which could also be attributed to

alterations in descending pain pathways in FM patients, therefore bolstering the above findings (Martucci et al., 2019). Nowadays, alterations in the descending pain pathways and the presence of central sensitization found in spinal cords affected by FM (Bosma et al., 2016; Martucci et al., 2019; Staud et al., 2021) have been one of key proposed causes behind the pain accompanying a clinical diagnosis. This example highlights the contribution that spinal cord fMRI can make in understanding unknown causes of neurological diseases.

Multiple sclerosis has also been studied with spinal cord fMRI. MS is a disease in which the immune system attacks and breaks down the myelin sheath coating white matter neurons, and can be characterized by an array of symptoms such as cognitive dysfunction, numbness/tingling, and incontinence (Tafti et al., 2022). The first to study MS with spinal cord fMRI was Agosta, et al. (2008), who utilized a tactile stimulation paradigm they firstly used in healthy controls (Agosta et al., 2009; Agosta, Valsasina, Caputo, et al., 2008). Their study found that patients presenting MS have an approximate 20% higher fMRI signal change within the C5-C8 spinal cord segments when tactile stimulation was administered compared to healthy controls (Agosta, Valsasina, Caputo, et al., 2008). Their later study found a similar increase when patients underwent a passive flexing task (Agosta, Valsasina, Rocca, et al., 2008). In line with this, Valsasina et al. (2010) reported that this higher level of activation than healthy controls was still observed in different sub-types of MS, i.e., relapsing-remitting (RR) and secondary progressive (SP) MS (Valsasina et al., 2010). Further work revealed that different MS sub-types also impact cord recruitment, as it was later discovered that SPMS has higher level of neuronal recruitment than primary progressive MS, despite the lack of obvious structural differences (Valsasina et al., 2012). Additionally, Rocca, et al. (2012) found decreased neuronal recruitment in RRMS patients with fatigue as compared to those without (Rocca et al., 2012). The cause for such

differences is speculated to be, not in the spinal cord, but in the brain, where it is hypothesized that changes in brain activation due to MS lesions affect how the spinal cord recruits neurons (Rocca et al., 2012; Valsasina et al., 2012). Alternatively, other evidence suggests that wider recruitment could be a compensatory effect or neuronal rewiring to make up for structural damage within the spinal cord (Agosta, Valsasina, Caputo, et al., 2008; Agosta, Valsasina, Rocca, et al., 2008; Combes et al., 2022; Conrad et al., 2018; Rocca et al., 2012; Valsasina et al., 2012). This is a case to demonstrate the usefulness of spinal cord fMRI in understanding pathologies of diseases beyond structural images.

The pathology resulting from the compression of the spinal cord due to injury or age has been studied with spinal cord fMRI as well, including SCI and cervical spondylotic myelopathy (CSM). SCI and CSM can both result in loss of function, chronic pain, and difficulties in coordinating or moving peripheral limbs. The first to study SCI with spinal cord fMRI was Stroman, et al. (2002), who reported that patients with complete injuries had altered areas of activity caudal to, or beneath, the site of injury in response to thermal stimulation, but with similar changes in signal intensities as compared with healthy controls (Stroman, Tomanek, et al., 2002), which was supported by later SCI studies (Kornelsen & Stroman, 2007; Stroman et al., 2004). On the contrary, patients with incomplete spinal cord injuries who could feel the stimulation were found to have activation similar to that of non-injured subjects (Stroman, Tomanek, et al., 2002), a finding supported by a later study from Stroman, et al. (2004) (Stroman et al., 2004). It was also found that those with complete or incomplete spinal cord injuries who could not feel stimulation had significantly diminished activity compared to healthy controls and those who could feel the stimulation (Stroman et al., 2004). Increased fMRI responses close to the site of injuries have been similarly observed in patients with spinal cord injuries using other

stimulation protocols. Cadotte, et al. (2012) reported an increased fMRI response when applying thermal stimulation above the site of an incomplete injury (Cadotte et al., 2012). Zhong, et al. (2017) had a similar finding when applying electrical stimulation to the elbow and palm (a methodology designed to evoke activation at the C5-C6 cord level) of incomplete injury patients with cervical cord injuries (Zhong et al., 2017). ALFF scores were also reported to be higher in CSM patients than healthy controls at resting state (Liu et al., 2016). Opposite phenomena have been noted in few spinal cord injury fMRI studies. In response to an active motor tasks, Kornelsen, et al. (2007) reported a lower amount of active voxels and a greater signal change in SCI patients than healthy controls (Kornelsen & Stroman, 2007). However, it is unclear whether this measurement was obtained from activation close to the injury site. Together, these discoveries imply that, similar to that in MS, the spinal cord compensates for impaired white and gray matter tracts by increasing neuronal activity in areas surrounding the damage or injury.

It is important to note that some of the clinical applications discussed above are enabled by the technological advancements that were first established in healthy controls. For example, Conrad, et al. (2018) (Conrad et al., 2018) took advantage of 7T MRI, i.e., increased BOLD contrast and increased ability in MS lesion detections, to investigate the effect lesions have on regional functional connectivity. The protocols for resting-state studies have also provided independent evidence of disease mechanisms that is congruent with those from task-based studies (Combes et al., 2022; Conrad et al., 2018; Liu et al., 2016; Martucci et al., 2019) and could be more widely implemented in clinical studies than task-based studies as no patient efforts are required in finishing tasks in resting-state study protocols.

2.4. Functional Stimulation Paradigms to Investigate DCM

As previously mentioned, there are several task-based paradigms that can be used to interrogate specific spinal cord reactions with fMRI. There is an enormous benefit in applying task-based paradigms over resting state, especially to isolate specific pathways that would experience impediment under pathological conditions. Popular examples can include thermal and tactile stimulation for sensory responses and tapping or flexing to illicit activation of motor pathways, which have been applied to study spinal cord pathologies like FM, MS, and SCI. However, previous studies have noted that DCM patients experience motor (Muhammad et al., 2023) and sensory (Hameed et al., 2024) deficits during disease progression. This introduces a new problem when trying to apply fMRI to investigate functional activity in DCM patients because these deficits could prevent consistent and normalized performances of task-based paradigms by patients.

A solution to this problem could be electrical stimulation, which can be individualized for every participant to elicit the same reaction, regardless of disease status. Electrical stimulation of the median nerve specifically has been used as an fMRI paradigm in healthy controls (Backes et al., 2001b; Xie et al., 2007) and SCI patients (Zhong et al., 2017), where it was proven to be able to evoke a cervical spinal cord fMRI response. Electrical median nerve stimulation has also been used as a common paradigm in neurophysiological studies (Akaza et al., 2021; Desmedt & Cheron, 1981; el-Negamy & Sedgwick, 1978) of the cervical spinal cord. Its established ability to evoke an electrophysiological and fMRI response in the cervical spinal cord could make it a valuable tool in studying DCM patients, as fMRI can interrogate the lower cervical spinal cord (where compression commonly occurs) and allow for insights into any functional alterations of spinal cord pathways.

Chapter 3: Investigating MTR's ability to reflect WM damage in DCM

* The following chapter is based on the publication (Haynes et al., 2024) and has been reproduced with permission from Springer Nature (Supplemental Material D).

The white matter of the spinal cord plays a key role in the integration of the sensorimotor signals travelling to and from the peripheral nerves. Therefore, damage to these tracts resulting from DCM compression is commonly thought to be the primary driver of DCM symptoms, as interruptions to these pathways that can manifest as a wide array of sensory and motor symptoms. Therefore, damage to the white matter regions could be established as a leading biomarker of the disease, especially for tracts that are responsible for different processes. However, it has not been established whether objective white matter measures – like those extracted from advanced spinal cord MRI methods – can distinguish the severities. The following chapter investigates this relationship and gives insight into structural injury patterns as myelopathy severity increases.

3.1. Introduction

The most commonly used clinical grading assessment scale for DCM severity is the modified Japanese Orthopaedic Association (mJOA) survey (Hejrati et al., 2023; Lannon & Kachur, 2021). The mJOA survey reflects common DCM symptoms that manifest as a result of compressive damage in the spinal cord and has been demonstrated to reliably classify mild, moderate, and severe myelopathy by assessing upper and lower limb motor dysfunction, upper limb sensory loss, and sphincter dysfunction (Tetreault et al., 2017). Though multiple treatments and therapies exist (Hejrati et al., 2023; Lannon & Kachur, 2021), DCM compression can only

be permanently corrected with surgical decompression (Fehlings et al., 2015; Fehlings et al., 2013), typically recommended for moderate and severe cases, but it cannot guarantee neurological recovery (Sampath et al., 2000; Zhang et al., 2016; Zhang et al., 2018). Symptom duration has been shown to be an important factor in predicting post-surgical recovery because it is theorized to reflect permanent damages resulting from demyelination of spinal cord white matter (Pandita et al., 2019; Zhang et al., 2016). The exclusion of mild DCM patients as surgical candidates potentially leaves patients in the early stages of DCM vulnerable to worsening symptoms (Sampath et al., 2000), however whether there are white matter differences between non-surgical (i.e., mild DCM) and surgical (i.e., moderate and severe DCM) groups is unknown.

There are several imaging methodologies that can be used to indirectly measure myelin levels within the spinal cord, such as diffusion tensor imaging (Aung et al., 2013; D'Souza M et al., 2017), myelin water fraction (MacKay & Laule, 2016), and synthetic MRI (Liu et al., 2023). One of these indirect methodologies is Magnetization Transfer Ratio (MTR), which can be calculated from structural MRI and has already been applied to study white matter damage in spinal cord pathologies like multiple sclerosis (Gloor et al., 2024) and spinal cord injury (Cohen-Adad et al., 2011). MTR measures within DCM patients have been shown to be lower than healthy controls (Cloney et al., 2018; Suleiman et al., 2018), which reflects the white matter tract volume loss associated with the manifestation of DCM symptoms (Hopkins et al., 2018). Early MTR studies have also shown that ventral spinal cord MTR is associated with pre-operative mJOA/JOA scores (Cloney et al., 2018; Filimonova, Abdaev, et al., 2024a) and post-operative mJOA recovery (Paliwal et al., 2020). Additionally, MTR from the rubrospinal tract was found to be associated with post-operative mJOA score recovery (Paliwal et al., 2020), as were spinocerebellar MTR tract values and pre-operative JOA scores (Filimonova, Abdaev, et al.,

2024a). However, these studies pose several design gaps that prevent them from impacting clinical intervention decision making. Firstly, the exclusion of key participant groups in some of these studies, e.g., clinically severe myelopathy patients (Paliwal et al., 2020) and healthy controls (Filimonova, Abdaev, et al., 2024a), limits the scope of the results because they can only be applied to specific clinical treatment groups. Secondly, only a limited amount of studies performed tract-based MTR extraction (Filimonova, Abdaev, et al., 2024a; Paliwal et al., 2020), which was further technically limited by their primary reliance on hand drawing spinal cord masks (Cloney et al., 2018; Paliwal et al., 2020) instead of automated cord segmentation. Therefore, the design and technical gaps within these studies prevent a full investigation into MTR's ability to reflect white matter damage in DCM severity at the individual tract level.

In the present study, we build upon these MTR studies to further investigate whether MTR has the ability to quantify the different severity levels of white matter damage in clinical DCM patient groups by using an automated, deep learning based spinal cord segmentation tool to focus on tract-based white matter analysis. To do so, we compared regional- and tract-based MTR between mJOA-based DCM treatment groups and their correlation to the clinical mJOA measures. Because white matter damage occurs as myelopathy continues to progress, MTR is expected to significantly differ between HC and DCM severity groups. Furthermore, because white matter damage leads to the impairment of the spinal cord's regions and tracts, regional- and tract-based MTRs are expected to correlate to mJOA measures relating to their corresponding sensory and motor functions.

3.2. Methods

3.2.1. Participants

Convenience sampling was used to recruit degenerative cervical myelopathy patients (n = 27, 15 female and 12 male) from the OU Health Physicians Neurosurgery Clinic. All DCM patients received a DCM diagnosis from a licensed clinician and had an mJOA score less than 18 (Table 2.1). Aged matched healthy control participants (n = 20, 14 female and 6 male) were recruited from the Laureate Institute for Brain Research (LIBR) in Tulsa, OK and the University

		Mild DCM (n = 11)	Moderate/Severe DCM (n = 16)	HC (n = 20)	p-value
Age		55.9 ± 8.3	52.6 ± 5.9	50.9 ± 6.7	0.161
Sex (F/M)		8/3	7/9	14/6	N/A
mJOA severity		16 ± 2.0	11 ± 3.3	18 ± 0.0	<0.0001
mJOA sub-scores	Upper limb	5.0 ± 0.0	4.0 ± 1.0	5.0 ± 0.0	<0.0001
	Lower limb	6.0 ± 2.0	4.0 ± 0.8	7.0 ± 0.0	<0.0001
	Sensory	2.0 ± 1.0	1.0 ± 1.0	3.0 ± 0.0	<0.0001
	Sphincter	3.0 ± 0.0	3.0 ± 1.0	3.0 ± 0.0	0.0018
Level of max compression		C3/C4 (n = 1) C4/C5 (n = 5) C5/C6 (n = 5)	C2/C3 (n = 1) C3/C4 (n = 2) C4/C5 (n = 2) C5/C6 (n = 11)	N/A	N/A

Table 2.1: Demographic, modified Japanese Orthopaedic Association (mJOA), and level of max compression data on the participants grouped in mild, moderate/severe degenerative cervical myelopathy (DCM), and healthy controls (HC).

of Oklahoma Health and Science Center (OUHSC). All participants were scanned between 2021 and 2023 and a signed, informed consent was collected before any data collection.

The following inclusion and exclusion criteria for this study is further described by Muhammad, et al. (2024) (Muhammad, Weber, Rohan, et al., 2024). Inclusion criteria for DCM patients included evidence of cervical spinal cord compression on a T2-weighed image and one of more of the following: (1) hyperreflexia, (2) a positive Hoffman sign, (3) hand coordination loss, (4) gait impairment, and/or (5) motor weakness. Furthermore, the following exclusion criteria were applied to all participants: (1) participant is less than 30 or more than 70 years of

age, (2) a history of spine surgery, (3) three or more co-morbid conditions, (4) diagnosis of a neurodegenerative disease, (5) diagnosis of a systemic rheumatological disease, (6) presences of isolated radiculopathy without myelopathy, (7) a history of active peripheral/vascular neuropathy, (8) pregnancy, (9) a history of seizure disorders, (10) any medical condition preventing the completion of study related procedures, (11) DCM patients in need of urgent decompressive surgery, and/or (12) participants with asymptomatic spinal cord compression (characterized by the presence of cervical canal stenosis, disk herniation, or hyperintense signal on a T2-weighted image, with no manifestation of clinical symptoms and an mJOA score of 18).

3.2.2. Statement of Ethics

This study was approved by the University of Oklahoma Health Sciences Center institutional review board (IRB #12068) and is in accordance with the Declaration of Helsinki. We certify that all applicable institutional and governmental regulations concerning the ethical use of human volunteers were followed during the course of this research.

3.2.3. Clinical assessment scales

All participants filled out a modified Japanese Orthopaedic Association (mJOA) survey (Tetreault et al., 2017). An mJOA score is broken into four sections, measuring four independent factors: upper extremity motor dysfunction (0-5), lower extremity motor dysfunction (0-7), sensation (0-3), and sphincter dysfunction (0-3). Answers for each question were summed and each participant was given a score of 0-18. DCM participants were then labeled as having mild, moderate, or severe myelopathy based on the mJOA severity groups established by Tretreault et al. (2016). Mild DCM was defined as a score of 15-17, moderate DCM as score of 12-14, and severe DCM as a score of 0-14 (Tetreault et al., 2017). DCM participants were sorted into mild (n = 11, 8 female and 3 male) and moderate/severe (n = 16, 7 female and 9 male) groups based

on their resulting mJOA scores to simulate treatment groups (i.e. non-surgical versus surgical). Healthy controls all received scores of 18, indicating the absence of neurological dysfunction. However, healthy controls with an mJOA of 18 were excluded if radiological signs of asymptomatic compression were present.

3.2.4. MRI protocol

All MRI data was collected at LIBR (Tulsa, OK) with a 3T MR750 GE scanner equipped with a 16-channel NovaCSpine coil. Participants were scanned in a supine position within the scanner and instructed to remain as still as possible. Spinal cord image acquisition for healthy controls and DCM patients followed the generic spine consensus protocol (Cohen-Adad et al., 2021). T2-weighted scans (TR = 120ms; TE = 2500ms; FOV = 256mm x 256mm; Thickness = 0.8mm) were collected for all participants. Additionally, two gradient echo T2*-weighted scans (TR = 35ms; TE = 4ms; Flip Angle = 9°; FOV = 172mm x 172mm; Resolution = 230mm x 230mm; Thickness = 5mm) were collected with (MT1) and without (MT0) a magnetization transfer (MT) pulse. The MT scans are centered at the C5 vertebra and cover the spinal cord region from the C3 to C7 vertebral levels.

3.2.5. MRI analysis

Quantitative MT image analysis from each participant was performed using the Spinal Cord Toolbox (SCT v6.1) (De Leener et al., 2017). Automatic segmentation of the spinal cord was performed on the MT1 images utilizing SCT's deep learning model (*sct_deepseg_sc* (Gros et al., 2019)). The accuracy of these segmentation masks was verified through a quality control report and manual corrections were applied to optimize automatic segmentation outcomes. A binary spinal cord mask with a diameter of 35mm was created on the MT1 image to define a region of interest (ROI) surrounding the spinal cord to avoid interference from irrelevant body

structures during the registration of the MT1 to MT0. The MT0 image was then registered to the MT1 using *sct_register_multimodal* and the ROI mask with a regularized slice-wise translation (Cohen-Adad et al., 2015). MTR was calculated using the *sct_compute_mtr*, which calculates MTR using the following formula for each voxel:

$$MTR = \frac{MT0 - MT1}{MT0} * 100 \quad (1)$$

Individual T2-weighted images were then registered to the PAM50 template (*sct_register_to_template* (De Leener et al., 2018)), which was then warped to the native T2-weighted space to define spinal cord regions and tracts with the PAM50 template. MT1 was also registered to a T2-weighted image using *sct_register_multimodal*. This makes group-level and region/track-based analysis possible. Detailed steps on how MTR images were processed and extracted are described in Supplemental Figure A.1 and a more detailed description of the anatomical processing code can be found in Muhammad, et. al. (2025) (Muhammad, Weber, Bédard, et al., 2025).

3.2.6. Regional and tract MTR extraction

For region- and tract-specific MTR extraction, we utilized *sct_extract_metric*, which uses the maximum a posteriori (MAP) method to estimate the maximum likelihood of the regions/tracts (Levy et al., 2015) and extract more accurate region/tracts-based MTR measures from the PAM50 white matter atlas (De Leener et al., 2018). The MAP method also helps to mitigate the partial volume effect caused by lower spatial resolution in MT images (De Leener et al., 2017). MTR measures from the total white matter; ventral, dorsal, and lateral white matter regions; and the ventral corticospinal, ventral reticulospinal, spino-olivary, rubrospinal, lateral corticospinal, lateral reticulospinal, spinal lemniscus, fasciculus gracilis, and fasciculus cuneatus tracts (Supplemental Figure A.2) were extracted from the two vertebral levels containing

maximum compression (Supplemental Figure A.1), which was identified on a T2w image. Reported MTR values were averaged across the two vertebral levels and over the regional/tract area.

3.2.7. Statistical analysis

Statistical analysis was performed with GraphPad PRISM version 10.2.2 software. ANOVAs were applied to compare participant characteristics (i.e. age, overall mJOA, and mJOA sub-scores), and region and tract-based MTRs of the HC, mild DCM, and moderate/severe DCM groups. Sample size was based on the results of a previous study, Paliwal et al. (2020) (Paliwal et al., 2020), which used samples sizes of 9 HCs and 13 DCM patients and observed significant differences between groups. In this study, sample size was increased to 20 HCs and 27 DCM patients to ensure adequate statistical power. Shapiro-Wilk normality tests were applied to the groups before statistical tests were conducted. For data that was normally distributed, a one-way ANOVA with Bonferroni multiple comparison correction was applied. A Kruskal-Wallis test with a Dunns multiple comparison test was applied to data that were not normally distributed. Center values for normally distributed data are represented by the mean and standard deviation (SD), and for non-parametric tests are represented by the median and interquartile range (IQR). Post-hoc corrections were performed separately for each characteristic, region-based, and tract-based comparison. Finally, to evaluate the relationships between the MTR measures and clinical assessment (i.e., mJOA) of DCM patients, a two-tailed Spearman's correlation was applied due to the non-normal distribution of the data. Differences and correlations with a p-value of <0.05 were considered statistically significant.

3.3. Results

3.3.1. Participant Characteristics

This cross-sectional study included 27 DCM patients and an age-matched HC group of 20 participants. The mJOA scores among the DCM patients ranged from 8 to 17. DCM patients were categorized into two severity groups based on their mJOA scores: 11 with mJOA scores from 15-17 were categorized into a mild DCM group and 16 with mJOA below 15 were categorized into a moderate and severe (moderate/severe) DCM group. The median (± IQR) mJOA score was 16 (± 2.0) for the mild DCM group and 11 (± 3.3) for the moderate/severe DCM group. The mJOA scores were also divided into sub-scores, which included measures for upper limb motor, lower limb motor, upper limb sensory, and sphincter disfunction. Mild and moderate/severe groups had mean upper limb mJOA scores of 5.0 (± 0.0) and 4.0 (± 1.0), lower limb mJOA scores of 6.0 (± 2.0) and 4.0 (± 0.8), sensory mJOA scores of 2.0 (± 1.0) and 1.0 (± 1.0), and sphincter mJOA scores of 3.0 (± 0.0) and 3.0 (± 1.0), respectively. Statistical testing revealed existing differences in overall and sub-scale mJOA scores between groups (Table 2.1). The mean (± SD) ages for the HC (50.9 ± 6.7), mild DCM (55.91 ± 8.3), and moderate/severe DCM (52.63 ± 5.9) were not statistically significantly different between the groups ($p = 0.16$). Detailed clinical and demographic characteristics of study participants are shown in Table 2.1.

3.3.2. Comparison of region-based MTR in DCM and HC groups

Significant differences in region-based MTR measures (Supplemental Figure A.2) were observed between the HC and moderate/severe DCM groups. In the total white matter, the moderate/severe DCM group had significantly lower MTR compared to the HC ($p = 0.0065$) (Figure 2.1A). Similarly, the moderate/severe DCM group had significantly lower MTR in the ventral region compared to the HC group ($p = 0.0009$) (Figure 2.1B). However, no significant

differences were observed in the lateral (p = 0.085) (Figure 2.1C) or dorsal (p = 0.0574) (Figure 2.1D) regions between these two groups. Heatmaps illustrating the average region-based MTR

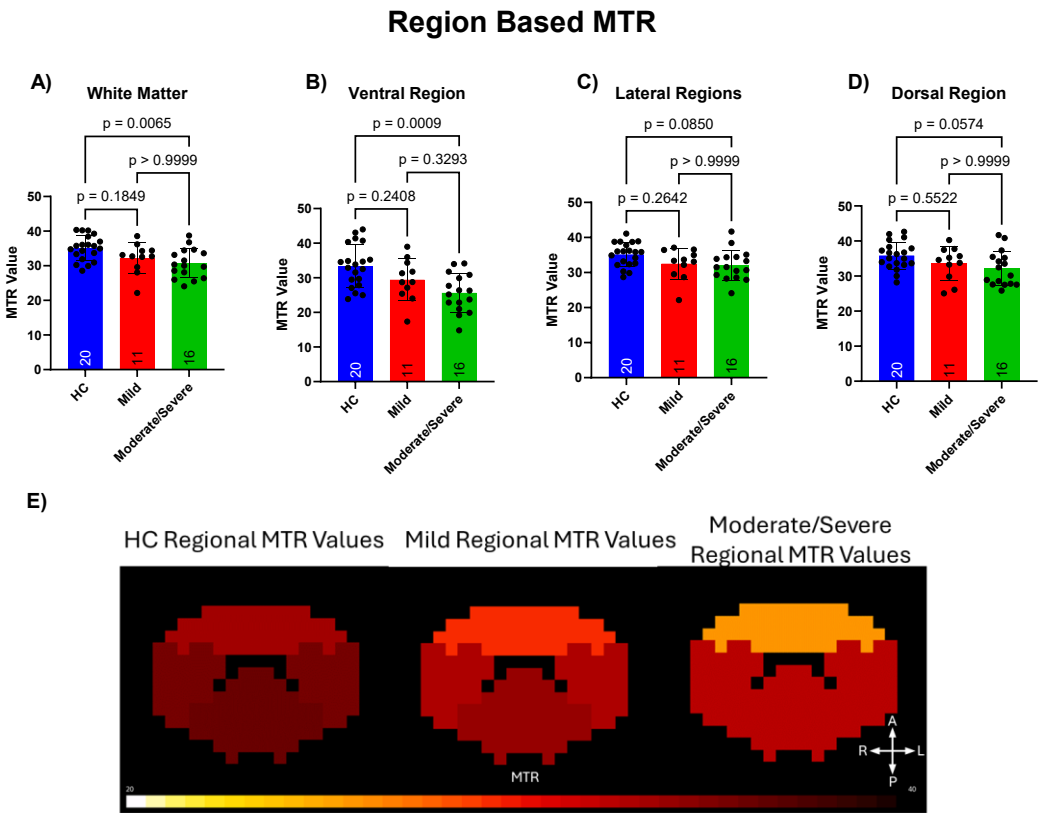

Figure 2.1: Region based magnetization transfer ratio (MTR) calculations between healthy controls (HC), and degenerative myelopathy (DCM) patients with mild and moderate/severe mJOA scores. A One-Way ANOVA and a Bonferroni multiple comparison test was used for all comparisons. Error bars represent the mean and standard deviation of the dataset. Significant differences in MTR values were found between HC and the moderate/severe DCM groups in the white matter (p = 0.0065) (A) and ventral (p = 0.0009) (B) regions. A heatmap of average regional- specific MTR values (E) depicts differences in HC (left), mild DCM (middle), and moderate/severe DCM (right) participants.

measures (i.e., ventral, dorsal, and lateral regions) are shown in Figure 2.1E, which also indicate that greater MTR differences occur within the ventral region. In general, the total white matter and region-based MTR decreased with DCM severity, but there were no significant differences observed between neighboring groups (i.e., HC vs mild DCM and mild DCM vs moderate/severe DCM) in either measure.

3.3.3. Comparison of tract-based MTR in DCM and HC groups

Tract-based MTR comparisons showed results consistent with the regional MTR comparisons. Significant differences in MTR were mainly observed between the HC and moderate/severe DCM groups for tracts located in the ventral region, including the ventral corticospinal ($p = 0.0101$) (Figure 2.2A) and ventral reticulospinal ($p = 0.0084$) (Figure 2.2B). Significant differences were also found in the spinal lemniscus ($p = 0.0079$) (Figure 2.2D),

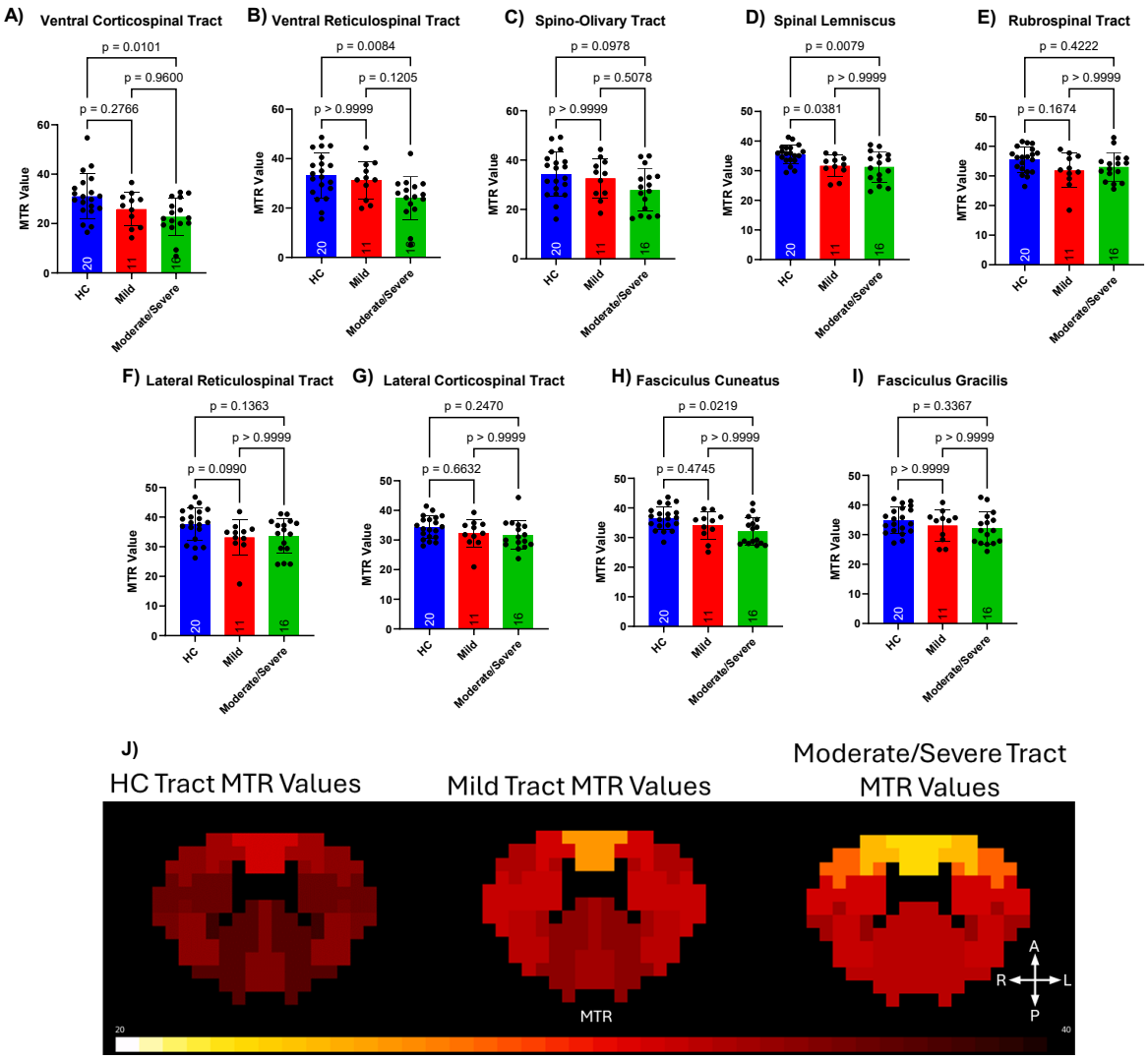

Figure 2.2: Tract-based magnetization transfer ratio (MTR) calculations between healthy controls (HC), and degenerative myelopathy (DCM) patients with mild and moderate/severe mJOA scores. A One-Way ANOVA and a Bonferroni multiple comparison test was applied to comparisons for A-E, G, and I, and a Kruskal-Wallis ANOVA and Dunn multiple correction test was applied to comparisons F and H. The error bars represent the mean and standard deviation of the dataset. Significant differences in MTR values were found between HC and the moderate/severe DCM groups in the ventral corticospinal ($p = 0.0101$) and reticulospinal ($p = 0.0084$), and spinal lemniscus ($p = 0.0079$) tracts. Significant differences were also found between the MTR values of HCs and mild DCM groups in the fasciculus cuneatus tract ($p = 0.0219$). A heatmap of average tract- specific MTR values (J) depicts differences in HC (left), mild DCM (middle), and moderate/severe DCM (right) participants.

which is a tract located within the lateral region but close to the ventral region. In the dorsal region, the fasciculus cuneatus ($p = 0.0219$) showed a significant difference (Figure 2.2H)

between the HC and moderate/severe DCM groups. Heatmaps illustrating the average tract-based MTR measures are shown in Figure 2.2J, which also indicate that the maximal differences occur within the ventral region. Similar to the region-based results, tract-based MTR generally decreased with DCM severity. An exception to this observation was the rubrospinal tract, which contained an increase in MTR between the mild and moderate/severe DCM groups. Only one significant difference was observed between neighboring groups (i.e., either HC vs mild DCM or mild DCM vs moderate/severe DCM), which was between the HC and mild DCM groups in the spinal lemniscus ($p = 0.0381$) (Figure 2.2D).

3.3.4. Association between MTR measures and mJOA scores

At the regional level, no significant correlation ($p > 0.05$) was found between region-based MTR and the overall or sub-scale (i.e., upper limb motor, lower limb motor, upper limb sensory, and sphincter) mJOA measures. The correlations between ventral region MTR values

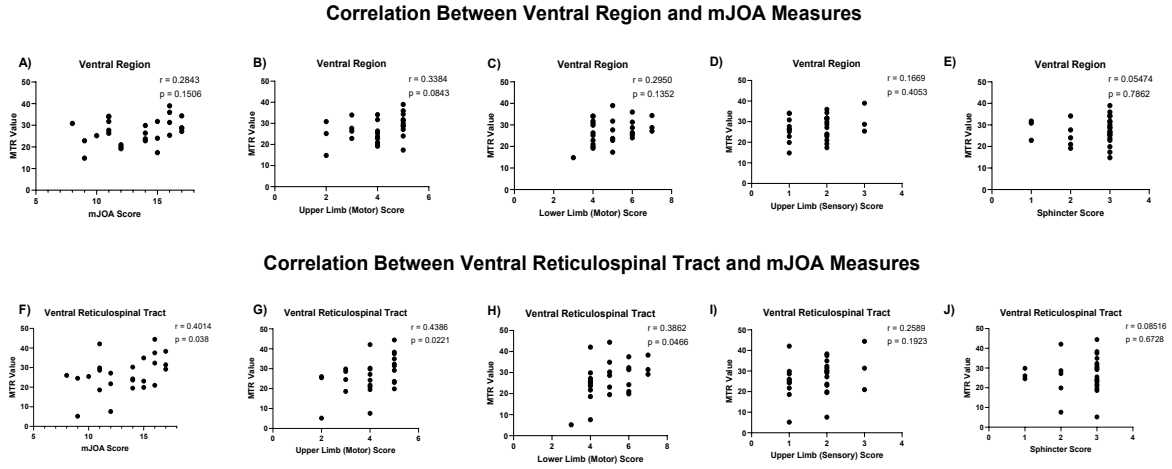

Figure 2.3: Correlations between the ventral region (A-E) and ventral reticulospinal tract (F-J) magnetization transfer ratio (MTR) values and modified Japanese Orthopaedic Association (mJOA) scores and measures. A Spearman's correlation was used to determine whether any correlations existed between values. There were no significant correlations found, but overall mJOA, upper limb motor, and lower limb motor scores were noted due to tract-specific correlations. Significant correlations were found between the ventral reticulospinal tract MTR values and overall mJOA ($r = 0.4014$; $p = 0.038$) (F), upper limb motor ($r = 0.4386$; $p = 0.0221$) (G), and lower limb motor ($r = 0.3862$; $p = 0.0466$) (H) scores.

and the overall mJOA (Figure 2.3A) and the sub-scale mJOA scores (Figure 2.3B-E) were included to compare tract-based results from the ventral region (see discussion below).

Ventral reticulospinal tract MTR was found to be significantly associated with overall mJOA scores ($r = 0.401$; $p = 0.038$) (Figure 2.3F), as well as the upper ($r = 0.439$; $p = 0.022$) (Figure 2.3G) and lower ($r = 0.386$; $p = 0.047$) (Figure 2.3H) limb motor sub-scale scores. However, the ventral reticulospinal MTR measures were not significantly correlated to the upper limb sensory ($r = 0.259$; $p = 0.192$) (Figure 2.3I) and sphincter ($r = 0.085$; $p = 0.673$) (Figure 2.3J) sub-scale scores. No other significant correlations ($p > 0.05$) between MTR measures and overall/sub-scale mJOA scores occurred, and it is important to note that no other tracts showing significant MTR decreases between groups (Figure 2.2A, 2.2D, and 2.2H) were found to correlate to overall or sub-scale mJOA scores. These included the ventral corticospinal (upper limb motor: $r = 0.328$; $p = 0.095$, lower limb motor: $r = 0.146$; $p = 0.469$) tract, the spinal lemniscus (upper limb sensory: $r = -0.045$; $p = 0.822$), and the fasciculus cuneatus (upper limb sensory: $r = 0.293$; $p = 0.138$). It is also noted that no significant correlations were observed between tract-based MTR and the upper limb sensory or sphincter sub-scale mJOA measures. Detailed r- and p-values for the Spearman's correlation between regions displaying significant MTR differences and mJOA scores/sub-scores can be found in Table 2.2.

Region/Tract	mJOA Score/Sub-Score	r-value	p-value
White Matter	mJOA Score	0.1682	0.4017
	Upper Limb	0.0889	0.6593
	Lower Limb	0.1373	0.4948
	Sensory	0.2256	0.2578
	Sphincter	0.2524	0.2040
Ventral Region	mJOA Score	0.2843	0.1506
	Upper Limb	0.3384	0.0842
	Lower Limb	0.2950	0.1352
	Sensory	0.1669	0.4053
	Sphincter	0.0547	0.7862
Ventral Reticulospinal	mJOA Score	**0.4014**	**0.0380**
	Upper Limb	**0.4386**	**0.0221**
	Lower Limb	**0.3862**	**0.0466**
	Sensory	0.2589	0.1923
	Sphincter	0.0852	0.6728
Ventral Corticospinal	mJOA Score	0.1362	0.4983
	Upper Limb	0.3281	0.0948
	Lower Limb	0.1456	0.4688
	Sensory	0.0176	0.9304
	Sphincter	-0.1095	0.5867
Spinal Lemniscus	mJOA Score	-0.0687	0.7335
	Upper Limb	-0.0766	0.7041
	Lower Limb	0.0122	0.9520
	Sensory	-0.0455	0.8219
	Sphincter	0.0852	0.6728
Fasciculus Cuneatus	mJOA Score	0.2070	0.3002
	Upper Limb	0.1319	0.5120
	Lower Limb	0.1337	0.5060
	Sensory	0.2928	0.1383
	Sphincter	0.3041	0.1230

Table 2.2: Spearman's r-values and their corresponding p-values. Correlation calculations were done between white matter regions displaying significant Magnetization Transfer Ratio (MTR) differences (Figures 1 and 2) and mJOA scores and sub-scores.

3.4. Discussion

Degenerative cervical myelopathy (DCM) is a common cause of chronic spinal cord injury in patients. While cord compression is an omnipresent finding in these patients, clinical symptoms of DCM are poorly predicted by standard MRI alone. Previous studies have shown that regional- (Cloney et al., 2018) and tract-specific (Filimonova, Abdaev, et al., 2024a; Paliwal et al., 2020) MTR measures in the spinal cords of DCM patients are lower compared to their healthy counterparts, likely reflecting white matter myelin loss (Hopkins et al., 2018). However, these works exclude key participant groups (i.e. severe DCM patients (Paliwal et al., 2020) and

healthy controls (Filimonova, Abdaev, et al., 2024a)) and solely employ manual MTR extraction methodologies. The current study seeks to evaluate region- and tract-specific DCM white matter injuries and how they result in various levels of clinical disability.

In general, MTR measured at multiple resolutions (i.e., overall white matter, regions, and tracts) decreased with DCM severity (Figures 2.1 and 2.2), indicating the global impact compression has on the spinal cord white matter of DCM patients. More importantly, our present study demonstrates that region- and tract-specific MTR changes within the spinal cord can reflect the heterogeneous nature of the white matter damage occurring in DCM patients, aligning with other studies demonstrating regional MTRs are impacted differently in the spinal cord white matter (Cloney et al., 2018). In a previous study done by Hopkins et al., white matter volume was found to significantly decrease in some of the ventral white matter tracts of DCM patients (Hopkins et al., 2018). Our results aligned with Hopkins et al.'s findings and showed that MTR significantly decreased in the ventral region between healthy controls and moderate/severe patients (Figure 2.1B). Evidence for the heterogeneous white matter damage in DCM patients is further revealed in significant tract-specific MTR changes (Figure 2.2). Most of the significant MTR decreases in DCM patients occurred in the motor tracts (i.e., the ventral corticospinal and ventral reticulospinal tracts) within the ventral cord, which is consistent with region-based MTR changes. However, no significant decrease in MTR was found in the spino-olivary tract, which is a sensory tract also contained within the ventral cord. Within the lateral and dorsal regions, two sensory tracts (i.e., the spinal lemniscus tract in the lateral region and the fasciculus cuneatus in the dorsal region), exhibited significant MTR changes while the rest did not. This mixture of significant and non-significant tract-specific changes explains the reasoning behind the non-significant region-based MTR decreases occurring within these two regions, which trend towards

significance between the HC and moderate/severe DCM groups (lateral: $p = 0.085$; dorsal: $p = 0.0574$, Figure 2.1). These observations testify to the benefit of tract-based MTR analysis because they can be used to evaluate the heterogeneity in white matter damage in progressive DCM. The benefits of tract-based MTR analysis is further supported by the correlation analysis between MTR and mJOA scores, where the only significant correlation was identified from tract-specific MTR (Figure 2.3F-H) and not the regional.

Because DCM is a heterogeneous disease with various symptom combinations, we expect tract-specific white matter changes to allow for a better quantification of impairment by allowing us to measure white matter damage occurring in specific motor and sensory tracts. Our most profound findings, that MTR changes within the motor tracts of the ventral region, were consistently observable at multiple spatial resolutions (i.e., regional vs tract). It also reflects a common pattern of injury in DCM patients where initial injury occurs in the ventral white and gray matter (Ito et al., 1996) and impacts the motor tracts within the region (Hardy, 2021). Motor processes like gait, balance, dexterity, and grip strength are commonly impacted by DCM and have been shown to be significantly decreased when compared to HC/asymptomatic controls (Doita et al., 2006; Haddas, Ju, et al., 2019; Nagata et al., 2012; Omori et al., 2018; Yukawa et al., 2009). The NIH Toolbox Motor Battery has also revealed functional motor differences between DCM and HC groups (Muhammad et al., 2023), and correlations with regional- and tract-based MTR values (Muhammad, Weber, Haynes, et al., 2025). Furthermore, patient reported outcome measures (PROMIS) upper extremity scores, which has patients self-assess their upper extremity functionality, and PROMIS mobility scores, measuring lower extremity dysfunction, are significantly lower in DCM patients than healthy and asymptomatic controls (Hameed et al., 2024). Previous findings that establish ventral MTR's correlation to overall

mJOA scores (Cloney et al., 2018) also align with our finding of correlations between the ventral reticulospinal tract MTR and overall, upper and lower limb motor mJOA sub-scores. However, our data allow for a tract-specific look into MTR's correlation with different measures of clinical severity that more closely pertain to the motor roles of the ventral reticulospinal tract.

A factor behind this ventral horn damage could potentially be the degree of cervical kyphosis – a condition in which the curve of the spine inverts – within the spinal column of DCM patients. This can cause the spinal cord to press against anterior part of the vertebrae and lead to tension in the cord, increased intramedullary pressure, and reduced blood supply (Ames et al., 2013; Buell et al., 2018). T1-slope was also found to impact the size of the C5-C7 neural foramina (i.e. nerve root) (Patwardhan et al., 2018), which is where common DCM symptoms are suspected to originate, and correlated with cervical lordosis measures and mJOA scores (Yuan et al., 2017). Furthermore, cervical malalignment can further impact the spinal cord when exposed to dynamic movements, like flexion and extension. For example, flexion can cause the cord to further lengthen and compress against the vertebrae and extension can reduce available cord space and is a risk factor for causing high-intensity lesions on T2w images (Ames et al., 2013; Buell et al., 2018). Because previous studies have provided evidence for the role that cervical malalignment plays in DCM, complementary imaging, like full length x-rays, dynamic MRI and films, and standing radiographs, when investigating its pathogenesis and progression could be an integral future step in understanding the mechanisms behind white matter damage and symptom manifestation.

Additionally, though only non-significant MTR decreases in the lateral and dorsal regions of DCM patients were noted, tract-based MTR analysis revealed significant changes in the sensory tracts of the dorsal (i.e., the fasciculus cuneatus) and lateral (i.e., the spinal lemniscus,

consisting of the spinothalamic and spinoreticular tracts (De Leener et al., 2018)) regions (Figure 2.2H and 2.2D). Damage to ascending sensory tracts aligns with findings that pain interference PROMIS scores, which measure self-reported pain and its impact on an individual's well-being, were significantly different between DCM patients and healthy/asymptomatic controls (Hameed et al., 2024). However, correlation between sensory tract MTRs and clinical severity measures were not observed (Figure 2.3), which might indicate that sensory tract white matter damage varies between individual patients and is not the result of a consistent injury pattern, like that occurring in the motor tracts of the ventral regions (Hardy, 2021; Ito et al., 1996). At the same time, it is also reasonable to observe this damage, as we would expect white matter injury to spread to the lateral and dorsal portions of the cord as myelopathy progresses.

3.4.1. Limitations

This study contains several limitations. Firstly, while the sample size was increased from previous studies (Cloney et al., 2018; Paliwal et al., 2020), sample size is still limited and should be expanded further in future studies in order to gain more robust results for a wider range of DCM patients. Secondly, while significant improvements in spinal cord MRI analysis tools, like the Spinal Cord Toolbox, have been made and the spinal cord can now be automatically segmented, manual corrections were still required in the vast majority of DCM patients due to the spinal cord compression. However, use of automated tools, like the deep learning based spinal cord segmentation, makes segmentation less biased than previous studies using hand drawn masks. Spinal cord imaging technology also still heavily limits data quality. MT imaging specifically has a low spatial resolution, making it susceptible to the partial volume effect, and MT1 and MT0 images are not acquired simultaneously, which could lead to issues with alignment and MTR calculation. However, advances in analysis methodologies, like the

automated registration of MT images to T2w for obtaining regional- and tract-based MTR data based on the PAM50 white matter atlases, helps to limit these effects by providing an image with higher spatial resolution to make data extraction more accurate and reproducible than previous studies. An additional limitation of this imaging technique is the static, supine position of the participants during imaging. Due to this limitation, investigation into the relationship between MTR values and cervical alignment and mobility parameters, which could provide insight into the manifestation and progression of DCM, could not be completed. Finally, while MTR is a validated strategy in quantifying white matter DCM damage, our analysis was constrained to the white matter tracts and did not include gray matter measurements. Since gray matter damage within the spinal cord is expected to occur alongside white matter loss in DCM patients (Ito et al., 1996), investigation into gray matter damage is warranted in future studies.

3.5. Conclusion

DCM is a progressive disease that can cause motor and sensory dysfunction that can ultimately result in permanent neurological damage if left untreated. Currently, surgical decompression is the only corrective treatment; however, surgery is typically reserved for moderate and severe cases, as measured by mJOA. In this study, we established that tract-specific MTR can reflect white matter changes in moderate/severe myelopathy patients that would be lost at the regional/tract level and that upper and lower limb motor mJOA scores correlate with MTR in the ventral reticulospinal tract. This provides evidence that tract-based MTR can reflect white matter damage resulting from cervical spinal cord compression.

Chapter 4: Establishing the Relationship Between Structural DCM Damage and Spinal Cord Reflex Arcs

* The following chapter has been reprinted, with permission, from (Haynes, Muhammad, Weber, Khan, Hameed, Ding, et al., 2025) (© 2025 IEEE). In reference to IEEE copyrighted material, which is used with permission in this thesis, the IEEE does not endorse any of the University of Oklahoma's products or services. Internal or personal use of this material is permitted (Supplemental Material E).

In combination with past white matter (WM) literature (Cloney et al., 2018; Filimonova, Abdaev, et al., 2024a; Hopkins et al., 2018; Paliwal et al., 2020), the findings described in the previous chapter (Haynes et al., 2024) help to establish the role that WM damage plays in DCM severity. However, despite the evidence establishing WM damage as a leading driver of DCM symptoms and key biomarker, it is not the only indicator. Compressive damage manifesting in the gray matter (GM) horns – which is significantly less investigated than its WM counterpart – could possibly be a secondary driver of symptoms, especially due to its role in segmental intraspinal connectivity. The following chapter aims to address this gap by investigating the relationships between GM loss and a required increase in involuntary motor threshold.

4.1. Introduction

Previous studies have investigated the impact of compressive damage to the microstructural content of the cord itself. Several studies have reported a decrease in magnetization transfer ratio (MTR), an indirect measure of WM content, between healthy controls (HCs) and patients with DCM (Cloney et al., 2018; Haynes et al., 2024), as well as a loss in WM tract volume (Hopkins et al., 2018). This WM damage has reportedly been correlated

with both pre- (Cloney et al., 2018; Haynes et al., 2024) and post-surgical (Paliwal et al., 2020) clinical measures. Furthermore, significant decreases in morphometric measures, e.g., cross-sectional area, at the level of maximum compression were correlated with decreases in motor performances (Muhammad, Weber, Bedard, et al., 2024), which have been reported to occur in DCM (Muhammad et al., 2023). These findings play key roles in understanding DCM pathology, as the loss of myelinated axons in impacted motor tracts could be the underlying cause of motor symptom manifestation (Haynes et al., 2024; Muhammad, Weber, Haynes, et al., 2025). Similarly, GM loss has also been reported in DCM patients (Smith et al., 2020), where it has been associated with clinical measures (Smith et al., 2020) and neurodegeneration in WM tracts (Grabher et al., 2017). Considering GM's intermediary role connecting the sensory and motor neurons of the spinal cord, understanding this relationship can provide additional insight into DCM symptom manifestation, pathogenesis, and treatment decisions. However, the impact of GM loss on motor function in DCM has not been investigated.

In this study, we investigate the relationships between GM volume and motor threshold to understand the role GM loss plays in the pathophysiology of DCM. To achieve this, we compared overall and regional GM volume measurements between HC and DCM patients to electrical stimulation motor thresholds. Previously, median nerve stimulation has been used to induce spinal cord reflex arcs connecting the sensory and motor neurons of the GM region (Knikou, 2008) and functional activation similar to hand clenching in healthy controls (Backes et al., 2001a). Therefore, median nerve electrophysiology makes it a primary target to interrogate the relationship between changes in GM volumes and motor threshold. This is because the ventral part of the cord houses motor neurons and tracts and is commonly impacted in DCM

(Haynes et al., 2024; Ito et al., 1996), and we can expect a decrease in GM volume, reflecting the loss of cell bodies, to indicate the increase in stimulation required to overcome motor inhibition.

4.2. Methods

4.2.1. Participants

HCs participants (n = 19; female = 14, male = 5) were recruited from the Laureate Institute for Brain Research (LIBR) in Tulsa, OK and the University of Oklahoma Health and Sciences Center (OUHSC). DCM patients (n = 28; female = 15, male = 13) were recruited from the OUHSC Neurosurgery clinic. Both groups were aged-matched to control for age-related changes. Demographic data for all participants can be found in Table 3.1. The study protocols were approved by OUHSC's Institutional Review Board (IRB #12068), and signed consent was collected from all participants before data collection. Inclusion and exclusion criteria for this study are described in Muhammad et al. (2025) (Muhammad, Weber, Bédard, et al., 2025).

4.2.2. Electrical Stimulation

Ag/AgCl electrodes were placed on the participant's dominant upper limb. The anode was placed about 1 cm proximal to the flexor retinaculum (wrist), and the cathode was placed 2-3 cm proximal to the medial epicondyle (elbow) along the median nerve. This methodology targets the median nerve and can elicit motor activation comparable to voluntary hand clenching in healthy controls (Backes et al., 2001a). Motor threshold was determined on a participant-to-participant basis and was defined as the minimal level of stimulation required to elicit a thumb or finger twitching in the hand. Visual twitching in the thumb or finger was also used as confirmation that the median nerve was successfully targeted, as the nerve innervates those appendages (Mazurek & Shin, 2001). The stimulation was delivered in single monophasic pulses (2ms) with a constant current stimulator (DS7A Digitimer, UK).

4.2.3. MRI Protocol

MRI data were collected with a GE Discovery MR750 3T scanner (software version 26, GE Healthcare, Milwaukee, WI, USA), equipped with a 16-channel NovaCSpine coil, at LIBR (Tulsa, OK). Participants were placed in a supine position during scanning and were instructed to remain as still as possible. All spinal cord acquisitions followed the generic spine consensus protocol (Cohen-Adad et al., 2021). Multi-echo gradient-echo (MERGE) T2* scans (TR = 600ms; Flip Angle = 30; FOV = 224mm; Matrix = 448 x 224 x 224; Slice Thickness = 5mm) were collected from each participant. Additionally, two gradient-echo T2* scans (TR = 35ms; TE = 4ms; Flip Angle = 9°; FOV = 172mm; Matrix = 256 x 230 x 230; Thickness = 5mm) were also collected from each participant with (MTon) and without (MToff) a magnetization transfer saturation pulse.

4.2.4. MRI Analysis

MRI scans were analyzed using the Spinal Cord Toolbox (v6.1) (De Leener et al., 2017). Deep learning segmentation was performed on each image (sct_deepseg_sc (Gros et al., 2019)) and manually corrected as needed. GM masks were automatically segmented from the spinal cord (sct_deepseg_gm (Perone et al., 2018)). To make the WM masks, the GM masks were subtracted from masks of the whole cord. The PAM50 T2* atlas and WM masks were then registered to the participant's native image space (sct_register_multimodal (De Leener et al., 2018)) before the PAM50 atlases (De Leener et al., 2018) were warped (sct_warp_template). GM metrics were extracted (sct_extract_metric) from the maximum compression level (MCL) using the PAM50 atlases and the maximum a posteriori (MAP) method (De Leener et al., 2018). Further details about MRI analysis in compressed DCM spinal cords can be found in Muhammad et al. (2025) (Muhammad, Weber, Bédard, et al., 2025).

4.2.5. Statistical Analysis

To test for normality, Shapiro-Wilk tests were performed. To compare the differences between HC and DCM groups, an unpaired t-test was used for normally distributed data and a Mann-Whitney test was used for non-normally distributed data. If standard deviations differed by a factor of two or greater, a Welch's t-test was used. For correlation calculations, Pearson's correlation was used for normally distributed data and Spearman's correlation for non-normally distributed data.

4.3. Results

4.3.1. Participant Characteristics

The mean age (± SD) for the HC (51.16 ± 6.1) and DCM (54.61 ± 7.41) groups were not statistically significant ($p = 0.010$). A detailed breakdown of clinical and demographic information for both groups is further described in Table 3.1.

	HC (n = 19)	DCM (n = 28)	P-value
Age (Years)	51.16 ± 6.08	54.61 ± 7.41	0.010
Sex (F/M)	14/5	15/13	N/A
Motor Threshold (mA)	3.3 ± 1.3	4.5 ± 1.7	0.008
MCL	N/A	C3 = 2 C4 = 6 C5 = 4 C6 = 16	N/A

Table 3.1: Demographic, motor threshold, and level of max compression (MCL) data on the degenerative cervical myelopathy (DCM) and healthy control (HC) groups.

4.3.2. Gray Matter Volume Between HC and DCM Groups

Overall, GM volume was significantly decreased in DCM patients compared to HCs (Figure 3.1A; $p < 0.001$). This significance was retained in the dorsal (Figure 3.1B; $p = 0.001$), intermediate zone (Figure 3.1C; $p < 0.001$), and ventral (Figure 3.1D; $p < 0.001$) regions.

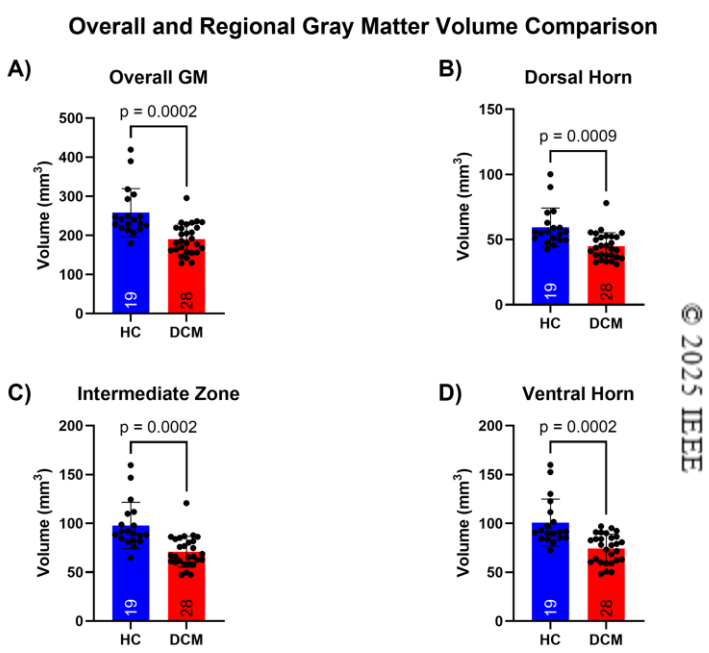

Figure 3.1: Bar graphs depicting significant decreases in the gray matter volume of DCM patients within the overall (A), dorsal horn (B), intermediate zone (C), and ventral horn (D) regions. A Welch's t-test was used to determine these differences.

4.3.3. Regional GM Volume Correlation to WM MTR

Correlation analysis between regional GM volume and WM MTR values revealed significant correlation between the ventral horn and ventral column measures of DCM patients (Figure 3.2D; $r = 0.485$, $p = 0.009$). No other significant correlations between the overall (Figure 3.2A; $r = 0.158$, $p = 0.853$), dorsal (Figure 3.2B; $r = -0.23023$, $p = 0.23424$), and

intermediate/lateral (Figure 3.2C; r = 0.084, p = 0.672) regions existed in the DCM group. No significant correlations arose for the HC group.

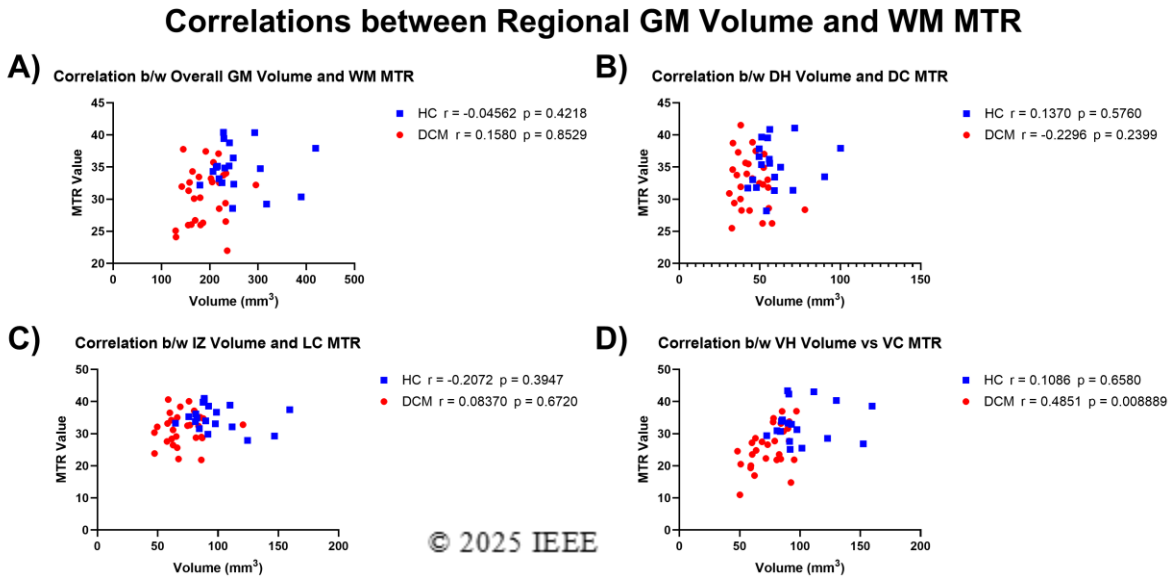

Figure 3.2: Graphs depicting correlations between gray (GM) and white matter (WM) measures in the overall spinal cord (A), the dorsal horn (DH) and dorsal column (DC) (B), the intermediate zone (IZ) and lateral columns (LC) (C), and the ventral horn (VH) and ventral column (VC) (D). GM measures were taken in volume (mm^3) and WM measures were taken in the form of magnetization transfer ratio (MTR). A Pearson's correlation was used for all comparisons.

4.3.4. Stimulation Motor Threshold Between HC and DCM Groups

The mean motor thresholds (± SD) for HC and DCM groups were 3.3 ± 1.3 mA and 4.5 ± 1.7 mA, respectfully (Table 3.1). A t-test performed between the motor threshold values of HC and DCM groups revealed a significant increase in stimulation intensity required to elicit a motor response in DCM patients (Figure 3.3, p = 0.008). For healthy controls, the stimulation ranged from 0.7 to 5.5mA. For DCM patients, the range of motor stimulation was 2.1-8.2mA.

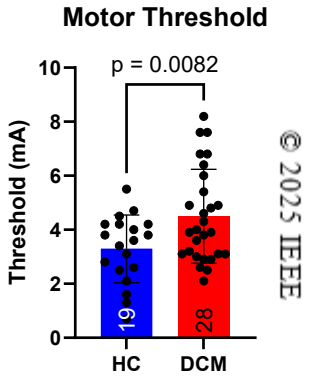

Figure 3.3: A bar graph depicting significant increases in motor threshold (p = 0.0082). A Welch's t-test was used to determine this difference.

4.3.5. Regional GM Volume Correlation with Stimulation Motor Threshold

No significant correlation existed between the GM volume of the overall (Figure 3.4A; HC: r = 0.112, p = 0.649; DCM: r = 0.03, p = 0.881), dorsal (Figure 3.4B; HC: r = 0.106, p = 0.667; DCM: r = -0.085, p = 0.666), intermediate zone (Figure 3.4C; HC: r = 0.091, p = 0.71;

DCM: r = -0.002, p = 0.992), or ventral (Figure 3.4D; HC: r = 0.011, p = 0.963; DCM: r = 0.034, p =0.863) GM regions and motor threshold in either HC or DCM groups.

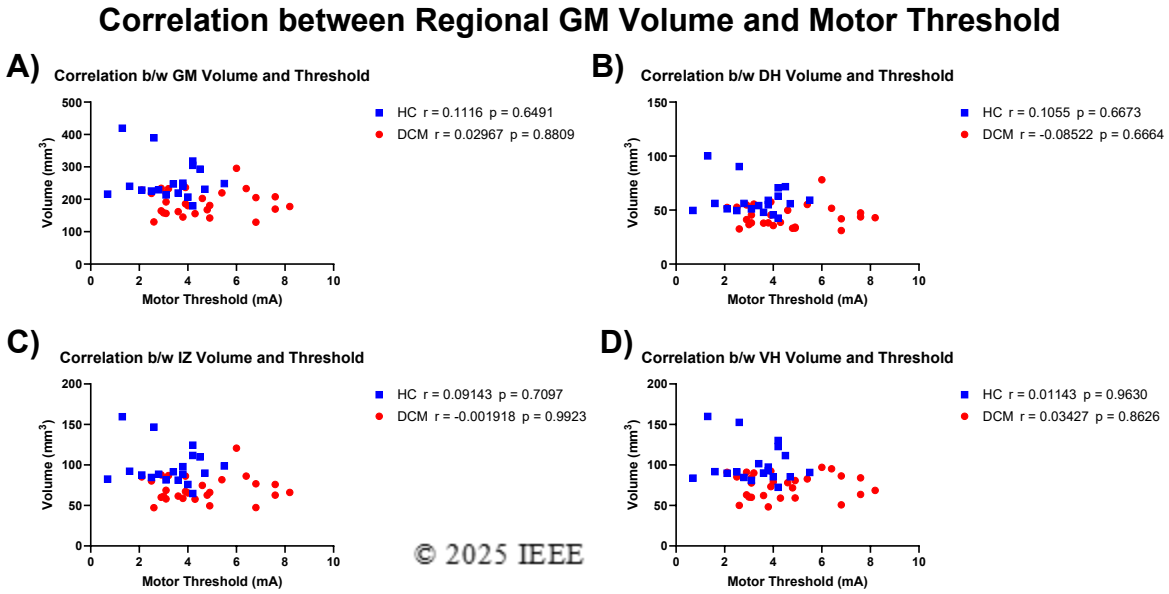

Figure 3.4: Graphs depicting correlations between gray matter (GM) volumes in the overall spinal cord (A), the dorsal horn (DH) (B), the intermediate zone (IZ) (C), and the ventral horn (VH) (D). GM measures were taken in volume (mm^3), and a combination of Pearson's correlation and Spearman's correlation was used for the comparisons.

4.4. Discussion

Degenerative cervical myelopathy (DCM) is a common form of non-traumatic compression within the cervical spine related to age. Previous studies have described decreases in GM volume (Smith et al., 2020) and WM MTR (Cloney et al., 2018; Haynes et al., 2024), however, it is unknown whether the loss of GM volume impacts motor threshold in DCM patients. Therefore, the aim of the present study is to assess whether GM volume loss relates to changes in involuntary motor threshold and to establish a link between structural and functional measures that may provide a more objective biomarker for motor pathway impairment in DCM.

Our results show that DCM patients have decreased GM volume as compared to their HC counterparts, at the overall and all regional (i.e. dorsal, ventral, and intermediate) levels (Figure

3.1), which aligns with previous studies of GM volume loss in DCM patients (Smith et al., 2020) and provides possible evidence that the GM area is more easily impacted by degenerative compression than WM regions because of its smaller volume within the cord. However, despite compression exhibited in all GM regions, GM volume decreases in the ventral horn remain the most significant (Figure 3.1D) and have the only positive correlation with the corresponding ventral column MTR, i.e., indirect WM measurements (Figure 3.2D), which are absent in other regions and HCs. These findings indicate that the changes in ventral GM and WM could be caused by the same underlying source, likely compression, impacting the same region. Moreover, both of these results align with patterned DCM damage previously shown to occur first in the ventral column WM (Cloney et al., 2018; Haynes et al., 2024). The loss of GM and WM in the ventral region, which is responsible for the delivery of motor signals to peripheral nerves and muscles, could also potentially explain motor deficits found in DCM patients (Muhammad et al., 2023). Structural imaging has revealed that decreases in ventral horn GM and tract-based ventral column MTR have been associated with decreases in clinical measures of motor movement (Haynes et al., 2024; Smith et al., 2020), indicating the possible presence of motor pathway damage.

Electrically inducing a spinal cord reflex could potentially complement other clinical and imaging diagnostic tools, which lack ways to objectively measure functional components. However, despite a higher motor threshold in DCM patients (Figure 3.3), GM volume did not display any correlation to motor threshold (Figure 3.4). The absence of a direct relationship between GM volume and motor threshold suggests that additional mechanisms may be contributing to motor pathway dysfunction in DCM. For example, changes in brain structure have been shown to occur within DCM patients (Freund et al., 2024; Muhammad, Weber,

Rohan, et al., 2024; Rafati Fard et al., 2024), but should not be impacting the motor threshold because they do not contribute to the motor response elicited during the spinal cord reflex. Additionally, previous studies have even concluded that overall resting motor threshold, elicited by TMS in the brain, did not differ between HC and DCM groups (Zdunczyk et al., 2018). Other explanations may also include supraspinal changes, as previously reported in DCM (Lebret et al., 2023; Muhammad, Weber, Bedard, et al., 2024; Vallotton et al., 2021), or peripheral nerve impairment resulting from comorbid conditions like cervical radiculopathy, which is estimated to be present in 50-75% of DCM patients (Choi et al., 2017; Wepking et al., 2013). However, further investigations into these potential sources of impairment would be needed to determine the precise origin of the required DCM motor threshold increase. For example, incorporating the recording of peripheral muscle activity, via EMG, in the muscles responsible for a decline in motor performances, like slower gait speed (Haddas, Cox, et al., 2019; Malone et al., 2013), in DCM patients could prove to be useful in interrogating the unknown mechanism.

This study does face several limitations, including those related to the stimulation paradigm. For example, we defined motor threshold with a visual twitching of the thumb/forefinger, which overlooks the smaller muscle contractions happening at lower amplitudes. Monitoring peripheral nerve stimulation with electromyography (EMG) could help to ensure the validity of the set motor threshold in the future. Furthermore, while participants with comorbidities, like cervical radiculopathy, should ideally be excluded, its prevalence in DCM in combination with limited diagnostic accuracy to distinguish between the two may make their complete exclusion unfeasible.

In addition to the previously mentioned study protocol improvements, there are several avenues that future research could take. For example, an investigation into the relationship

between the metrics described in this paper (i.e., motor threshold and GM volume) to disease severity metrics like mJOA and Nurick Grade. This could help lead to the establishment of new structural and functional DCM biomarkers by providing insight into whether motor threshold and GM volume are reflected in clinical measures and DCM progression. This can further be bolstered by a longitudinal study that follows patients not receiving surgical treatment, which can help establish how the structural and functional integrity of DCM spinal cords develop over time.

Chapter 5: Applying Task-Based Spinal fMRI to Reveal Functional Alterations in DCM

* The following chapter is based on the article (Haynes, Muhammad, Weber, Khan, Hameed, Shakir, et al., 2025) and has been reused with permission of the authors. It is currently under review at *Imaging Neuroscience*.

In the previous two chapters, it has been established that DCM significantly impacts both the white and gray matter (Haynes, Muhammad, Weber, Khan, Hameed, Ding, et al., 2025; Haynes et al., 2024). However, the applied imaging techniques (i.e., MTR and T2*), while insightful, are only capable of assessing structural damage. These structural changes have been the primary focus of DCM research, with little to no attention to the functional alterations to the spinal cord pathways. The following chapter applies an involuntary motor threshold stimulation as a task-based fMRI paradigm to establish what functional alterations – if any – occur in spinal cords impacted by DCM compression.

5.1. Introduction

One technique that could provide a way of evaluating the injury to the spinal cord and its resulting impact on functionality is functional MRI (fMRI), which can employ sensory (e.g. tactile or thermal stimulation) (Weber et al., 2020; Weber et al., 2018) and motor (e.g. fist clenching or finger abductions) (Kinany, Pirondini, et al., 2023; Landelle et al., 2021) tasks to interrogate the functional pathways. These paradigms have been primarily used in subjects with healthy spinal cords, but they do also serve as an important foundation for applying task-based fMRI methods in cervical spinal diseases to study alterations in functional pathways (Haynes et al., 2023). However, only resting-state fMRI has been applied to study DCM-induced injury,

demonstrating that the Amplitude of Low Frequency Fluctuation (ALFF) in the cervical cord is associated with myelopathy severity (Liu et al., 2016). Clinical impairments associated with DCM manifestation (Hameed et al., 2024; Muhammad et al., 2023) means that the performance of task-based paradigms normally applied in healthy spinal cords can be negatively impacted.

Therefore, in this study, we apply direct electrical stimulation to the median nerve as a task-based fMRI paradigm to avoid the challenges that arise with subject-driven motor tasks and evaluate the functional pathways in the cervical spine of DCM patients by activating spinal cord reflexes. To date, median nerve stimulation has not been applied in DCM fMRI studies, but has been used in several fMRI papers involving healthy controls (Backes et al., 2001a; Wilmink et al., 2003; Xie et al., 2007) where it was found to induce activation in the lower cervical spine (Backes et al., 2001a; Wilmink et al., 2003; Xie et al., 2007) comparable to fist clenching (Backes et al., 2001a; Wilmink et al., 2003). Direct stimulation is also a common electrodiagnostic tool used to study and diagnose functional changes in DCM patients (Dvorak et al., 2003) and median nerve stimulation specifically has been established to induce activation in areas commonly impacted by DCM compression (e.g., lower cervical spine) (Muhammad, Weber, Bedard, et al., 2024; Vallotton et al., 2021). Because this chronic compression can lead to progressive injury of the motor and sensory GM horns, we seek to demonstrate that median nerve stimulation can reveal functional impairment of sensorimotor pathways in DCM. Specifically, we focus on segmental recruitment in the lower cervical cord, recruitment differences between sub-motor and motor activation, and the spatial distribution of responses across GM, WM, and lateralized pathways.

5.2. Methods

5.2.1. Participants

DCM patients (n = 23, 17 females) were recruited from OU Health Adult Neurosurgery Clinic in Oklahoma City. All patients were evaluated independently by spine neurosurgeons (ZAS, HJS). Healthy control participants in this study (n = 23, 15 females) were simultaneously recruited from the Laureate Institute for Brain Research (LIBR) in Tulsa, OK and the University of Oklahoma Health Sciences Center (OUHSC). The HC (49.7 ± 2.23 years) and DCM (54.4 ± 2.03 years) groups were age-matched and had no significant age difference ($p = 0.12$). All participants were right-handed. All participants were scanned between March 2021 and May 2024 and signed an informed consent document before data collection began. Details about this cohort, including inclusion and exclusion criteria, can be found in Muhammad, *et al.* (2025) (Muhammad, Weber, Bédard, et al., 2025). All imaging experiments performed in this study were approved by the University of OUHSC and LIBR institutional review boards (IRB #12068) and performed according to IRB regulation guidelines.

5.2.2. MRI Data Acquisition

Structural and functional cervical spine MRI data were collected with a Signa 3T MR750 scanner (GE Healthcare, Milwaukee, WI) equipped with a 32-channel NovaCSpine coil at LIBR. Participants laid supine in the scanner with no visual stimulation and were instructed to remain still while undergoing scanning. Isotropic T2-weighted sagittal and axial CUBE images (TR = 2500ms; TE = 120ms; FOV = 256 x 256mm; Thickness = 0.8mm; Resolution = 0.8 x 0.8mm) and a multi-echo gradient-echo T2*-weighted (TR = 600ms; FOV = 224 x 224mm; Thickness = 5mm; Resolution = 0.5 x 0.5mm) scan were collected according to the generic spine protocol (Cohen-Adad et al., 2021). Functional MRI (fMRI) scans were acquired with single-shot echo-

planar imaging (SS-EPI) (TR = 2000ms; TE = 29.5ms; Flip Angle = 90 degrees; FOV = 128 x 128mm; Thickness = 5mm; Resolution = 1 x 1mm) covering the C3-T2 vertebral levels and the field of view was centered at C5.

5.2.3. fMRI Task Design: Stimulation Paradigm and MRI Setup Conditions

Ag/AgCl electrodes were placed on the center, inner wrist (cathode), and above the inner elbow (anode) of the subject's right upper limb (Figure 4.1B). This placement of electrodes was based on the anatomy of the median nerve, which runs beneath the bicipital aponeurosis at the elbow and the carpal tunnel at the wrist (Mazurek & Shin, 2001). Due to individual neurological differences, stimulation thresholds could not be generalized for all subjects and were, therefore, determined individually. To do this, single monophasic electrical pulses were delivered in increments of 0.5 mA until a consistent involuntary twitching in the thumb or forefinger was

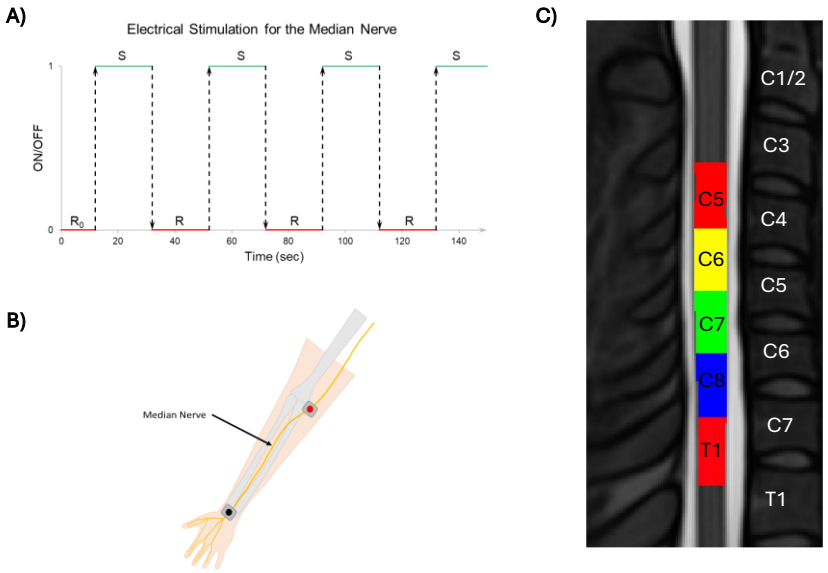

Figure 4.1: Overview of the spinal cord task-based fMRI stimulation paradigm and segmental localization. (A) Stimulation block design showing the timing of electrical median nerve stimulation. The paradigm begins with a 12-second initial rest period (R_0), followed by alternating 20-second stimulation (S) and rest (R) defined time period across four cycles. (B) Schematic showing the surface localizations of median nerve in the forearm, illustrating the placement of surface electrodes. (C) Anatomical segmentation and masks of the cervical (C5-C8) and upper thoracic (T1) spinal segments using the PAM50 template. Colored masks correspond to spinal cord segments from C5 to T1, used for segmental voxel extraction.

observed. The amplitude of the pulse was then decreased by 0.1mA until the strength of the stimulation was only capable of inducing a minimally observable finger twitching (motor threshold). The sub-motor threshold was set at 15% below motor threshold.

These thresholds were then applied in 2ms pulses at 1 Hz for twenty seconds during the course of an 8 minutes, 12 seconds fMRI run, where they alternated with twenty second rest periods until the end of the scan (Figure 4.1A). Each subject underwent two fMRI runs, which used the sub-motor and the motor threshold stimuli respectively. To deliver consistent stimulation pulses during functional MRI scans, a series of trigger pulses was generated with a timed code synchronized with the beginning of the scan. Digital signals from a laptop were delivered to the input port of a high-voltage, constant current stimulator (Digitimer DS7A),

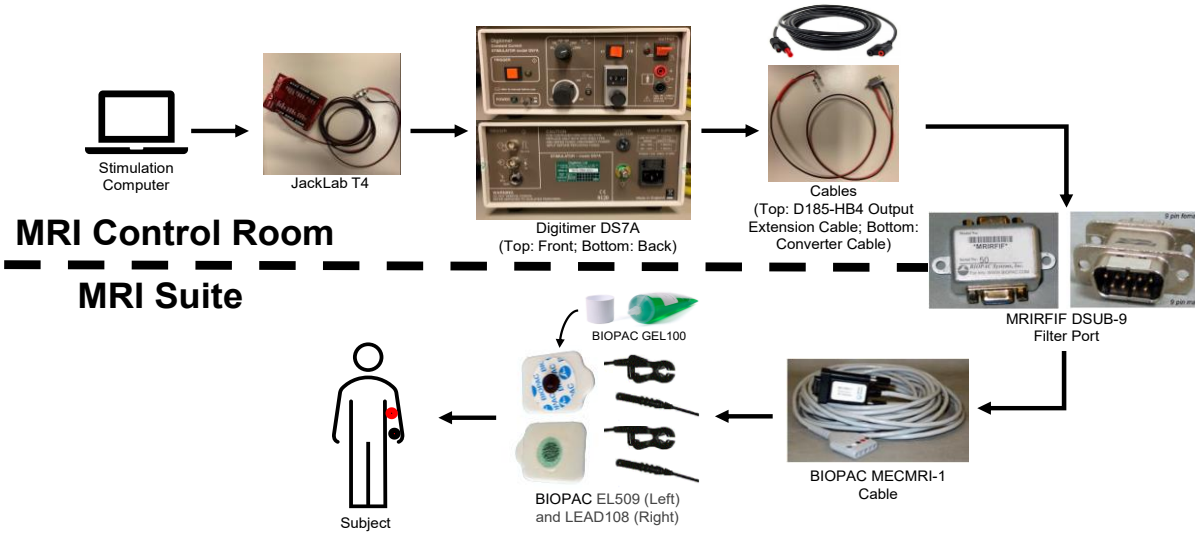

Figure 4.2: MRI-compatible electrical stimulation setup for median nerve stimulation. The stimulation protocol begins in the MRI control room, where the stimulation computer delivers the stimulation commands through JackLab T4 device. This device interfaces with a Digitimer (DS7A constant current stimulator (top: front view, bottom: rear view with connections). Stimulation pulses are routed through a series of output and converter cables that passed through an MRIRFIF DSUB-9 filter port into the MRI suite. Inside the MRI suite, filtered signals are transmitted via a BIOPAC MECMRI-1 cable to surface electrodes (BIOPAC EL509 and LEAD108) placed over the median nerve on the subject's forearm. Conductive gel (BIOPAC GEL100) is applied to ensure correct contact and signal delivery during scanning.

which outputted to a filtered 9-pinned series port (BIOPAC MRIRFIF DSUB-9) connected to an

MRI compatible electrode cable (BIOPAC MECMRI-1) inside of the MRI suite. Anode and cathode leads then delivered the pulse to the electrodes located on the subject's dominant (i.e., right) arm. Figure 4.2 demonstrates how the equipment was set up in an MRI environment.

5.2.4. MRI Processing

Spinal Cord Toolbox (SCT) (v.7) (De Leener et al., 2017) was used for structural image preprocessing for individual subjects. Spinal cord segmentation was performed using the *sct_deepseg_sc* function (Gros et al., 2019) and registered to the PAM50 template using *sct_register_to_template* (Ullmann et al., 2014) (Figure 4.1C). The structural spinal cord was registered to the PAM50 template using *sct_register_to_template* (De Leener et al., 2018). Lastly, the PAM50 templates were warped to the native space using *sct_warp_template*. Spinal cord segmentation was also created for the T2* images using *sct_deepseg_sc* (Gros et al., 2019). Gray matter (GM) segmentation was also extracted from the T2* images using *sct_deepseg_gm*, which was used in combination with the cord mask to create a white matter (WM) mask. The T2* image and white matter segmentation were then registered to the PAM50 template and warped to the native space using *sct_register_multimodal* and *sct_warp_template*. Further details about how anatomical images with compressed spinal cords were preprocessed can be found in Muhammad et al. (2025) (Muhammad, Weber, Bédard, et al., 2025).

5.2.5. Functional Pre-Processing

The fMRI data were preprocessed using a combination of SCT (v.7) (De Leener et al., 2017) and FMRIB Software Library (FSL) (Jenkinson et al., 2012). The preprocessing steps follow similar descriptions in previous studies using similar methodologies (Banerjee et al., 2025; Oliva et al., 2025; Weber et al., 2016a, 2016b). These preprocessing steps include:

5.2.5.1. Motion Correction

Motion correction was performed in two stages using a custom 2D slice-wise registration pipeline optimized for spinal cord fMRI (Weber et al., 2020; Weber et al., 2016a, 2016b). First, a temporal mean image was generated from the raw BOLD time series using *sct_maths,* and the spinal cord was segmented using *sct_deepseg_sc.* A mask of the spinal canal was also created using *sct_propseg -CSF* (De Leener et al., 2015; Oliva et al., 2025), and the two masks were combined and dilated (disk shape, 5 voxels, 2D) to define a robust registration mask.

In the first motion correction step, each volume was registered slice-by-slice to the middle volume of the functional time series to limit motion correction to the region within the registration mask. In the second step, the temporally averaged motion-corrected image from the first pass was used as the new reference volume, and all volumes were realigned to it using the updated registration mask. This two-pass approach improves motion correction by refining alignment across both time and anatomical structure, accounting for non-rigid, slice-specific motion frequently observed in spinal cord data (Weber et al., 2016a, 2016b).

5.2.5.2. Segmentation and Registration to the Template Space

Following motion correction, spinal cord segmentation was performed on the motion-corrected mean functional image. A subject-specific spinal cord mask was obtained by applying SCT's EPI-trained deep learning segmentation tool (*sct_deepseg sc_epi*), which is optimized for EPI images (Banerjee et al., 2025). The spinal canal was then segmented using *sct_propseg -CSF* (De Leener et al., 2015), and this mask was dilated in-plane (disk, 3 voxels) to define the CSF region surrounding the cord.

For spatial normalization, functional data were registered to the PAM50 T2* spinal cord template using *sct_register_multimodal.* The registration steps included (1) slicewise

segmentation-based alignment to the center of mass (i.e. *centermass*), (2) non-linear symmetric normalization alignment using b-splines (i.e. *bsplinesyn*), and (3) intensity-based refinement using non-linear symmetric normalization (i.e *syn*) with cross-correlation. Subject-specific warps derived from high-resolution T2* structural scans were used to initialize the registration. Finally, *sct_warp_template* was used to warp PAM50 template labels into functional space, enabling spinal level localization and group-level comparisons.

5.2.5.3. Physiological Noise Modeling

Physiological denoising was performed using the RETROICOR-based approach, which modeled and removed cardiac and respiratory artifacts from the fMRI data using the phase regressors derived from the physiological recordings (Glover et al., 2000). We also extracted the time courses from WM and CSF masks. The PAM50 T2* template was registered to each subject's motion-corrected mean functional image using the *sct_register_multimodal* and *sct_warp_template*. The PAM50 WM mask and the segmented CSF canal (*sct_propseg -CSF* (De Leener et al., 2015)) were warped and binarized to extract mean time series from each axial slice. These were concatenated into regressors. These physiological regressors were entered into the denoising model implemented using the FSL's FMRI Expert Analysis Tool (FEAT) (Weber et al., 2016a, 2016b).

5.2.5.4. Slice-timing Correction and Smoothing

Denoised data were corrected for slice-timing offsets using FSL's *slicetimer* tool, and the resulting volumes were warped to PAM50 template space using *sct_apply_tranfo* and previously estimated warp fields. Voxels falling outside of the automated spinal cord segmentation mask space were then removed using a spinal cord mask warped to template space. The images were then smoothed using FSL's *susan* with a 2mm Full Width at Half Maximum (FWHM) Gaussian

kernel (Smith & Brady, 1997). A representative example of signal stability in the spinal cord (via temporal signal to noise ratio) can be seen in Supplemental Figure B.1.

5.2.6. Statistical Analysis

5.2.6.1. First-Level Analysis

Subject-level analysis was performed in FSL's FEAT (Woolrich et al., 2001) using a General Linear model (GLM) framework based on a square-shaped ON/OFF stimulation paradigm (Figure 4.1A) convolved with a gamma hemodynamic response function. A high-pass filter (cut-off: 0.01Hz) was then applied to remove low-frequency noise. DVARS-derived motion outliers (i.e. volumes where the difference between root-mean-squared values is greater than the 100^{th} percentile) were used as covariates of no interest. Temporal autocorrelation was modeled and corrected using FMRIB's Improved Linear Model (FILM) (Woolrich et al., 2001). Voxel-wise activation was assessed using z-statistics and a threshold of $z > 2.3$ (uncorrected p-value of < 0.05) was applied to define activation.

5.2.6.2. Group Level Analysis

Group-level statistical analysis was performed using the Higher-Level Analysis functionality of FSL's FEAT tool (Woolrich et al., 2004). Analyses were performed for each contrast using GLMs implemented in FSL, with variance modeled at the group level. Three statistical tests were applied to compare group level activation results. The first tests were one-sample t-tests to detect whether BOLD signal changes were significantly different from zero within each group (HC and DCM) and condition (sub-motor and motor threshold stimulations). These tests identify voxels that exhibited positive (BOLD z-statistic > 0) or negative (BOLD z-statistic < 0) activation. The second tests were paired two-sample t-tests applied within each group (HC and DCM) to compare motor threshold vs sub-motor stimulation, identifying

condition-driven differences in BOLD activation (i.e., motor threshold > sub-motor and sub-motor > motor threshold). The final approach applied was unpaired two-sample t-tests to compare activation between HCs and DCM groups during both stimulation conditions (i.e. HC > DCM and DCM < HC), assessing for disease-related differences. All GLMs were set up according to FSL's recommended guidelines for group analysis and details can be found on the FSL – FMRIB Software Library website. All analyses were performed independently per contrast.

Each model produced a z-statistics maps, which were thresholded using a fixed-effect, voxel-wise threshold of $z > 1.64$ with a cluster-wise correction of $z > 1.64$ (p-value < 0.05) to identify significantly active voxels. These maps were overlaid on the PAM50 T2w spinal cord template (De Leener et al., 2017) to visualize activation across the cervical spinal cord (Figure 4.3). Segmental activation distributions were quantified using SCT's PAM50 spinal segment masks (PAM50_spinal_levels.nii.gz) specifically from the C5 to C8 spinal cord segments (Figure 4.1C, Figures 4.3, 4.4, and 4.6). To further characterize the spatial distribution of spinal cord activity, two voxel-based ratios were computed. The first was the Gray/White Matter Ratio (GW Ratio), which quantified the relative distribution of significant voxels across GM and WM by dividing the percentage of active GM voxels by those in WM (Weber et al., 2020). The second was the Left/Right Index (LR Index), which measured lateralization by computing the normalized difference between active voxels in the left and right hemicords, and dividing the difference by the sum (Weber et al., 2020; Weber et al., 2016b).

5.3. Results

5.3.1. Spinal Cord fMRI Responses to Sub-motor and Motor Threshold Median Nerve Stimulation

To identify regions with statistically significant BOLD activation (BOLD z-statistic > 0) and deactivation (BOLD z-statistic < 0), we performed a one-sample t-test at the group level for HCs and DCM groups. Significant BOLD responses were observed in both HC and DCM during sub-motor and motor threshold stimulations (Figure 4.3A and Supplemental Figure B.2). In the HC group, motor threshold stimulation elicited greater activation across the C5-C8 segments (1155 voxels) compared to sub-motor stimulation (496 voxels), while deactivation remained

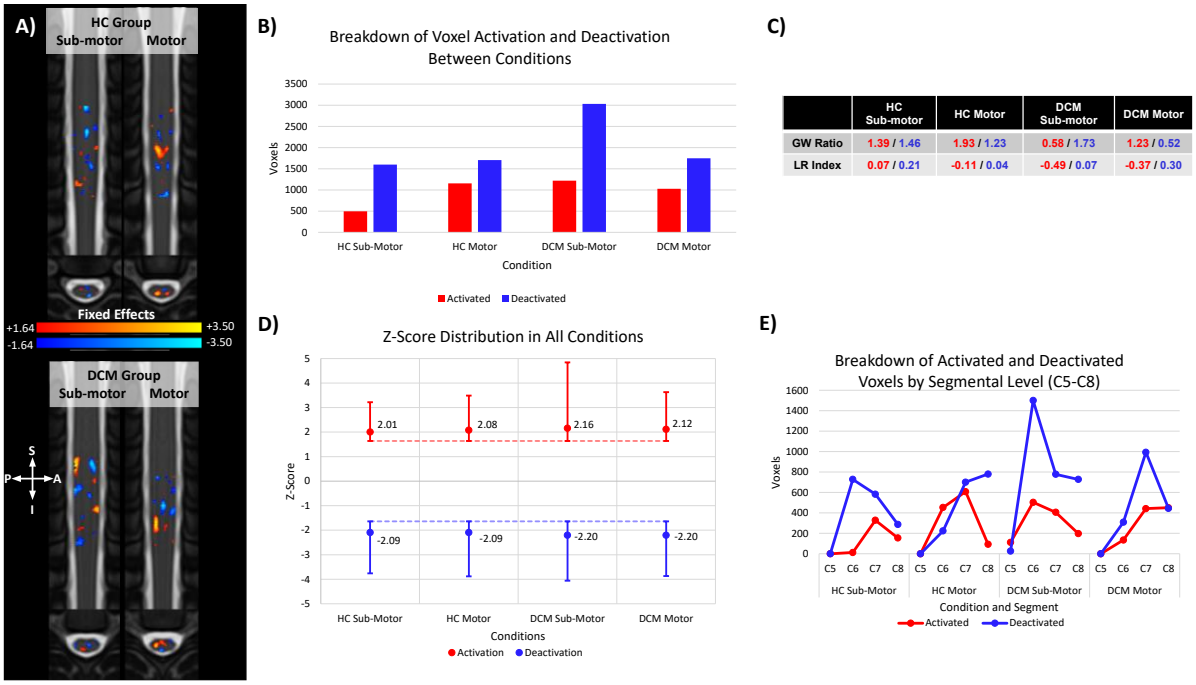

Figure 4.3: Spinal cord task-based fMRI BOLD response in healthy controls and patients with DCM. (A) Fixed-effects activation maps for sub-motor and motor conditions in healthy controls (HC, top row) and DCM (bottom row). Activations (red-yellow) and deactivations (blue-light blue) are displayed on axial and sagittal spinal cord T2w (PAM50) templates spanning cervical segments C5–C8. Cluster thresholds are set at ±1.64 to ±3.50. (B) Group-level Voxel count summary showing the number of significantly activated (red) and deactivated (blue) voxels for each condition and group. (C) Summary table showing the gray matter (GM) to white matter (WM) activation ratios (GW Ratio) and left-right laterality indices (LR Index) across conditions. (D) Average Z-score distributions for activated (red) and deactivated (blue) voxels across all conditions, with standard error bars. (E) Segmental-level analysis (C5–C8) of voxel-wise activation and deactivation, indicating condition-specific and segmental variations in BOLD signal in DCM and HC.

relatively consistent across both conditions (1598 vs 1705 voxels, Figure 4.3B). In contrast, DCM patients showed a robust decline in deactivation between sub-motor and motor threshold conditions (3032 vs 1747 voxels), while activation remained relatively stable (1220 vs 1028 voxels, Figure 4.3B).

Spatial distribution in the HC group was predominantly localized to the GM in both sub-motor and motor threshold conditions (GW Ratio: sub-motor = 1.39; motor = 1.93) (Figure 4.3C). However, the DCM group showed a reverse in GM localization during the sub-motor condition (0.57), but aligned more with HCs during motor threshold stimulation (1.23) (Figure 4.3C). Furthermore, lateralization patterns (LR index) in HCs were relatively balanced (sub-motor: 0.07; motor threshold: -0.11), whereas the DCM group showed right-sided lateralization (sub-motor: -0.49; motor threshold: -0.37) (Figure 4.3C). Across the two conditions, the mean z-scores for activation was similar between groups (HCs: sub-motor = 2.01, motor threshold = 2.08; DCM: sub-motor = 2.16, motor threshold = 2.12) (Figure 4.3D). The z-scores for deactivation were also comparable (HC: sub-motor = -2.09, motor threshold = -2.09; DCM: sub-motor = -2.20, motor threshold = -2.20) across both conditions (Figure 4.3D).

The segmental level (C5-C8) activation revealed condition-specific differences. In the HC group, motor threshold stimulation elicited caudally increasing activation from C6 (453 voxels) to C7 (608 voxels) (Figure 4.3E). Sub-motor responses were reduced across all segments (C6: 13 voxels, C7: 328 voxels, C8: 155 voxels) compared to their motor threshold counterparts, with the exception of C8 (Figure 4.3E). In DCM patients, activation decreased caudally from C6 (504 voxels), C7 (406 voxels), and C8 (198 voxels) segments during sub-motor stimulation and increased slightly during motor threshold stimulation (C6: 135 voxels, C7: 442 voxels, C8: 451 voxels) (Figure 4.3E). Notably, the motor threshold activation in the DCM group was lower than

in the HC group across most spinal segments, particularly at C6 and C7. Deactivation in HCs had a caudal decrease during sub-motor stimulation across C6 (728 voxels), C7 (583 voxels), and C8 (287 voxels), but increased across the same segmental levels (C6: 224 voxels, C7: 701 voxels, C8: 780 voxels) during motor threshold stimulation (Figure 4.3E). Deactivation in DCM was elevated in C6 (1500 voxels), C7 (778 voxels), and C8 (728 voxels) segments during sub-motor stimulation. During motor threshold stimulation, deactivation responses decreased, with the exception of C7, (C6: 309 voxels, C7: 993 voxels, C8: 445 voxels), but still remained higher than in HC, with the exception of C8 (Figure 4.3E). Additionally, during sub-motor stimulation, the DCM group showed both activation (112 voxels) and deactivation (26 voxels) at C5, which was not observed in the HC group (Figures 4.3E).

5.3.2. Group Level Changes Between Sub-motor and Motor Threshold Stimulation

To determine the changes in spinal cord activation across stimulation intensities, we performed a paired, two-sample t-test comparing motor threshold and sub-motor stimulations in each group. Significant activation differences were detected in all comparisons (motor threshold > sub-motor and sub-motor > motor threshold; Figure 4.4). In the HC group, motor threshold stimulation evoked a greater increase in activation compared to sub-motor stimulation, activation with a 4.09% difference in active voxels during motor threshold vs 2.12% during sub-motor (i.e. difference in active voxels divided by number of total voxels in the C5-C8 mask) (Figure 4.4B).

Different patterns of segmental responses were observed between HC and DCM due to changes in the stimulation intensities. In the HC group, the comparison of motor threshold > sub-motor revealed the largest increase in activation at C6, followed by a decrease caudally (C6: 9.41%; C7: 5.35%; C8: 1.22%). In contrast, the sub-motor > motor threshold comparison showed a caudal increase in activation with more voxels at lower segments (C6: 1.15%; C7:

3.44%; C8: 4.53%), suggesting that the sub-motor threshold preferentially recruited lower spinal segments in HCs (Figure 4.4C). The DCM group exhibited a different response pattern. The sub-motor > motor threshold comparison revealed larger increases in activation overall than the motor threshold > sub-motor comparison. Specifically, the sub-motor > motor threshold comparison showed increasing activation from C6 (5.39%) to a peak at C7 (8.89%), then C8 (6.86%). In contrast, the motor threshold > sub-motor response was weaker across all segments

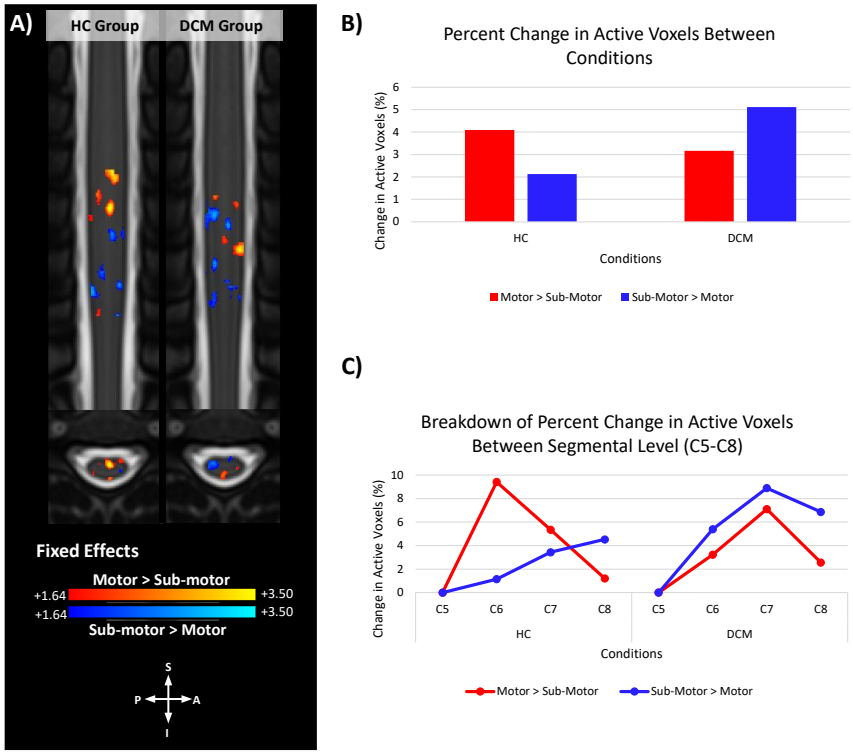

Figure 4.4: Motor and sub-motor threshold contrasts-driven BOLD responses in HC and DCM. (A) Fixed effects activation maps of threshold response showing where motor > sub-motor (red-yellow) and sub-motor > motor (blue-light blue) responses in HC (left) and in DCM (right). Activations maps are overlaid on T2 w axial and sagittal (PAM50) template. Separate comparison maps are shown for HC and DCM groups. (B) Percent change in the number of active voxels between motor and sub-motor conditions within each group (C) Segmental-level (C5–C8) distribution of active voxels in motor > sub-motor (red) or sub-motor > motor (blue) contrasts.

(C6: 3.23%; C7: 7.11%; C8: 2.57%) (Figure 4.4C). This divergent pattern indicates that an increase in stimulation intensity does not enhance spinal cord activation in DCM patients and that responses to motor threshold and sub-motor stimulations may be less distinct than in HC.

5.3.3. Voxel Activation at Subject Level

To further examine individual responses and variability within each group, we analyzed subject-level changes in the number of active voxels between sub-motor and motor threshold conditions (Figure 4.5A). More HCs had a modest increase in active voxels from sub-motor to motor threshold stimulation (13/23 in the HC group compared to 5/23 in the DCM group) (Figure 4.5A). Furthermore, patients in the DCM group showed a less consistent response with the majority showing reduced activation during motor threshold stimulation (18/23). On average, the DCM group exhibited a decrease of 212 voxels when transitioning from sub-motor to motor

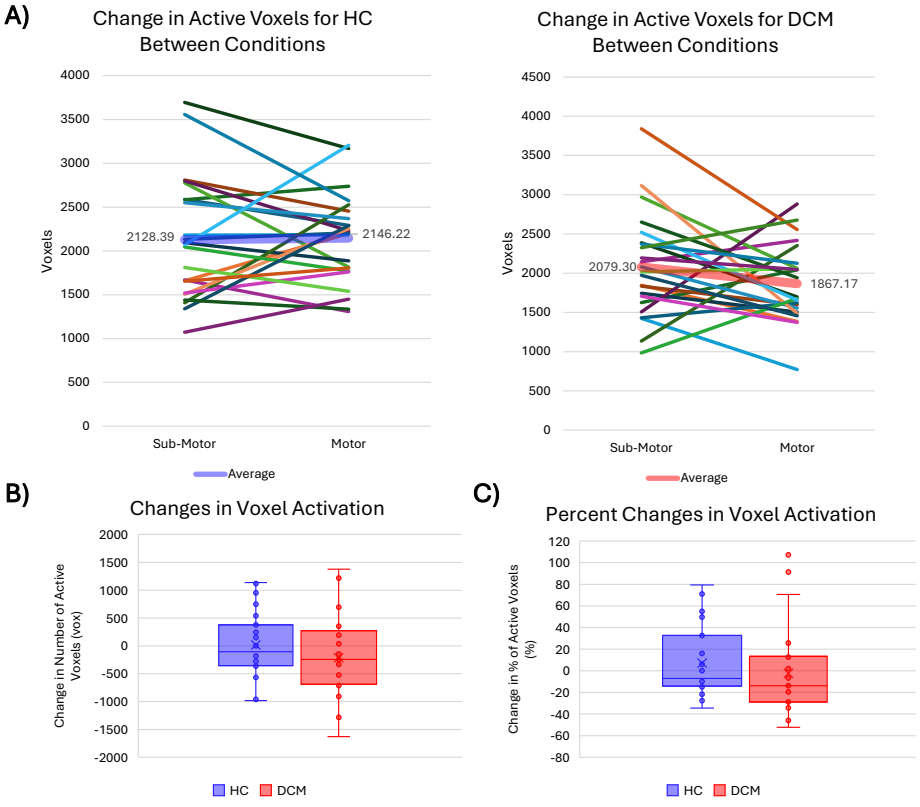

Figure 4.5: Subject-level changes in spinal cord activation between motor and sub-motor conditions in HC and DCM. (A) Line plots showing individual changes in active voxel counts between sub-motor and motor conditions for each subject, in HC (left) and DCM (right) groups. Mean voxel change between the conditions are overlaid in color (HC: blue and DCM: red). (B) Boxplot of the absolute differences in voxel activation per subject between conditions (motor minus sub-motor) for each group (C) Boxplot of percent difference in active voxels between conditions per subject. Box plot, *HC: blue, DCM: red.*

threshold stimulation, while the HC group exhibited a modest positive shift in mean voxel counts (17.83 voxels ± 588.3) (Figure 4.5B). The DCM group also showed a greater inter-subject variability and a negative shift (-212.1 voxels ± 725.5) (Figure 4.5B). When the percent changes were calculated, HCs again showed a small increase in activation (7.06% ± 31.9), whereas DCM patients exhibited an overall decrease (-2.23% ± 41.8) (Figure 4.5C). However, these differences at the subject level were not statistically significant.

5.3.4. Group Level BOLD Changes Between HC and DCM

While the earlier analyses characterized responses within each group, here we directly compared HC and DCM activation patterns using unpaired, two-sample t-tests between (HC > DCM; DCM > HC) for both sub-motor and motor threshold stimulation conditions. This analysis allowed us to quantify and spatially map group-level differences (Figure 4.6A)**.** Overall, HCs showed greater differences in the amounts of active voxels during sub-motor and motor threshold stimulations over DCM between groups (3.84% and 4.04% respectively, with the difference in active voxels being divided by the number of total voxels in the C5-C8 mask) (Figure 4.6B).

Segmental level comparisons (Figure 4.1C) provided additional insight into these group differences. In HCs, motor threshold stimulation exhibited the greatest increase in activation than DCM at C7 (8.88%) (Figure 4.6C). In contrast, the DCM-HC motor threshold stimulation showed a progressive caudal increase (C6: 0.47%; C7: 4.3%; C8: 8.43%), peaking at C8, and suggesting a shift in segmental response between the two groups. Furthermore, the HC-DCM difference peaked at C8 (7.61%) during sub-motor stimulation, whereas the DCM-HC pattern shifted rostrally peaking at C6 (6.48%) (Figure 4.6C). These suggest that DCM patients exhibited enhanced sub-motor responses at slightly more rostral segments compared to motor

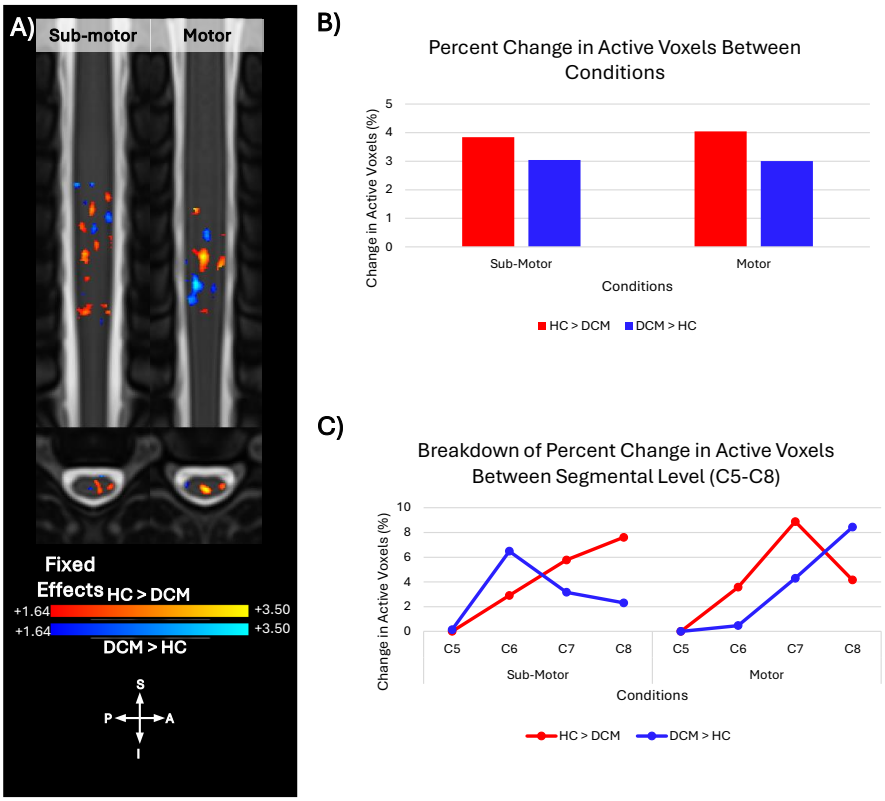

Figure 4.6: Group level differences comparing HC and DCM across the sub-motor and motor conditions. (A) Fixed-effects contrast maps showing voxel-wise differences between HC and DCM groups during sub-motor and motor tasks. Red-yellow indicates HC > DCM, while blue-light blue indicates DCM > HC. BOLD activation maps overlaid on axial and sagittal T2w PAM50 templates. (B) Percent change in the number of significantly active voxels by group and condition derived from unpaired two sample t test. Red bars is activation in HC > DCM, while blue bars reflect DCM > HC. (C) Segmental-level breakdown of differential activation (C5–C8), showing voxel-wise segmental group difference.

threshold stimulation, which adds to the evidence indicating alterations in the localization of spinal cord activation in DCM.

5.4. Discussion

Degenerative cervical myelopathy can cause progressive damage to both the WM and GM pathways of the spinal cord (Cloney et al., 2018; Haynes et al., 2024; Hopkins et al., 2018; Smith et al., 2020). Although WM and structural injury have been well studied (Bedard et al., 2025a; Cloney et al., 2018; Filimonova, Abdaev, et al., 2024b; Haynes et al., 2024; Muhammad, Weber, Bedard, et al., 2024; Paliwal et al., 2020), less is known about the functional consequences of GM injury, despite its role in sensory input and motor output. Defining these changes is clinically important because a greater injury burden predicts poorer surgical outcomes (Kopjar et al., 2018; L. A. Tetreault et al., 2015). In this study, we apply a task-based fMRI paradigm using peripheral median nerve stimulation, a method that helps to avoid reliance on voluntary motor performance to provide a more consistent measure of spinal cord functional activity.

In healthy controls, our group level analysis of spinal cord activation shows an expected increase between sub-motor and motor threshold conditions. This enhanced activation response to an increase in stimulation is expected, as the motor threshold is aimed at recruiting the neurons that were not activated during sub-motor threshold (i.e. motor neurons). Furthermore, the strongest recruitment was seen at C6 and C7, which aligns with the spinal nerve root origins of the median nerve and electrophysiological studies showing that stimulation results in a higher current amplitude in the vertebral levels aligning with the C7/C8 segments (Akaza et al., 2021). However, DCM patients showed a paradoxical decrease in BOLD activated voxels when the stimulation intensity increased and abnormal recruitment at C6 and C8 during sub-motor

stimulation. This expansion of activation suggests impairments in localized neuronal recruitment and the presence of compensatory reorganization in DCM. Sub-motor stimulation responses were also exaggerated relative to motor threshold, pointing to abnormal excitability or impaired inhibition of compressed pathways. This excessive sub-motor response was specifically pronounced in the C6 segment, increasing by comparison to its HC counterpart, which aligns with the vertebral levels commonly associated with DCM compression (i.e. C5 and C6) (Muhammad, Weber, Bedard, et al., 2024; Vallotton et al., 2021). Finally, activation lateralization, determined by the LR index, appeared to be primarily bilateral in HCs. Ipsilateral responses in the spinal cord are expected because the incoming peripheral signals and the motor responses involved in the induced spinal cord reflex arc (i.e. Hoffmann's reflex) will enter and exit on the ipsilateral side of the stimulation. Contralateral activation (i.e., the side opposite the stimulation) is also consistent with interneuronal crossover at the spinal cord level and has been previously reported in other task-based fMRI paradigms (Agosta et al., 2009; Bouwman et al., 2008; Brooks et al., 2012; Maieron et al., 2007; Ng et al., 2008). This type of contralateral activation is likely due to the presence of commissural interneurons (i.e. interneurons that cross the midline of the spinal cord to the contralateral side) (Landelle et al., 2021; Maxwell & Soteropoulos, 2020). Little is known about the commissural interneurons of the cervical spine, but it is speculated that they are organized similarly to those in the lumbar spine, which are known to play a significant role in locomotion (Maxwell & Soteropoulos, 2020). DCM responses, however, were predominantly ipsilateral, implying that, in addition to the segmental shift in activation, DCM patients also experience an interruption in left-right connectivity that is reducing contralateral activation. This is potentially due to the mechanism of injury in degenerative myelopathy where the central part of the cord experiences the most amount of

stress (Levy et al., 2021), which ultimately results in damage to the commissural interneurons responsible for the contralateral activation seen in healthy controls.

In addition to regions of positive BOLD signal change (i.e. activation), regions of negative BOLD signal change (i.e. deactivation) were noted in all conditions. In the brain, deactivation has long been suspected to be the result of inhibition (Allison et al., 2000; Nakata et al., 2019; Schafer et al., 2012). This indicates that changes in deactivation patterns could also be important because they reflect additional alterations in neuronal processes. Deactivation has also been reported to extend to the spinal cord, where it indicated the inhibition of neuronal activity in the left ventral and dorsal horns during a motor task (Oliva et al., 2025). These findings in the spinal cord align with the well established presence of inhibitory interneurons, demonstrated over a century ago (Callister et al., 2020), which are known to help regulate the transmission of sensory signals (Bardoni et al., 2013; Goulding et al., 2014), especially pain (Hughes & Todd, 2020), and motor reflex coordination (Goulding et al., 2014). In our data, deactivation was observed to be consistent in HCs across stimulation intensities and showed a bilateral distribution (i.e. LR Index). In contrast, DCM patients exhibited a marked spike at C6 during sub-motor stimulation, far greater than its HC counterpart. This abnormal inhibitory signal coincided with increased activation and higher z-scores in sub-motor stimulation, suggesting that heightened excitation and inhibition co-occur at the same segment. Notably, this phenomenon was localized to the C6 segment (C5 vertebral level), the site most affected in DCM (Muhammad, Weber, Bedard, et al., 2024; Vallotton et al., 2021). This exaggerated inhibitory response could be a reflection of a maladaptive processing of the excitatory drive at a lower threshold (i.e., sub-motor) and underscores the role of inhibitory interneurons in shaping abnormal activity pattern (Bardoni et al., 2013; Goulding et al., 2014; Hughes & Todd, 2020).

Beyond indicating areas of deactivation, negative BOLD signals have been increasingly recognized as biologically meaningful. Altered deactivation patterns during spinal cord stimulation have been associated with pain processing in surgical spine patients (De Groote et al., 2018) and linked to inhibitory interneuron activity regulating sensory transmission and motor reflexes (Oliva et al., 2025). In combination with our own data, these studies support the idea that heightened inhibition in DCM reflects disrupted sensorimotor integration.

The resulting change in the recruitment of different segmental and lateral areas of the cord among DCM participants displayed by direct stimulation is likely reflective of the structural damage occurring during cord compression. Previous biomechanical DCM studies show that diffused compression on the anterior part of the cord causes the most stress (Levy et al., 2021) and results in the most detrimental symptomatic outcomes (Nishida et al., 2012). This stress can then cause disruption to the capillaries of the blood-spinal cord barrier, ultimately causing ischemia (i.e., lack of blood flow) to the spinal cord (Badhiwala et al., 2020; Blume et al., 2020; Tu et al., 2021) that can impair neural function through several mechanisms. The first is neuronal loss and impeded activation, which has been documented in the WM and GM (Badhiwala et al., 2020; Blume et al., 2020; Cloney et al., 2018; Haynes, Muhammad, Weber, Khan, Hameed, Ding, et al., 2025; Haynes et al., 2024; Hopkins et al., 2018; Smith et al., 2020; Tu et al., 2021) and indicates the presences of ventral horn atrophy and motor neuron degeneration. These structural changes align with clinical reports of motor performance deficits in DCM patients (Muhammad et al., 2023; Muhammad, Weber, Bedard, et al., 2024). The second possible explanation is that surviving neurons remain structurally intact but functionally impaired. Compressive DCM damage that results in axonal degeneration and demyelination (Akter et al., 2020; Dohle et al., 2023) will reduce conduction and responsiveness and therefore change

functional responses in the spinal cord. In response, spared axons can reach out to reroute or recruit alternative segments, a similar reaction to spinal cord injury (Sofroniew, 2018), which can result in reorganization of neuronal pathways and an abnormal spread of activation to the C5 and C8 segments. Finally, the ischemia may blunt BOLD signal sensitivity by reducing the amount of oxygenated blood being delivered to active regions (Glover, 2011). Together, these processes may account for the pathophysiological mechanisms for the functional alterations we observed in DCM patients during task-based fMRI.

The ability to detect functional changes in DCM patients with fMRI highlights the advantages of a median nerve stimulation paradigm. Backes et al. was the first to demonstrate that median nerve stimulation could evoke cervical spinal cord activation that was comparable to voluntary motor tasks such as fist clenching (Backes et al., 2001a). Subsequent work confirmed that median nerve stimulation can produce robust BOLD responses in the cervical spinal cord (Xie et al., 2007), validating the paradigm as a reproducible method to probe sensorimotor pathways. The HC group also displayed activation profiles aligning with electrophysiology of median nerve stimulation in the cervical spine (Akaza et al., 2021), supporting the validity of the paradigm. Furthermore, this approach avoids dependence on patient motor performance, which is a critical limitation of task-based DCM studies due to motor impairments (Muhammad et al., 2023), and reveals distinct functional alterations in DCM patients. This underscores the paradigm's potential as a method to assess spinal cord function in disease states.

Because of this, applying a direct median nerve stimulation fMRI paradigm in DCM patients could provide one of the first functional biomarkers to complement established structural imaging. In the past, structural MRI has helped to define cord compression, atrophy, and other degenerative changes (Bedard et al., 2025a; Cloney et al., 2018; Filimonova, Abdaev, et al.,

2024b; Haynes et al., 2024; Khan et al., 2023; Muhammad, Weber, Bedard, et al., 2024; Smith et al., 2020). However, it cannot capture functional activity. By utilizing techniques that rely on detecting changes in blood oxygenation (i.e., BOLD signal) within spinal cord segments affected by DCM, we demonstrate an approach that offers insight into the recruitment of different segmental and lateral cord areas and inhibitory alterations that are not accessible with structural imaging. The ability to indirectly map the functional changes within the regions of damage highlights the potential median nerve stimulation has to serve as a clinically relevant, functional DCM biomarker.

5.4.1. Limitations

There are several limitations to this study. First, spinal cord compression can distort cord anatomy and vertebral alignment, which may affect template registration and the normalization to the PAM50 template that is derived from healthy controls (De Leener et al., 2018). Second, spinal cord fMRI has challenges in reproducibility, particularly in response to stimulation where signal levels are typically lower than during voluntary motor tasks (Backes et al., 2001a; Wilmink et al., 2003). This may contribute to variability across individuals and limit the generalizability of group-level comparisons. Third, stimulation thresholds were determined based on observed finger twitch, which is inherently subjective and may introduce variability in application. While pilot work with EMGs has confirmed reflex responses for this paradigm, future studies should incorporate objective electrophysiological measures to improve consistency. We also observed that all DCM patients required higher motor thresholds to elicit comparable responses (Haynes, Muhammad, Weber, Khan, Hameed, Ding, et al., 2025), suggesting that there are disease-related differences in excitability that must be accounted for in future refinements of this technique.

5.4.2. Future Directions

The data presented here demonstrates functional changes in the spinal cords of DCM patients during sub-motor and motor threshold stimulation. To further investigate changes to spinal cord pathways, especially at the neuronal level, there are multiple types of measures that could be implemented in future research. For example, spinal cord EEG could be applied to achieve a better understanding of the inhibition to localized neuronal recruitment and the role commissural interneurons play in the lateralization of functional patterns observed. Tissue collection methodologies – like histology – could be applied to help provide a detailed, in-depth description of changes to glial populations in the spinal cord over low spatial resolution imaging methodologies. Additionally, little is known about reorganization of resting-state patterns in DCM. While dorsal and ventral resting-state networks have been defined in healthy controls (Barry et al., 2014; Kong et al., 2014), evidence in DCM is limited to a single study associating BOLD fluctuations with JOA scores (Liu et al., 2016). Examining resting-state patterns and comparing them to task-based stimulation responses could reveal whether the extended activation we observed at C5 and C8 represents maladaptive dysfunction or adaptive reorganization. Furthermore, because DCM is a progressive disease that can be classified by severity (Tetreault et al., 2017), future studies should investigate whether functional changes differ between mild and severe categories (i.e., moderate and severe). Such comparisons could improve understanding of DCM progression and may inform decisions on surgical intervention and predict outcomes, thereby positioning spinal fMRI as a prognostic tool of DCM. Lastly, an important next step will be to establish how these functional changes relate to clinical motor and sensory deficits in DCM. Linking functional activation and deactivation patterns to symptom severity could clarify the contribution that abnormal excitability and reorganization have on

disability. Further work should also examine how functional changes couple with established structural alterations, providing insight into how anatomy and physiology interact to shape disease progression.

5.5. Conclusion

In summary, median nerve stimulation combined with fMRI revealed functional alterations in DCM patients, which included abnormal segmental recruitment, exaggerated sub-motor responses, reduced motor threshold activation, altered lateralization, and increased inhibitory processing at compressed levels. These changes likely reflect compensatory mechanisms that allow partial motor function to be preserved despite tract damage. By capturing the functional disruptions not visible with structural imaging, this paradigm highlights a potential avenue for developing functional spinal cord biomarkers of DCM.

Chapter 6: Discussion

6.1. Summary of Aims and Contributions

In previous studies of DCM patients, the presence of white and gray matter structural damage has been extensively reported. Advanced MRI methodologies (i.e., magnetization transfer ratio (Cloney et al., 2018; Filimonova, Abdaev, et al., 2024a; Suleiman et al., 2018), myelin water fraction (Liu et al., 2017), and diffusion tensor imaging (Atchut et al., 2023)) have found indications of significantly decreased levels of white matter content in DCM patients. Furthermore, regional measures of gray matter volumes also decreased in DCM spinal cords when compared to HCs (Smith et al., 2020). These structural WM and GM changes in DCM have been primarily found in the ventral/anterior cord, which primarily houses motor pathways, and aligns with some of the most common DCM symptoms responsible for significant motor impediment (Muhammad et al., 2023).

6.1.1. Aim 1: Utilize improved spinal cord analysis methodologies to demonstrate MTR's ability to quantify white matter damage in DCM

Several notable gaps existed in the methodologies used in the aforementioned studies – primarily a lack of investigations into tract- and severity-based alterations – that led into the investigation of regional and tract-based white matter changes between different DCM severities (i.e., mild and moderate/severe). Through this investigation, it was confirmed that – compared to HCs – patients with moderate/severe DCM experience significant white matter decreases in the overall spinal cord, the ventral region, the ventral corticospinal and reticulospinal tracts, the spinal lemniscus, and the fasciculus cuneatus (Haynes et al., 2024).

6.1.2. Aim 2: Test the relationship between DCM damage and the impediment of spinal cord reflex arcs

In order to fully quantify the impact of volume loss in DCM spinal cords, volume changes in the GM horns and their correlations to WM loss and measures of motor function were also investigated (Haynes, Muhammad, Weber, Khan, Hameed, Ding, et al., 2025). Significant decreases were found in all the GM regions (overall, ventral, intermediate, and dorsal regions) of DCM patients, as well as significant increases in the threshold required to induce a minimal motor response. Despite significant changes, there was no correlation between the GM volumes and motor thresholds. However, ventral horn GM volume did correlate with ventral region MTR values, further emphasizing the development of a ventral region injury pattern in DCM patients.

6.1.3. Aim 3: Interrogate changes in functional activation with an electrical stimulation paradigm capable of inducing an involuntary motor reaction

Despite these two investigations indicating WM and GM changes, they could not give insight into one important factor – function. Previous task-based fMRI studies have shown evidence of functional reorganization in other pathologies (Haynes et al., 2023), but none of the previous reports have explored DCM. By implementing a task-based fMRI paradigm – electrical stimulation of the median nerve – we showed that DCM spinal cords undergo overall, segmental, and lateralized functional reorganization (Haynes, Muhammad, Weber, Khan, Hameed, Shakir, et al., 2025).

6.2. Impact of Progressive DCM on the Ventral Spinal Cord

Through the investigations into regional and tract-based WM changes, significant decreases in the ventral region of moderate/severe DCM patients – specifically the ventral corticospinal and reticulospinal tracts – demonstrated a pattern of heterogeneous damage that

occurs with the progression of DCM (Haynes et al., 2024). Furthermore, this impact to the ventral cord and the tracts within can potentially help to explain the impairment in motor performance experienced by DCM patients as the pathology progresses. The ventral cord damage indicated by MTR also correlated with significant loss of gray matter volume in the same area (Haynes, Muhammad, Weber, Khan, Hameed, Ding, et al., 2025). This noted decrease in the ventral cord and ventral horn measures is bolstered by previous research done in different DCM cohorts, which showed similar decreases in anterior white and gray matter measures (Cloney et al., 2018; Dohle et al., 2023; Hopkins et al., 2018; Smith et al., 2020). However, neither gray nor white matter measures correlated with the amplitude of electrical stimulation required to induce a motor response (Haynes, Muhammad, Weber, Khan, Hameed, Ding, et al., 2025), indicating that further impairment might originate from the peripheral nerves rather than the spinal cord.

Damage to the ventral region and horn of the spinal cord during the progression of DCM aligns with previous autopsy studies reporting demyelination and neuronal loss in the white and gray matter, respectively (Dohle et al., 2023). Because the ventral horn houses motor neurons and their regulating interneurons and the majority of the ventral white matter tracts are descending (i.e. motor), damage in this region could provide an explanation for the manifestation of motor symptoms that DCM patients experience. A descending trend in MTR values, with significant decreases between the HC and moderate/severe groups, also gives insight into the mechanisms of DCM progression. For example, cervical kyphosis – an inversion of the spinal cord curve associated with myelopathy severity (Ames et al., 2013) – could be a possible mechanism behind this damage. Kyphosis can cause the spinal cord to press against the anterior part of the vertebrae and result in an increase in intermedullary pressure, cord tension, and a

decreased blood supply (ischemia) (Ames et al., 2013; Buell et al., 2018) that would ultimately impair neuronal function by either killing or damaging neurons (Haynes, Muhammad, Weber, Khan, Hameed, Shakir, et al., 2025).

6.3. Functional Alterations Resulting from Chronic DCM Compression

To investigate functional alterations induced by chronic DCM damage, the capability of the electrical stimulation paradigm to evoke functional activity aligning with neurophysiological expectations was established. For example, because motor neurons require a higher activation threshold (Gaines et al., 2018), they would only be recruited during the motor threshold condition. The expected result of the additional neuronal recruitment is an increase in the number of active voxels during the motor threshold condition. Furthermore, the LR Indices indicated a bilateral distribution of activation. Ipsilateral responses are expected, as the roots of the peripheral nerves enter on the ipsilateral side, and contralateral activation is representative of interneurons carrying the signal to the opposing side of the cord. Finally, a segmental breakdown of activation in HCs revealed that the primary levels activated were the C6 and C7, which aligns with the spinal cord segments where the median nerve is rooted (C5-T1).

Defining a HC response to median nerve stimulation provided a baseline to detect any functional alterations in DCM. For example, HCs experienced an increase between sub-motor and motor threshold runs, whereas DCM patients experienced a decrease. This deviation from HCs demonstrates the presence of functional alterations in DCM. Additionally, instead of a bilateral distribution like in HCs, activation in DCM patients remained primarily ipsilateral, which indicates potential impairments of the interneuronal pathways leading to the contralateral side of the cord. Finally, DCM patients experienced a noticeable increase at the C6 segment in sub-motor stimulation, which was reduced during motor threshold stimulation. This reaction was

the exact opposite at the C6 segment in HCs and occurred at a level commonly impacted by DCM compression (Muhammad, Weber, Bedard, et al., 2024; Vallotton et al., 2021). Deactivation – commonly considered to be the result of inhibition – also increased in the C6 segment during the sub-motor stimulation in DCM patients, possibly indicating that compensatory mechanisms from inhibitory interneurons are helping to regulate sensory and motor signal transmission (Goulding et al., 2014).

Establishing these functional alterations in DCM gives insight into how the structural damage previously found could manifest as impairments and how the spinal cord adapts to chronic compression in order to retain some functionality. For example, structural imaging of the spinal cord tells us that remote segments above or below the regions of compression of the spinal cord are altered in DCM (Baucher et al., 2021; Maier et al., 2020; Martin et al., 2017; Muhammad, Weber, Haynes, et al., 2025; Vallotton et al., 2021), but functional imaging can reveal activity shifts to different segmental and lateral regions (Haynes, Muhammad, Weber, Khan, Hameed, Shakir, et al.). Functional MRI has been used previously to define functional reorganization that occurs in spinal cord pathologies like spinal cord injury, fibromyalgia, and multiple sclerosis (Haynes et al., 2023). These changing functional patterns can possibly reflect axonal restructuring, which is known to occur in spinal cord injury, and may help to retain partial sensory and motor functions (Sofroniew, 2018). However, this study marks the first to demonstrate these types of functional changes in DCM with fMRI and could open a path for the future development of clinically useful fMRI biomarkers.

6.4. Limitations

Despite many advances since its inception, spinal cord imaging still faces many limitations that impact the aforementioned studies. For example, the length of the cord and the

surrounding vertebrae can cause difficulties in obtaining quality images of the cord. Additionally, the spinal cord is not a static structure and is constantly subject to the voluntary and involuntary movements of surrounding physiological processes. While most voluntary movement is preventable in an MRI setting, involuntary movement impacting spinal cord imaging like breathing, heart rate, and CSF flow is not. However, in advanced MRI methodologies like fMRI, many of these movements can be corrected via pre-processing methods (i.e.. motion correction and physiological noise model regression) that help to correct for gross movement and signals involved with the physiological noises. Furthermore, hypo- or hyperintense signals in compressed areas of the cord can impact the quality of the automatic segmentation algorithms and result in inaccurate segmentation of the spinal cord. Though steps are being made to improve these algorithms in pathological spinal cords (Bedard et al., 2025b), segmentation errors still require manual correction that can result in human error impacting analysis. Despite this, however, automated segmentation limits human error and provides a less biased method of segmentation than those drawn completely by hand.

Despite attaining spinal cord images using advanced techniques, these images – like MTR, T2*, and fMRI – have low spatial resolution. This can further lead to the partial volume effect, which incorporates the signal from multiple tissue types into one voxel and blurs the boundaries between different tissues and structures. Not only can this cause an issue with anatomical imaging, especially for the distinction between gray and white matter and cerebrospinal fluid, but it can also result in errors in analysis for functional active voxels. In the human spinal cord, the largest supplying blood vessel can reach up to 0.8mm in diameter, with its smaller branches ranging from 0.06-0.4mm (Santillan et al., 2012). With a 1 x 1 x 5mm resolution, many of these vessels will be lumped together into the same voxel during functional

imaging. This could either diminish or exaggerate how many neurons are active in a single voxel and how strong their signals are.

Finally, data extraction from the spinal cord is subject to error due to the nature of the template used for extraction. SCT's PAM50 templates are made from HCs, which can result in difficulties registering pathological morphometric spinal cord changes to the normalized space. DCM patients especially have been noted to have significant morphometric changes along the axial plane (i.e. decreases in cross-sectional area, anterior-posterior diameter, and right-left diameter (Muhammad, Weber, Bedard, et al., 2024)) and superior-inferior axis (Nouri et al., 2015). Though extreme care was taken to make sure that registration was accurate, these morphometric changes can result in the misalignment of the native spinal cord image to the template and result in errors when extracting data using the PAM50 templates (i.e. gray and white matter atlases, root levels, vertebral levels).

6.5. Future Directions

Establishing a stimulation paradigm capable of revealing functional differences between HC and DCM patients opens the way to further investigation into changes of functional patterns that can help to give insight into the pathophysiology of DCM. One direction that is key to investigate in future studies is the impact that DCM severity has on functional reorganization. Currently, surgical interventions are typically reserved for moderate and severe DCM cases, but correlations have been drawn between the duration of symptoms and post-surgical recovery (L. A. Tetreault et al., 2015). Furthermore, there is evidence suggesting that moderate/severe patients experience significant white matter damage in comparison to HCs and mild DCM patients (Haynes et al., 2024). This implies that not only are moderate and severe patients experiencing neurological damage and are therefore less likely to fully recover, but patients with

mild disease are left vulnerable to permanent damage. Therefore, while there is evidence that the spinal cord can compensate to some degree in DCM, patients can still experience progressive, potentially permanent DCM-induced damage that could result in severe impairment if left untreated. Defining objective structural and functional imaging markers that can distinguish between mild and moderate/severe patients can help to lessen the likelihood that this permanent damage will occur before surgery, which will improve post-surgical recovery and quality of life for DCM patients.

Additionally, functional investigations with different amplitudes of stimulation could provide more insight into functional alterations for a broader range of intensities. A single investigation into the resting-state function of DCM patients (i.e., with no stimulation) revealed that fluctuations in BOLD signals increased with DCM severity (Liu et al., 2016). However, there have been no studies which have interrogated potential changes to the resting-state networks, which have been defined in HCs (Barry et al., 2014; Kong et al., 2014). An additional condition that could be useful to apply in future investigations is supra-motor stimulation (i.e., a stimulation greater than motor threshold). As previously stated, DCM patients have a history of motor impairment (Muhammad et al., 2023) that can impede their performance in fMRI settings. DCM patients also had a noticeable decrease in activated voxels during motor stimulation (Haynes, Muhammad, Weber, Khan, Hameed, Shakir, et al., 2025). However, these differences were detected at the minimal threshold needed to induce a motor response and do not investigate how much impairment, if any, occurs during conditions that evoke a stronger motor response. An investigation applying a resting-state and supra-motor stimulation paradigm could help to establish what type of functional pattern alteration occurs, if any, by providing alternative conditions aimed at evoking to interrogate these varying conditions.

6.6. Conclusion

Through the course of my investigations, I characterized an injury pattern in DCM patients that reveals how the ventral cord and horn are impacted as compression worsens. I also provided evidence for a task-based fMRI paradigm capable to interrogate the functional differences in DCM patients, opening future research avenues to investigate the functional alterations in DCM pathogenesis and progression.

REFERENCES

Agosta, F., Valsasina, P., Caputo, D., Rocca, M. A., & Filippi, M. (2009). Tactile-associated fMRI recruitment of the cervical cord in healthy subjects. *Hum Brain Mapp*, *30*(1), 340-345. https://doi.org/10.1002/hbm.20499

Agosta, F., Valsasina, P., Caputo, D., Stroman, P. W., & Filippi, M. (2008). Tactile-associated recruitment of the cervical cord is altered in patients with multiple sclerosis. *Neuroimage*, *39*(4), 1542-1548. https://doi.org/10.1016/j.neuroimage.2007.10.048

Agosta, F., Valsasina, P., Rocca, M. A., Caputo, D., Sala, S., Judica, E., Stroman, P. W., & Filippi, M. (2008). Evidence for enhanced functional activity of cervical cord in relapsing multiple sclerosis. *Magn Reson Med*, *59*(5), 1035-1042. https://doi.org/10.1002/mrm.21595

Akaza, M., Kawabata, S., Ozaki, I., Miyano, Y., Watanabe, T., Adachi, Y., Sekihara, K., Sumi, Y., & Yokota, T. (2021). Noninvasive measurement of sensory action currents in the cervical cord by magnetospinography. *Clin Neurophysiol*, *132*(2), 382-391. https://doi.org/10.1016/j.clinph.2020.11.029

Akter, F., Yu, X., Qin, X., Yao, S., Nikrouz, P., Syed, Y. A., & Kotter, M. (2020). The Pathophysiology of Degenerative Cervical Myelopathy and the Physiology of Recovery Following Decompression. *Front Neurosci*, *14*, 138. https://doi.org/10.3389/fnins.2020.00138

Al-Shawwa, A., Craig, M., Ost, K., Anderson, D., Casha, S., Jacobs, W. B., Evaniew, N., Tripathy, S., Bouchard, J., Lewkonia, P., Nicholls, F., Soroceanu, A., Swamy, G., Thomas, K. C., duPlessis, S., Yang, M. M., Cohen-Adad, J., Dea, N., Wilson, J. R., & Cadotte, D. W. (2025). Spinal cord demyelination predicts neurological deterioration in

patients with mild degenerative cervical myelopathy. *BMJ Neurol Open*, *7*(1), e000940. https://doi.org/10.1136/bmjno-2024-000940

Ali, T. F. T., & Badawy, A. E. (2013). Feasibility of H-MR Spectroscopy in evaluation of cervical spondylotic myelopathy. *Egyptian Journal of Radiology and Nuclear Medicine*, *44*(1), 93-99. https://doi.org/10.1016/j.ejrnm.2012.11.001

Allison, J. D., Meador, K. J., Loring, D. W., Figueroa, R. E., & Wright, J. C. (2000). Functional MRI cerebral activation and deactivation during finger movement. *Neurology*, *54*(1), 135-142. https://doi.org/10.1212/wnl.54.1.135

Ames, C. P., Blondel, B., Scheer, J. K., Schwab, F. J., Le Huec, J. C., Massicotte, E. M., Patel, A. A., Traynelis, V. C., Kim, H. J., Shaffrey, C. I., Smith, J. S., & Lafage, V. (2013). Cervical radiographical alignment: comprehensive assessment techniques and potential importance in cervical myelopathy. *Spine (Phila Pa 1976)*, *38*(22 Suppl 1), S149-160. https://doi.org/10.1097/BRS.0b013e3182a7f449

Atchut, K. A., Shetty, L., & Ravichandran, K. (2023). Role of diffusion tensor imaging in stenotic and non-stenotic spinal canal. *J Med Imaging Radiat Sci*, *54*(4), 699-706. https://doi.org/10.1016/j.jmir.2023.09.022

Aung, W. Y., Mar, S., & Benzinger, T. L. (2013). Diffusion tensor MRI as a biomarker in axonal and myelin damage. *Imaging Med*, *5*(5), 427-440. https://doi.org/10.2217/iim.13.49

Backes, W. H., Mess, W. H., & Wilmink, J. T. (2001a). Functional MR imaging of the cervical spinal cord by use of median nerve stimulation and fist clenching. *AJNR Am J Neuroradiol*, *22*(10), 1854-1859. https://www.ncbi.nlm.nih.gov/pubmed/11733315

Backes, W. H., Mess, W. H., & Wilmink, J. T. (2001b). Functional MR imaging of the cervical spinal cord by use of median nerve stimulation and fist clenching. *AJNR Am J Neuroradiol*, *22*(10), 1854-1859. http://www.ajnr.org/content/22/10/1854

Badhiwala, J. H., Ahuja, C. S., Akbar, M. A., Witiw, C. D., Nassiri, F., Furlan, J. C., Curt, A., Wilson, J. R., & Fehlings, M. G. (2020). Degenerative cervical myelopathy - update and future directions. *Nat Rev Neurol*, *16*(2), 108-124. https://doi.org/10.1038/s41582-019-0303-0

Badhiwala, J. H., Witiw, C. D., Nassiri, F., Akbar, M. A., Mansouri, A., Wilson, J. R., & Fehlings, M. G. (2019). Efficacy and Safety of Surgery for Mild Degenerative Cervical Myelopathy: Results of the AOSpine North America and International Prospective Multicenter Studies. *Neurosurgery*, *84*(4), 890-897. https://doi.org/10.1093/neuros/nyy133

Bakhsheshian, J., Mehta, V. A., & Liu, J. C. (2017). Current Diagnosis and Management of Cervical Spondylotic Myelopathy. *Global Spine J*, *7*(6), 572-586. https://doi.org/10.1177/2192568217699208

Balmaceno-Criss, M., Singh, M., Daher, M., Buchbinder, R., Diebo, B. G., & Daniels, A. H. (2024). Degenerative Cervical Myelopathy: History, Physical Examination, and Diagnosis. *J Clin Med*, *13*(23). https://doi.org/10.3390/jcm13237139

Banerjee, R., Kaptan, M., Tinnermann, A., Khatibi, A., Dabbagh, A., Buchel, C., Kundig, C. W., Law, C. S. W., Pfyffer, D., Lythgoe, D. J., Tsivaka, D., Van De Ville, D., Eippert, F., Muhammad, F., Glover, G. H., David, G., Haynes, G., Haaker, J., Brooks, J. C. W., . . . Cohen-Adad, J. (2025). EPISeg: Automated segmentation of the spinal cord on echo

planar images using open-access multi-center data. *Imaging Neurosci (Camb)*, *3*. https://doi.org/10.1162/IMAG.a.98

Bardoni, R., Takazawa, T., Tong, C. K., Choudhury, P., Scherrer, G., & Macdermott, A. B. (2013). Pre- and postsynaptic inhibitory control in the spinal cord dorsal horn. *Ann N Y Acad Sci*, *1279*, 90-96. https://doi.org/10.1111/nyas.12056

Barry, R. L., Conrad, B. N., Smith, S. A., & Gore, J. C. (2018). A practical protocol for measurements of spinal cord functional connectivity. *Sci Rep*, *8*(1), 16512. https://doi.org/10.1038/s41598-018-34841-6

Barry, R. L., Rogers, B. P., Conrad, B. N., Smith, S. A., & Gore, J. C. (2016). Reproducibility of resting state spinal cord networks in healthy volunteers at 7 tesla. *Neuroimage*, *133*, 31-40. https://doi.org/10.1016/j.neuroimage.2016.02.058

Barry, R. L., Smith, S. A., Dula, A. N., & Gore, J. C. (2014). Resting state functional connectivity in the human spinal cord. *Elife*, *3*, e02812. https://doi.org/10.7554/eLife.02812

Barry, R. L., Vannesjo, S. J., By, S., Gore, J. C., & Smith, S. A. (2018). Spinal cord MRI at 7T. *Neuroimage*, *168*, 437-451. https://doi.org/10.1016/j.neuroimage.2017.07.003

Baucher, G., Rasoanandrianina, H., Levy, S., Pini, L., Troude, L., Roche, P. H., & Callot, V. (2021). T1 Mapping for Microstructural Assessment of the Cervical Spinal Cord in the Evaluation of Patients with Degenerative Cervical Myelopathy. *AJNR Am J Neuroradiol*, *42*(7), 1348-1357. https://doi.org/10.3174/ajnr.A7157

Bedard, S., Valosek, J., Seif, M., Curt, A., Schading-Sassenhausen, S., Pfender, N., Freund, P., Hupp, M., & Cohen-Adad, J. (2025a). Normalizing spinal cord compression measures in

degenerative cervical myelopathy. *Spine J*, *25*(9), 1951-1963. https://doi.org/10.1016/j.spinee.2025.03.012

Bedard, S., Valosek, J., Seif, M., Curt, A., Schading-Sassenhausen, S., Pfender, N., Freund, P., Hupp, M., & Cohen-Adad, J. (2025b). Normalizing spinal cord compression measures in degenerative cervical myelopathy. *Spine J*. https://doi.org/10.1016/j.spinee.2025.03.012

Benzel, E. C., Lancon, J., Kesterson, L., & Hadden, T. (1991). Cervical laminectomy and dentate ligament section for cervical spondylotic myelopathy. *J Spinal Disord*, *4*(3), 286-295. https://doi.org/10.1097/00002517-199109000-00005

Bhargava, J., & Hurley, J. A. (2023). Fibromyalgia. In *StatPearls [Internet]*. StatPearls Publishing. https://www.ncbi.nlm.nih.gov/pubmed/31082018

Blume, C., Geiger, M. F., Brandenburg, L. O., Muller, M., Mainz, V., Kalder, J., Albanna, W., Clusmann, H., & Mueller, C. A. (2020). Patients with degenerative cervical myelopathy have signs of blood spinal cord barrier disruption, and its magnitude correlates with myelopathy severity: a prospective comparative cohort study. *Eur Spine J*, *29*(5), 986-993. https://doi.org/10.1007/s00586-020-06298-7

Bosma, R. L., Ameli Mojarad, E., Leung, L., Pukall, C., Staud, R., & Stroman, P. W. (2015). Neural correlates of temporal summation of second pain in the human brainstem and spinal cord. *Hum Brain Mapp*, *36*(12), 5038-5050. https://doi.org/10.1002/hbm.22993

Bosma, R. L., Mojarad, E. A., Leung, L., Pukall, C., Staud, R., & Stroman, P. W. (2016). FMRI of spinal and supra-spinal correlates of temporal pain summation in fibromyalgia patients. *Hum Brain Mapp*, *37*(4), 1349-1360. https://doi.org/10.1002/hbm.23106

Bosma, R. L., & Stroman, P. W. (2014). Assessment of data acquisition parameters, and analysis techniques for noise reduction in spinal cord fMRI data. *Magn Reson Imaging*, *32*(5), 473-481. https://doi.org/10.1016/j.mri.2014.01.007

Bosma, R. L., & Stroman, P. W. (2015). Spinal cord response to stepwise and block presentation of thermal stimuli: a functional MRI study. *J Magn Reson Imaging*, *41*(5), 1318-1325. https://doi.org/10.1002/jmri.24656

Bouwman, C. J., Wilmink, J. T., Mess, W. H., & Backes, W. H. (2008). Spinal cord functional MRI at 3 T: gradient echo echo-planar imaging versus turbo spin echo. *Neuroimage*, *43*(2), 288-296. https://doi.org/10.1016/j.neuroimage.2008.07.024

Brooks, J. C., Beckmann, C. F., Miller, K. L., Wise, R. G., Porro, C. A., Tracey, I., & Jenkinson, M. (2008). Physiological noise modelling for spinal functional magnetic resonance imaging studies. *Neuroimage*, *39*(2), 680-692. https://doi.org/10.1016/j.neuroimage.2007.09.018

Brooks, J. C., Kong, Y., Lee, M. C., Warnaby, C. E., Wanigasekera, V., Jenkinson, M., & Tracey, I. (2012). Stimulus site and modality dependence of functional activity within the human spinal cord. *J Neurosci*, *32*(18), 6231-6239. https://doi.org/10.1523/JNEUROSCI.2543-11.2012

Bryant, R. A., Williamson, T., Erlinger, M., Felmingham, K. L., Malhi, G., Hinton, M., Williams, L., & Korgaonkar, M. S. (2021). Neural activity during response inhibition associated with improvement of dysphoric symptoms of PTSD after trauma-focused psychotherapy-an EEG-fMRI study. *Transl Psychiatry*, *11*(1), 218. https://doi.org/10.1038/s41398-021-01340-8

Buell, T. J., Buchholz, A. L., Quinn, J. C., Shaffrey, C. I., & Smith, J. S. (2018). Importance of Sagittal Alignment of the Cervical Spine in the Management of Degenerative Cervical Myelopathy. *Neurosurg Clin N Am*, *29*(1), 69-82. https://doi.org/10.1016/j.nec.2017.09.004

Cadotte, D. W., Bosma, R., Mikulis, D., Nugaeva, N., Smith, K., Pokrupa, R., Islam, O., Stroman, P. W., & Fehlings, M. G. (2012). Plasticity of the injured human spinal cord: insights revealed by spinal cord functional MRI. *PLoS One*, *7*(9), e45560. https://doi.org/10.1371/journal.pone.0045560

Cahill, C. M., & Stroman, P. W. (2011). Mapping of neural activity produced by thermal pain in the healthy human spinal cord and brain stem: a functional magnetic resonance imaging study. *Magn Reson Imaging*, *29*(3), 342-352. https://doi.org/10.1016/j.mri.2010.10.007

Callister, R. J., Brichta, A. M., Schaefer, A. T., Graham, B. A., & Stuart, D. G. (2020). Pioneers in CNS inhibition: 2. Charles Sherrington and John Eccles on inhibition in spinal and supraspinal structures. *Brain Res*, *1734*, 146540. https://doi.org/10.1016/j.brainres.2019.146540

Chen, S., Wang, Y., Wu, X., Chang, J., Jin, W., Li, W., Song, P., Wu, Y., Zhu, J., Qian, Y., Shen, C., Yu, Y., & Dong, F. (2022). Degeneration of the Sensorimotor Tract in Degenerative Cervical Myelopathy and Compensatory Structural Changes in the Brain. *Front Aging Neurosci*, *14*, 784263. https://doi.org/10.3389/fnagi.2022.784263

Chikuda, H., Seichi, A., Takeshita, K., Shoda, N., Ono, T., Matsudaira, K., Kawaguchi, H., & Nakamura, K. (2010). Correlation between pyramidal signs and the severity of cervical myelopathy. *Eur Spine J*, *19*(10), 1684-1689. https://doi.org/10.1007/s00586-010-1364-3

Choi, B. W., Kim, S. S., Lee, D. H., & Kim, J. W. (2017). Cervical radiculopathy combined with cervical myelopathy: prevalence and characteristics. *Eur J Orthop Surg Traumatol*, *27*(7), 889-893. https://doi.org/10.1007/s00590-017-1972-2

Churchill, N. W., Hutchison, M. G., Graham, S. J., & Schweizer, T. A. (2019). Mapping brain recovery after concussion: from acute injury to 1 year after medical clearance. *Neurology*, *93*(21), e1980-e1992. https://doi.org/10.1212/WNL.0000000000008523

Cloney, M. B., Smith, Z. A., Weber, K. A., 2nd, & Parrish, T. B. (2018). Quantitative Magnetization Transfer MRI Measurements of the Anterior Spinal Cord Region are Associated With Clinical Outcomes in Cervical Spondylotic Myelopathy. *Spine (Phila Pa 1976)*, *43*(10), 675-680. https://doi.org/10.1097/BRS.0000000000002470

Cohen-Adad, J., Alonso-Ortiz, E., Abramovic, M., Arneitz, C., Atcheson, N., Barlow, L., Barry, R. L., Barth, M., Battiston, M., Buchel, C., Budde, M., Callot, V., Combes, A. J. E., De Leener, B., Descoteaux, M., de Sousa, P. L., Dostal, M., Doyon, J., Dvorak, A., . . . Xu, J. (2021). Generic acquisition protocol for quantitative MRI of the spinal cord. *Nat Protoc*, *16*(10), 4611-4632. https://doi.org/10.1038/s41596-021-00588-0

Cohen-Adad, J., El Mendili, M. M., Lehericy, S., Pradat, P. F., Blancho, S., Rossignol, S., & Benali, H. (2011). Demyelination and degeneration in the injured human spinal cord detected with diffusion and magnetization transfer MRI. *Neuroimage*, *55*(3), 1024-1033. https://doi.org/10.1016/j.neuroimage.2010.11.089

Cohen-Adad, J., Gauthier, C. J., Brooks, J. C., Slessarev, M., Han, J., Fisher, J. A., Rossignol, S., & Hoge, R. D. (2010). BOLD signal responses to controlled hypercapnia in human spinal cord. *Neuroimage*, *50*(3), 1074-1084. https://doi.org/10.1016/j.neuroimage.2009.12.122

Cohen-Adad, J., Levy, S., & Avants, B. (2015). *Slice-by-slice regularized registration for spinal cord MRI: SliceReg* ISMRM, Toronto, Canada. https://www.dropbox.com/s/v3bb3etbq4gb111/cohenadad_ismrm15_slicereg.pdf?dl=0

Combes, A. J. E., O'Grady, K. P., Rogers, B. P., Schilling, K. G., Lawless, R. D., Visagie, M., Houston, D., Prock, L., Malone, S., Satish, S., Witt, A. A., McKnight, C. D., Bagnato, F., Gore, J. C., & Smith, S. A. (2022). Functional connectivity in the dorsal network of the cervical spinal cord is correlated with diffusion tensor imaging indices in relapsing-remitting multiple sclerosis. *Neuroimage Clin*, *35*, 103127. https://doi.org/10.1016/j.nicl.2022.103127

Conrad, B. N., Barry, R. L., Rogers, B. P., Maki, S., Mishra, A., Thukral, S., Sriram, S., Bhatia, A., Pawate, S., Gore, J. C., & Smith, S. A. (2018). Multiple sclerosis lesions affect intrinsic functional connectivity of the spinal cord. *Brain*, *141*(6), 1650-1664. https://doi.org/10.1093/brain/awy083

D'Souza M, M., Choudhary, A., Poonia, M., Kumar, P., & Khushu, S. (2017). Diffusion tensor MR imaging in spinal cord injury. *Injury*, *48*(4), 880-884. https://doi.org/10.1016/j.injury.2017.02.016

Davies, B. M., Phillips, R., Clarke, D., Furlan, J. C., Demetriades, A. K., Milligan, J., Witiw, C. D., Harrop, J. S., Aarabi, B., Kurpad, S. N., Guest, J. D., Wilson, J. R., Kwon, B. K., Vaccaro, A. R., Fehlings, M. G., Rahimi-Movaghar, V., & Kotter, M. R. N. (2022). Establishing the Socio-Economic Impact of Degenerative Cervical Myelopathy Is Fundamental to Improving Outcomes [AO Spine RECODE-DCM Research Priority Number 8]. *Global Spine J*, *12*(1_suppl), 122S-129S. https://doi.org/10.1177/21925682211039835

De Groote, S., De Jaeger, M., Van Schuerbeek, P., Sunaert, S., Peeters, R., Loeckx, D., Goudman, L., Forget, P., De Smedt, A., & Moens, M. (2018). Functional magnetic resonance imaging: cerebral function alterations in subthreshold and suprathreshold spinal cord stimulation. *J Pain Res*, *11*, 2517-2526. https://doi.org/10.2147/JPR.S160890

De Leener, B., Cohen-Adad, J., & Kadoury, S. (2015). Automatic Segmentation of the Spinal Cord and Spinal Canal Coupled With Vertebral Labeling. *IEEE Trans Med Imaging*, *34*(8), 1705-1718. https://doi.org/10.1109/TMI.2015.2437192

De Leener, B., Fonov, V. S., Collins, D. L., Callot, V., Stikov, N., & Cohen-Adad, J. (2018). PAM50: Unbiased multimodal template of the brainstem and spinal cord aligned with the ICBM152 space. *Neuroimage*, *165*, 170-179. https://doi.org/10.1016/j.neuroimage.2017.10.041

De Leener, B., Levy, S., Dupont, S. M., Fonov, V. S., Stikov, N., Louis Collins, D., Callot, V., & Cohen-Adad, J. (2017). SCT: Spinal Cord Toolbox, an open-source software for processing spinal cord MRI data. *Neuroimage*, *145*(Pt A), 24-43. https://doi.org/10.1016/j.neuroimage.2016.10.009

Denno, J. J., & Meadows, G. R. (1991). Early diagnosis of cervical spondylotic myelopathy. A useful clinical sign. *Spine (Phila Pa 1976)*, *16*(12), 1353-1355. https://doi.org/10.1097/00007632-199112000-00001

Desmedt, J. E., & Cheron, G. (1981). Prevertebral (oesophageal) recording of subcortical somatosensory evoked potentials in man: the spinal P13 component and the dual nature of the spinal generators. *Electroencephalogr Clin Neurophysiol*, *52*(4), 257-275. https://doi.org/10.1016/0013-4694(81)90055-9

Dohle, E., Beardall, S., Chang, A., Mena, K. P. C., Jovanovic, L., Nath, U., Lee, K. S., Smith, A. H., Thirunavukarasu, A. J., Touzet, A. Y., Norton, E. J., Mowforth, O. D., Kotter, M. R. N., & Davies, B. M. (2023). Human spinal cord tissue is an underutilised resource in degenerative cervical myelopathy: findings from a systematic review of human autopsies. *Acta Neurochir (Wien)*, *165*(5), 1121-1131. https://doi.org/10.1007/s00701-023-05526-5

Doita, M., Sakai, H., Harada, T., Nishida, K., Miyamoto, H., Kaneko, T., & Kurosaka, M. (2006). Evaluation of impairment of hand function in patients with cervical myelopathy. *J Spinal Disord Tech*, *19*(4), 276-280. https://doi.org/10.1097/01.bsd.0000203275.97627.9f

Dvorak, J., Sutter, M., & Herdmann, J. (2003). Cervical myelopathy: clinical and neurophysiological evaluation. *Eur Spine J*, *12 Suppl 2*(Suppl 2), S181-187. https://doi.org/10.1007/s00586-003-0631-y

Eippert, F., Kong, Y., Winkler, A. M., Andersson, J. L., Finsterbusch, J., Buchel, C., Brooks, J. C. W., & Tracey, I. (2017). Investigating resting-state functional connectivity in the cervical spinal cord at 3T. *Neuroimage*, *147*, 589-601. https://doi.org/10.1016/j.neuroimage.2016.12.072

el-Negamy, E., & Sedgwick, E. M. (1978). Properties of a spinal somatosensory evoked potential recorded in man. *J Neurol Neurosurg Psychiatry*, *41*(8), 762-768. https://doi.org/10.1136/jnnp.41.8.762

Farah, K., McHinda, S., Pini, L., Baucher, G., Roche, P. H., Fuentes, S., & Callot, V. (2025). T1 mapping using MP2RAGE in degenerative cervical myelopathy: a longitudinal study. *Eur Spine J*, *34*(2), 731-740. https://doi.org/10.1007/s00586-025-08652-z

Fehlings, M. G., Ibrahim, A., Tetreault, L., Albanese, V., Alvarado, M., Arnold, P., Barbagallo, G., Bartels, R., Bolger, C., Defino, H., Kale, S., Massicotte, E., Moraes, O., Scerrati, M., Tan, G., Tanaka, M., Toyone, T., Yukawa, Y., Zhou, Q., . . . Kopjar, B. (2015). A global perspective on the outcomes of surgical decompression in patients with cervical spondylotic myelopathy: results from the prospective multicenter AOSpine international study on 479 patients. *Spine (Phila Pa 1976)*, *40*(17), 1322-1328. https://doi.org/10.1097/BRS.0000000000000988

Fehlings, M. G., Tetreault, L. A., Kurpad, S., Brodke, D. S., Wilson, J. R., Smith, J. S., Arnold, P. M., Brodt, E. D., & Dettori, J. R. (2017). Change in Functional Impairment, Disability, and Quality of Life Following Operative Treatment for Degenerative Cervical Myelopathy: A Systematic Review and Meta-Analysis. *Global Spine J*, *7*(3 Suppl), 53S-69S. https://doi.org/10.1177/2192568217710137

Fehlings, M. G., Wilson, J. R., Kopjar, B., Yoon, S. T., Arnold, P. M., Massicotte, E. M., Vaccaro, A. R., Brodke, D. S., Shaffrey, C. I., Smith, J. S., Woodard, E. J., Banco, R. J., Chapman, J. R., Janssen, M. E., Bono, C. M., Sasso, R. C., Dekutoski, M. B., & Gokaslan, Z. L. (2013). Efficacy and safety of surgical decompression in patients with cervical spondylotic myelopathy: results of the AOSpine North America prospective multi-center study. *J Bone Joint Surg Am*, *95*(18), 1651-1658. https://doi.org/10.2106/JBJS.L.00589

Figley, C. R., Leitch, J. K., & Stroman, P. W. (2010). In contrast to BOLD: signal enhancement by extravascular water protons as an alternative mechanism of endogenous fMRI signal change. *Magn Reson Imaging*, *28*(8), 1234-1243. https://doi.org/10.1016/j.mri.2010.01.005

Filimonova, E., Abdaev, M., Vasilenko, I., Kubetskij, Y., Prokhorov, O., & Rzaev, J. (2024a). Evaluation of the structural integrity of different spinal cord tracts with magnetization transfer ratio in degenerative cervical myelopathy. *Neuroradiology*, *66*(5), 839-846. https://doi.org/10.1007/s00234-024-03327-w

Filimonova, E., Abdaev, M., Vasilenko, I., Kubetskij, Y., Prokhorov, O., & Rzaev, J. (2024b). White matter spinal tracts impairment in patients with degenerative cervical myelopathy evaluated with the magnetization transfer saturation MRI technique. *Spinal Cord*, *62*(10), 590-596. https://doi.org/10.1038/s41393-024-01025-1

Filimonova, E., Letyagin, V., Zaitsev, B., Kubetsky, Y., & Rzaev, J. (2024). Application of the T1w/T2w mapping technique for spinal cord assessment in patients with degenerative cervical myelopathy. *Spinal Cord*, *62*(1), 6-11. https://doi.org/10.1038/s41393-023-00941-y

Fitzgerald, P. B., Srithiran, A., Benitez, J., Daskalakis, Z. Z., Oxley, T. J., Kulkarni, J., & Egan, G. F. (2008). An fMRI study of prefrontal brain activation during multiple tasks in patients with major depressive disorder. *Hum Brain Mapp*, *29*(4), 490-501. https://doi.org/10.1002/hbm.20414

Freund, P., Boller, V., Emmenegger, T. M., Akbar, M., Hupp, M., Pfender, N., Wheeler-Kingshott, C., Cohen-Adad, J., Fehlings, M. G., Curt, A., & Seif, M. (2024). Quantifying neurodegeneration of the cervical cord and brain in degenerative cervical myelopathy: A multicentre study using quantitative magnetic resonance imaging. *Eur J Neurol*, *31*(7), e16297. https://doi.org/10.1111/ene.16297

Fu, W., Xu, R., Wang, X., Li, H., Chen, X., Wang, L., Yuan, S., Tian, Y., & Liu, X. (2024). Can the 6-minute Walking Test Assess Ambulatory Function Impairment in Patients With

Cervical Spondylotic Myelopathy? *Spine (Phila Pa 1976)*, *49*(21), 1497-1503. https://doi.org/10.1097/BRS.0000000000005095

Funaba, M., Imajo, Y., Suzuki, H., Nishida, N., Nagao, Y., Sakamoto, T., Fujimoto, K., & Sakai, T. (2021). The associations between radiological and neurological findings of degenerative cervical myelopathy: radiological analysis based on kinematic CT myelography and evoked potentials of the spinal cord. *J Neurosurg Spine*, *35*(3), 308-319. https://doi.org/10.3171/2020.11.SPINE201626

Gaines, J. L., Finn, K. E., Slopsema, J. P., Heyboer, L. A., & Polasek, K. H. (2018). A model of motor and sensory axon activation in the median nerve using surface electrical stimulation. *J Comput Neurosci*, *45*(1), 29-43. https://doi.org/10.1007/s10827-018-0689-5

Giulietti, G., Giove, F., Garreffa, G., Colonnese, C., Mangia, S., & Maraviglia, B. (2008). Characterization of the functional response in the human spinal cord: impulse-response function and linearity. *Neuroimage*, *42*(2), 626-634. https://doi.org/10.1016/j.neuroimage.2008.05.006

Glaser, J. A., Cure, J. K., Bailey, K. L., & Morrow, D. L. (2001). Cervical Spinal Cord Compression and the Hoffman Sign. *Iowa Orthop J.*, *21*, 49-52. https://pmc.ncbi.nlm.nih.gov/articles/PMC1888193/

Gloor, M., Andelova, M., Gaetano, L., Papadopoulou, A., Burguet Villena, F., Sprenger, T., Radue, E. W., Kappos, L., Bieri, O., & Garcia, M. (2024). Longitudinal analysis of new multiple sclerosis lesions with magnetization transfer and diffusion tensor imaging. *Eur Radiol*, *34*(3), 1680-1691. https://doi.org/10.1007/s00330-023-10173-6

Glover, G. H. (2011). Overview of functional magnetic resonance imaging. *Neurosurg Clin N Am*, *22*(2), 133-139, vii. https://doi.org/10.1016/j.nec.2010.11.001

Glover, G. H., Li, T. Q., & Ress, D. (2000). Image-based method for retrospective correction of physiological motion effects in fMRI: RETROICOR. *Magn Reson Med*, *44*(1), 162-167. https://doi.org/10.1002/1522-2594(200007)44:1<162::aid-mrm23>3.0.co;2-e

Goulding, M., Bourane, S., Garcia-Campmany, L., Dalet, A., & Koch, S. (2014). Inhibition downunder: an update from the spinal cord. *Curr Opin Neurobiol*, *26*, 161-166. https://doi.org/10.1016/j.conb.2014.03.006

Govers, N., Beghin, J., Van Goethem, J. W., Michiels, J., van den Hauwe, L., Vandervliet, E., & Parizel, P. M. (2007). Functional MRI of the cervical spinal cord on 1.5 T with fingertapping: to what extent is it feasible? *Neuroradiology*, *49*(1), 73-81. https://doi.org/10.1007/s00234-006-0162-4

Grabher, P., Mohammadi, S., David, G., & Freund, P. (2017). Neurodegeneration in the Spinal Ventral Horn Prior to Motor Impairment in Cervical Spondylotic Myelopathy. *J Neurotrauma*, *34*(15), 2329-2334. https://doi.org/10.1089/neu.2017.4980

Grodzinski, B., Durham, R., Mowforth, O., Stubbs, D., Kotter, M. R. N., & Davies, B. M. (2021). The effect of ageing on presentation, management and outcomes in degenerative cervical myelopathy: a systematic review. *Age Ageing*, *50*(3), 705-715. https://doi.org/10.1093/ageing/afaa236

Gros, C., De Leener, B., Badji, A., Maranzano, J., Eden, D., Dupont, S. M., Talbott, J., Zhuoquiong, R., Liu, Y., Granberg, T., Ouellette, R., Tachibana, Y., Hori, M., Kamiya, K., Chougar, L., Stawiarz, L., Hillert, J., Bannier, E., Kerbrat, A., . . . Cohen-Adad, J. (2019). Automatic segmentation of the spinal cord and intramedullary multiple sclerosis

lesions with convolutional neural networks. *Neuroimage*, *184*, 901-915. https://doi.org/10.1016/j.neuroimage.2018.09.081

Haddas, R., Cox, J., Belanger, T., Ju, K. L., & Derman, P. B. (2019). Characterizing gait abnormalities in patients with cervical spondylotic myelopathy: a neuromuscular analysis. *Spine J*, *19*(11), 1803-1808. https://doi.org/10.1016/j.spinee.2019.06.005

Haddas, R., Ju, K. L., Boah, A., Kosztowski, T., & Derman, P. B. (2019). The Effect of Surgical Decompression on Functional Balance Testing in Patients With Cervical Spondylotic Myelopathy. *Clin Spine Surg*, *32*(9), 369-376. https://doi.org/10.1097/BSD.0000000000000889

Hameed, S., Muhammad, F., Haynes, G., Smith, L., Khan, A. F., & Smith, Z. A. (2024). Early neurological changes in aging cervical spine: insights from PROMIS mobility assessment. *Geroscience*, *46*(3), 3123-3134. https://doi.org/10.1007/s11357-023-01050-7

Hardy, T. A. (2021). Spinal Cord Anatomy and Localization. *Continuum (Minneap Minn)*, *27*(1), 12-29. https://doi.org/10.1212/CON.0000000000000899

Harita, S., & Stroman, P. W. (2017). Confirmation of resting-state BOLD fluctuations in the human brainstem and spinal cord after identification and removal of physiological noise. *Magn Reson Med*, *78*(6), 2149-2156. https://doi.org/10.1002/mrm.26606

Harrison, O. K., Guell, X., Klein-Flugge, M. C., & Barry, R. L. (2021). Structural and resting state functional connectivity beyond the cortex. *Neuroimage*, *240*, 118379. https://doi.org/10.1016/j.neuroimage.2021.118379

Harrop, J. S., Naroji, S., Maltenfort, M., Anderson, D. G., Albert, T., Ratliff, J. K., Ponnappan, R. K., Rihn, J. A., Smith, H. E., Hilibrand, A., Sharan, A. D., & Vaccaro, A. (2010). Cervical myelopathy: a clinical and radiographic evaluation and correlation to cervical

spondylotic myelopathy. *Spine (Phila Pa 1976)*, *35*(6), 620-624. https://doi.org/10.1097/BRS.0b013e3181b723af

Haynes, G., Muhammad, F., Khan, A. F., Mohammadi, E., Smith, Z. A., & Ding, L. (2023). The current state of spinal cord functional magnetic resonance imaging and its application in clinical research. *J Neuroimaging*, *33*(6), 877-888. https://doi.org/10.1111/jon.13158

Haynes, G., Muhammad, F., Weber, K. A., 2nd, Khan, A. F., Hameed, S., Ding, L., & Smith, Z. A. (2025). Increased Involuntary Motor Threshold Stimulation in Patients with Degenerative Cervical Myelopathy. *IEEE EMBS NER*, *In Press*.

Haynes, G., Muhammad, F., Weber, K. A., 2nd, Khan, A. F., Hameed, S., Shakir, H., Van Hal, M., Dickson, D., Rohan, M., Dhaher, Y., Parrish, T., Ding, L., & Smith, Z. A. (2024). Tract-specific magnetization transfer ratio provides insights into the severity of degenerative cervical myelopathy. *Spinal Cord*, *62*(12), 700-707. https://doi.org/10.1038/s41393-024-01036-y

Haynes, G., Muhammad, F., Weber, K. A., 2nd, Khan, A. F., Hameed, S., Shakir, H. J., Rohan, M., Ding, L., & Smith, Z. A. (2025). The application of peripheral nerve stimulation for functional MRI in Degenerative Cervical Myelopathy *bioRxiv*. https://doi.org/10.1101/2025.09.17.675603

Heine, L., Soddu, A., Gomez, F., Vanhaudenhuyse, A., Tshibanda, L., Thonnard, M., Charland-Verville, V., Kirsch, M., Laureys, S., & Demertzi, A. (2012). Resting state networks and consciousness: alterations of multiple resting state network connectivity in physiological, pharmacological, and pathological consciousness states. *Front Psychol*, *3*, 295. https://doi.org/10.3389/fpsyg.2012.00295

Hejrati, N., Pedro, K., Alvi, M. A., Quddusi, A., & Fehlings, M. G. (2023). Degenerative cervical myelopathy: Where have we been? Where are we now? Where are we going? *Acta Neurochir (Wien)*, *165*(5), 1105-1119. https://doi.org/10.1007/s00701-023-05558-x

Hirai, T., Otani, K., Sekiguchi, M., Kikuchi, S. I., & Konno, S. I. (2021). Epidemiological study of cervical cord compression and its clinical symptoms in community-dwelling residents. *PLoS One*, *16*(8), e0256732. https://doi.org/10.1371/journal.pone.0256732

Holly, L. T. (2009). Management of cervical spondylotic myelopathy with insights from metabolic imaging of the spinal cord and brain. *Curr Opin Neurol*, *22*(6), 575-581. https://doi.org/10.1097/WCO.0b013e3283325ea7

Holly, L. T., Freitas, B., McArthur, D. L., & Salamon, N. (2009). Proton magnetic resonance spectroscopy to evaluate spinal cord axonal injury in cervical spondylotic myelopathy. *J Neurosurg Spine*, *10*(3), 194-200. https://doi.org/10.3171/2008.12.SPINE08367

Hopkins, B. S., Weber, K. A., 2nd, Cloney, M. B., Paliwal, M., Parrish, T. B., & Smith, Z. A. (2018). Tract-Specific Volume Loss on 3T MRI in Patients With Cervical Spondylotic Myelopathy. *Spine (Phila Pa 1976)*, *43*(20), E1204-E1209. https://doi.org/10.1097/BRS.0000000000002667

Horak, T., Horakova, M., Svatkova, A., Kadanka, Z., Kudlicka, P., Valosek, J., Rohan, T., Kerkovsky, M., Vlckova, E., Kadanka, Z., Deelchand, D. K., Henry, P. G., Bednarik, J., & Bednarik, P. (2021). In vivo Molecular Signatures of Cervical Spinal Cord Pathology in Degenerative Compression. *J Neurotrauma*, *38*(21), 2999-3010. https://doi.org/10.1089/neu.2021.0151

Houten, J. K., & Noce, L. A. (2008). Clinical correlations of cervical myelopathy and the Hoffmann sign. *J Neurosurg Spine*, *9*(3), 237-242. https://doi.org/10.3171/SPI/2008/9/9/237

Hughes, D. I., & Todd, A. J. (2020). Central Nervous System Targets: Inhibitory Interneurons in the Spinal Cord. *Neurotherapeutics*, *17*(3), 874-885. https://doi.org/10.1007/s13311-020-00936-0

Islam, H., Law, C. S. W., Weber, K. A., Mackey, S. C., & Glover, G. H. (2019). Dynamic per slice shimming for simultaneous brain and spinal cord fMRI. *Magn Reson Med*, *81*(2), 825-838. https://doi.org/10.1002/mrm.27388

Ito, T., Oyanagi, K., Takahashi, H., Takahashi, H. E., & Ikuta, F. (1996). Cervical spondylotic myelopathy. Clinicopathologic study on the progression pattern and thin myelinated fibers of the lesions of seven patients examined during complete autopsy. *Spine (Phila Pa 1976)*, *21*(7), 827-833. https://doi.org/10.1097/00007632-199604010-00010

Jenkinson, M., Beckmann, C. F., Behrens, T. E., Woolrich, M. W., & Smith, S. M. (2012). Fsl. *Neuroimage*, *62*(2), 782-790. https://doi.org/10.1016/j.neuroimage.2011.09.015

Jiang, Z., Davies, B., Zipser, C., Margetis, K., Martin, A., Matsoukas, S., Zipser-Mohammadzada, F., Kheram, N., Boraschi, A., Zakin, E., Obadaseraye, O. R., Fehlings, M. G., Wilson, J., Yurac, R., Cook, C. E., Milligan, J., Tabrah, J., Widdop, S., Wood, L., . . . Incubator, A. O. S. R.-D. D. C. (2024). The value of Clinical signs in the diagnosis of Degenerative Cervical Myelopathy - A Systematic review and Meta-analysis. *Global Spine J*, *14*(4), 1369-1394. https://doi.org/10.1177/21925682231209869

Kalsi-Ryan, S., Rienmueller, A. C., Riehm, L., Chan, C., Jin, D., Martin, A. R., Badhiwala, J. H., Akbar, M. A., Massicotte, E. M., & Fehlings, M. G. (2020). Quantitative Assessment of

Gait Characteristics in Degenerative Cervical Myelopathy: A Prospective Clinical Study. *J Clin Med*, *9*(3). https://doi.org/10.3390/jcm9030752

Kato, S., & Fehlings, M. (2016). Degenerative cervical myelopathy. *Curr Rev Musculoskelet Med*, *9*(3), 263-271. https://doi.org/10.1007/s12178-016-9348-5

Kato, S., Oshima, Y., Oka, H., Chikuda, H., Takeshita, Y., Miyoshi, K., Kawamura, N., Masuda, K., Kunogi, J., Okazaki, R., Azuma, S., Hara, N., Tanaka, S., & Takeshita, K. (2015). Comparison of the Japanese Orthopaedic Association (JOA) score and modified JOA (mJOA) score for the assessment of cervical myelopathy: a multicenter observational study. *PLoS One*, *10*(4), e0123022. https://doi.org/10.1371/journal.pone.0123022

Khan, A. F., Haynes, G., Mohammadi, E., Muhammad, F., Hameed, S., & Smith, Z. A. (2023). Utility of MRI in Quantifying Tissue Injury in Cervical Spondylotic Myelopathy. *J Clin Med*, *12*(9). https://doi.org/10.3390/jcm12093337

Khatibi, A., Vahdat, S., Lungu, O., Finsterbusch, J., Buchel, C., Cohen-Adad, J., Marchand-Pauvert, V., & Doyon, J. (2022). Brain-spinal cord interaction in long-term motor sequence learning in human: an fMRI study. *Neuroimage*, *253*, 119111. https://doi.org/10.1016/j.neuroimage.2022.119111

Kinany, N., Khatibi, A., Lungu, O., Finsterbusch, J., Buchel, C., Marchand-Pauvert, V., Van De Ville, D., Vahdat, S., & Doyon, J. (2023). Decoding cerebro-spinal signatures of human behavior: application to motor sequence learning. *Neuroimage*, *275*, 120174. https://doi.org/10.1016/j.neuroimage.2023.120174

Kinany, N., Pirondini, E., Micera, S., & Van De Ville, D. (2020). Dynamic functional connectivity of resting-state spinal cord fMRI reveals fine-grained intrinsic architecture. *Neuron*, *108*(3), 424-435. https://doi.org/10.1016/j.neuron.2020.07.024

Kinany, N., Pirondini, E., Micera, S., & Van De Ville, D. (2022). Spinal Cord fMRI: A New Window into the Central Nervous System. *Neuroscientist*, 10738584221101827. https://doi.org/10.1177/10738584221101827

Kinany, N., Pirondini, E., Micera, S., & Van De Ville, D. (2023). Spinal Cord fMRI: A New Window into the Central Nervous System. *Neuroscientist*, *29*(6), 715-731. https://doi.org/10.1177/10738584221101827

Knikou, M. (2008). The H-reflex as a probe: pathways and pitfalls. *J Neurosci Methods*, *171*(1), 1-12. https://doi.org/10.1016/j.jneumeth.2008.02.012

Kong, Y., Eippert, F., Beckmann, C. F., Andersson, J., Finsterbusch, J., Buchel, C., Tracey, I., & Brooks, J. C. (2014). Intrinsically organized resting state networks in the human spinal cord. *Proc Natl Acad Sci U S A*, *111*(50), 18067-18072. https://doi.org/10.1073/pnas.1414293111

Kopjar, B., Bohm, P. E., Arnold, J. H., Fehlings, M. G., Tetreault, L. A., & Arnold, P. M. (2018). Outcomes of Surgical Decompression in Patients With Very Severe Degenerative Cervical Myelopathy. *Spine (Phila Pa 1976)*, *43*(16), 1102-1109. https://doi.org/10.1097/BRS.0000000000002602

Kornelsen, J., Smith, S. D., McIver, T. A., Sboto-Frankenstein, U., Latta, P., & Tomanek, B. (2013). Functional MRI of the thoracic spinal cord during vibration sensation. *J Magn Reson Imaging*, *37*(4), 981-985. https://doi.org/10.1002/jmri.23819

Kornelsen, J., & Stroman, P. W. (2004). fMRI of the lumbar spinal cord during a lower limb motor task. *Magn Reson Med*, *52*(2), 411-414. https://doi.org/10.1002/mrm.20157

Kornelsen, J., & Stroman, P. W. (2007). Detection of the neuronal activity occurring caudal to the site of spinal cord injury that is elicited during lower limb movement tasks. *Spinal Cord*, *45*(7), 485-490. https://doi.org/10.1038/sj.sc.3102019

Kowalczyk, I., Duggal, N., & Bartha, R. (2012). Proton magnetic resonance spectroscopy of the motor cortex in cervical myelopathy. *Brain*, *135*(Pt 2), 461-468. https://doi.org/10.1093/brain/awr328

Landelle, C., Lungu, O., Vahdat, S., Kavounoudias, A., Marchand-Pauvert, V., De Leener, B., & Doyon, J. (2021). Investigating the human spinal sensorimotor pathways through functional magnetic resonance imaging. *Neuroimage*, *245*, 118684. https://doi.org/10.1016/j.neuroimage.2021.118684

Lannon, M., & Kachur, E. (2021). Degenerative Cervical Myelopathy: Clinical Presentation, Assessment, and Natural History. *J Clin Med*, *10*(16). https://doi.org/10.3390/jcm10163626

Lebret, A., Levy, S., Pfender, N., Farshad, M., Altorfer, F. C. S., Callot, V., Curt, A., Freund, P., & Seif, M. (2023). Investigation of perfusion impairment in degenerative cervical myelopathy beyond the site of cord compression. *Sci Rep*, *13*(1), 22660. https://doi.org/10.1038/s41598-023-49896-3

Leung, R. H., & Stroman, P. W. (2016). Functional magnetic resonance imaging of the human brainstem and cervical spinal cord during cognitive modulation of pain. *Crit Rev Biomed Eng*, *44*(1-2), 47-71. https://doi.org/10.1615/CritRevBiomedEng.2016016541

Levy, S., Baucher, G., Roche, P. H., Evin, M., Callot, V., & Arnoux, P. J. (2021). Biomechanical comparison of spinal cord compression types occurring in Degenerative Cervical

Myelopathy. *Clin Biomech (Bristol)*, *81*, 105174. https://doi.org/10.1016/j.clinbiomech.2020.105174

Levy, S., Benhamou, M., Naaman, C., Rainville, P., Callot, V., & Cohen-Adad, J. (2015). White matter atlas of the human spinal cord with estimation of partial volume effect. *Neuroimage*, *119*, 262-271. https://doi.org/10.1016/j.neuroimage.2015.06.040

Liu, H., MacMillan, E. L., Jutzeler, C. R., Ljungberg, E., MacKay, A. L., Kolind, S. H., Madler, B., Li, D. K. B., Dvorak, M. F., Curt, A., Laule, C., & Kramer, J. L. K. (2017). Assessing structure and function of myelin in cervical spondylotic myelopathy: Evidence of demyelination. *Neurology*, *89*(6), 602-610. https://doi.org/10.1212/WNL.0000000000004197

Liu, Q., Shao, H., Liu, C., Liu, W. V., Saeed, A., Zhang, Q., Lu, J., Zhang, G., Li, L., Tang, X., Du, G., & Zhu, W. (2023). Quantitative evaluation of the spinal cord compression in patients with cervical spondylotic myelopathy using synthetic MRI. *Front Physiol*, *14*, 1140870. https://doi.org/10.3389/fphys.2023.1140870

Liu, X., Qian, W., Jin, R., Li, X., Luk, K. D., Wu, E. X., & Hu, Y. (2016). Amplitude of low frequency fluctuation (ALFF) in the cervical spinal cord with stenosis: a resting state fMRI study. *PLoS One*, *11*(12), e0167279. https://doi.org/10.1371/journal.pone.0167279

MacKay, A. L., & Laule, C. (2016). Magnetic Resonance of Myelin Water: An in vivo Marker for Myelin. *Brain Plast*, *2*(1), 71-91. https://doi.org/10.3233/BPL-160033

Madi, S., Flanders, A. E., Vinitski, S., Herbison, G. J., & Nissanov, J. (2001). Functional MR imaging of the human cervical spinal cord. *AJNR Am J Neuroradiol*, *22*(9), 1768-1774. https://www.ncbi.nlm.nih.gov/pubmed/11673177

Maier, I. L., Hofer, S., Eggert, E., Schregel, K., Psychogios, M. N., Frahm, J., Bahr, M., & Liman, J. (2020). T1 Mapping Quantifies Spinal Cord Compression in Patients With Various Degrees of Cervical Spinal Canal Stenosis. *Front Neurol*, *11*, 574604. https://doi.org/10.3389/fneur.2020.574604

Maieron, M., Iannetti, G. D., Bodurka, J., Tracey, I., Bandettini, P. A., & Porro, C. A. (2007). Functional responses in the human spinal cord during willed motor actions: evidence for side- and rate-dependent activity. *J Neurosci*, *27*(15), 4182-4190. https://doi.org/10.1523/JNEUROSCI.3910-06.2007

Malone, A., Meldrum, D., Gleeson, J., & Bolger, C. (2013). Electromyographic characteristics of gait impairment in cervical spondylotic myelopathy. *Eur Spine J*, *22*(11), 2538-2544. https://doi.org/10.1007/s00586-013-2928-9

Martin, A. R., Aleksanderek, I., Cohen-Adad, J., Tarmohamed, Z., Tetreault, L., Smith, N., Cadotte, D. W., Crawley, A., Ginsberg, H., Mikulis, D. J., & Fehlings, M. G. (2016). Translating state-of-the-art spinal cord MRI techniques to clinical use: A systematic review of clinical studies utilizing DTI, MT, MWF, MRS, and fMRI. *Neuroimage Clin*, *10*, 192-238. https://doi.org/10.1016/j.nicl.2015.11.019

Martin, A. R., De Leener, B., Cohen-Adad, J., Cadotte, D. W., Kalsi-Ryan, S., Lange, S. F., Tetreault, L., Nouri, A., Crawley, A., Mikulis, D. J., Ginsberg, H., & Fehlings, M. G. (2017). A Novel MRI Biomarker of Spinal Cord White Matter Injury: T2*-Weighted White Matter to Gray Matter Signal Intensity Ratio. *AJNR Am J Neuroradiol*, *38*(6), 1266-1273. https://doi.org/10.3174/ajnr.A5162

Martucci, K. T., Weber, K. A., 2nd, & Mackey, S. C. (2019). Altered cervical spinal cord resting-state activity in fibromyalgia. *Arthritis Rheumatol*, *71*(3), 441-450. https://doi.org/10.1002/art.40746

Maxwell, D. J., & Soteropoulos, D. S. (2020). The mammalian spinal commissural system: properties and functions. *Journal of Neurophysiology*, *123*(1), 4-21. https://doi.org/10.1152/jn.00347.2019

Mazurek, M. T., & Shin, A. Y. (2001). Upper extremity peripheral nerve anatomy: current concepts and applications. *Clin Orthop Relat Res*(383), 7-20. https://doi.org/10.1097/00003086-200102000-00004

Moffitt, M. A., Dale, B. M., Duerk, J. L., & Grill, W. M. (2005). Functional magnetic resonance imaging of the human lumbar spinal cord. *J Magn Reson Imaging*, *21*(5), 527-535. https://doi.org/10.1002/jmri.20314

Muhammad, F., Baha, A., Haynes, G., Shakir, H., Omini, M., Martin, M., Weber, K. A., 2nd, Paliwal, M., Van Hal, M., Dickson, D., Dhaher, Y., Zhao, Y. D., & Smith, Z. A. (2023). Isolating Neurologic Deficits in Cervical Spondylotic Myelopathy: A Case-Controlled Study, Using the NIH Toolbox Motor Battery. *Neurol Clin Pract*, *13*(2), e200126. https://doi.org/10.1212/CPJ.0000000000200126

Muhammad, F., Weber, K. A., 2nd, Bedard, S., Haynes, G., Smith, L., Khan, A. F., Hameed, S., Gray, K., McGovern, K., Rohan, M., Ding, L., Van Hal, M., Dickson, D., Tamimi, M. A., Parrish, T., Dhaher, Y., & Smith, Z. A. (2024). Cervical spinal cord morphometrics in degenerative cervical myelopathy: quantification using semi-automated normalized technique and correlation with neurological dysfunctions. *Spine J*, *24*(11), 2045-2057. https://doi.org/10.1016/j.spinee.2024.07.002

Muhammad, F., Weber, K. A., 2nd, Bédard, S., Haynes, G., & Smith, Z. A. (2025). Semiautomated Pipeline Effectively Assesses Severity and Monitor Disease Progression in Compressed Spinal Cord of Degenerative Cervical Myelopathy Patients. *Neurosurgery Practice*, *6*(2). https://doi.org/10.1227/neuprac.0000000000000138

Muhammad, F., Weber, K. A., 2nd, Haynes, G., Villeneuve, L., Smith, L., Baha, A., Hameed, S., Khan, A. F., Dhaher, Y., Parrish, T., Rohan, M., & Smith, Z. A. (2025). Magnetization transfer MRI (MT-MRI) detects white matter damage beyond the primary site of compression in degenerative cervical myelopathy using a novel semi-automated analysis. *Comput Biol Med*, *197*(Pt B), 111083. https://doi.org/10.1016/j.compbiomed.2025.111083

Muhammad, F., Weber, K. A., 2nd, Rohan, M., & Smith, Z. A. (2024). Patterns of cortical thickness alterations in degenerative cervical myelopathy: associations with dexterity and gait dysfunctions. *Brain Commun*, *6*(5), fcae279. https://doi.org/10.1093/braincomms/fcae279

Mummaneni, P. V., Kaiser, M. G., Matz, P. G., Anderson, P. A., Groff, M., Heary, R., Holly, L., Ryken, T., Choudhri, T., Vresilovic, E., Resnick, D., Joint Section on Disorders of the, S., Peripheral Nerves of the American Association of Neurological, S., & Congress of Neurological, S. (2009). Preoperative patient selection with magnetic resonance imaging, computed tomography, and electroencephalography: does the test predict outcome after cervical surgery? *J Neurosurg Spine*, *11*(2), 119-129. https://doi.org/10.3171/2009.3.SPINE08717

Nagata, K., Yoshimura, N., Muraki, S., Hashizume, H., Ishimoto, Y., Yamada, H., Takiguchi, N., Nakagawa, Y., Oka, H., Kawaguchi, H., Nakamura, K., Akune, T., & Yoshida, M.

(2012). Prevalence of cervical cord compression and its association with physical performance in a population-based cohort in Japan: the Wakayama Spine Study. *Spine (Phila Pa 1976)*, *37*(22), 1892-1898. https://doi.org/10.1097/BRS.0b013e31825a2619

Nakata, H., Domoto, R., Mizuguchi, N., Sakamoto, K., & Kanosue, K. (2019). Negative BOLD responses during hand and foot movements: An fMRI study. *PLoS One*, *14*(4), e0215736. https://doi.org/10.1371/journal.pone.0215736

Ng, M. C., Wu, E. X., Lau, H. F., Hu, Y., Lam, E. Y., & Luk, K. D. (2008). Cervical spinal cord BOLD fMRI study: modulation of functional activation by dexterity of dominant and non-dominant hands. *Neuroimage*, *39*(2), 825-831. https://doi.org/10.1016/j.neuroimage.2007.09.026

Nishida, N., Kato, Y., Imajo, Y., Kawano, S., & Taguchi, T. (2012). Biomechanical analysis of cervical spondylotic myelopathy: the influence of dynamic factors and morphometry of the spinal cord. *J Spinal Cord Med*, *35*(4), 256-261. https://doi.org/10.1179/2045772312Y.0000000024

Nouri, A., Martin, A. R., Kato, S., Reihani-Kermani, H., Riehm, L. E., & Fehlings, M. G. (2017). The Relationship Between MRI Signal Intensity Changes, Clinical Presentation, and Surgical Outcome in Degenerative Cervical Myelopathy: Analysis of a Global Cohort. *Spine (Phila Pa 1976)*, *42*(24), 1851-1858. https://doi.org/10.1097/BRS.0000000000002234

Nouri, A., Martin, A. R., Mikulis, D., & Fehlings, M. G. (2016). Magnetic resonance imaging assessment of degenerative cervical myelopathy: a review of structural changes and measurement techniques. *Neurosurg Focus*, *40*(6), E5. https://doi.org/10.3171/2016.3.FOCUS1667

Nouri, A., Tetreault, L., Dalzell, K., Zamorano, J. J., & Fehlings, M. G. (2017). The Relationship Between Preoperative Clinical Presentation and Quantitative Magnetic Resonance Imaging Features in Patients With Degenerative Cervical Myelopathy. *Neurosurgery*, *80*(1), 121-128. https://doi.org/10.1227/NEU.0000000000001420

Nouri, A., Tetreault, L., Singh, A., Karadimas, S. K., & Fehlings, M. G. (2015). Degenerative Cervical Myelopathy: Epidemiology, Genetics, and Pathogenesis. *Spine (Phila Pa 1976)*, *40*(12), E675-693. https://doi.org/10.1097/BRS.0000000000000913

Nurick, S. (1972). The pathogenesis of the spinal cord disorder associated with cervical spondylosis. *Brain*, *95*(1), 87-100. https://doi.org/10.1093/brain/95.1.87

O'Donnell, L. J., & Westin, C. F. (2011). An introduction to diffusion tensor image analysis. *Neurosurg Clin N Am*, *22*(2), 185-196, viii. https://doi.org/10.1016/j.nec.2010.12.004

Ogawa, S., Tank, D. W., Menon, R., Ellermann, J. M., Kim, S. G., Merkle, H., & Ugurbil, K. (1992). Intrinsic signal changes accompanying sensory stimulation: functional brain mapping with magnetic resonance imaging. *Proc Natl Acad Sci U S A*, *89*(13), 5951-5955. https://doi.org/10.1073/pnas.89.13.5951

Oliva, V., Bedard, S., Kaptan, M., Pfyffer, D., Chy, B., Aufrichtig, S., Berhe, N., Chaudhari, A. S., Tharin, S., Hu, S. S., Ratliff, J., Smith, Z. A., Smith, A. C., Glover, G. H., Mackey, S., Law, C. S. W., & Weber, K. A. (2025). Mapping Hand Function with Simultaneous Brain-Spinal Cord Functional MRI. *Imaging Neuroscience*. https://doi.org/10.1162/IMAG.a.159

Oliva, V., Hartley-Davies, R., Moran, R., Pickering, A. E., & Brooks, J. C. (2022). Simultaneous brain, brainstem, and spinal cord pharmacological-fMRI reveals involvement of an

endogenous opioid network in attentional analgesia. *Elife*, *11*. https://doi.org/10.7554/eLife.71877

Omori, M., Shibuya, S., Nakajima, T., Endoh, T., Suzuki, S., Irie, S., Ariyasu, R., Unenaka, S., Sano, H., Igarashi, K., Ichimura, S., & Ohki, Y. (2018). Hand Dexterity Impairment in Patients with Cervical Myelopathy: A New Quantitative Assessment Using a Natural Prehension Movement. *Behav Neurol*, *2018*, 5138234. https://doi.org/10.1155/2018/5138234

Ouzzani, M., Hammady, H., Fedorowicz, Z., & Elmagarmid, A. (2016). Rayyan-a web and mobile app for systematic reviews. *Syst Rev*, *5*(1), 210. https://doi.org/10.1186/s13643-016-0384-4

Paliwal, M., Weber, K. A., 2nd, Hopkins, B. S., Cantrell, D. R., Hoggarth, M. A., Elliott, J. M., Dahdaleh, N. S., Mackey, S., Parrish, T. D., Dhaher, Y., & Smith, Z. A. (2020). Magnetization Transfer Ratio and Morphometrics of the Spinal Cord Associates with Surgical Recovery in Patients with Degenerative Cervical Myelopathy. *World Neurosurg*, *144*, e939-e947. https://doi.org/10.1016/j.wneu.2020.09.148

Pandita, N., Gupta, S., Raina, P., Srivastava, A., Hakak, A. Y., Singh, O., Darokhan, M. A., & Butt, M. F. (2019). Neurological Recovery Pattern in Cervical Spondylotic Myelopathy after Anterior Surgery: A Prospective Study with Literature Review. *Asian Spine J*, *13*(3), 423-431. https://doi.org/10.31616/asj.2018.0139

Patwardhan, A. G., Khayatzadeh, S., Havey, R. M., Voronov, L. I., Smith, Z. A., Kalmanson, O., Ghanayem, A. J., & Sears, W. (2018). Cervical sagittal balance: a biomechanical perspective can help clinical practice. *Eur Spine J*, *27*(Suppl 1), 25-38. https://doi.org/10.1007/s00586-017-5367-1

Perone, C. S., Calabrese, E., & Cohen-Adad, J. (2018). Spinal cord gray matter segmentation using deep dilated convolutions. *Sci Rep*, *8*(1), 5966. https://doi.org/10.1038/s41598-018-24304-3

Poitelon, Y., Kopec, A. M., & Belin, S. (2020). Myelin Fat Facts: An Overview of Lipids and Fatty Acid Metabolism. *Cells*, *9*(4). https://doi.org/10.3390/cells9040812

Rafati Fard, A., Mowforth, O. D., Yuan, M., Myrtle, S., Lee, K. S., Banerjee, A., Khan, M., Kotter, M. R., Newcombe, V. F. J., Stamatakis, E. A., & Davies, B. M. (2024). Brain MRI changes in degenerative cervical myelopathy: a systematic review. *EBioMedicine*, *99*, 104915. https://doi.org/10.1016/j.ebiom.2023.104915

Rao, R. D., Currier, B. L., Albert, T. J., Bono, C. M., Marawar, S. V., Poelstra, K. A., & Eck, J. C. (2007). Degenerative cervical spondylosis: clinical syndromes, pathogenesis, and management. *J Bone Joint Surg Am*, *89*(6), 1360-1378. https://doi.org/10.2106/00004623-200706000-00026

Rempe, T., Wolff, S., Riedel, C., Baron, R., Stroman, P. W., Jansen, O., & Gierthmuhlen, J. (2014). Spinal fMRI reveals decreased descending inhibition during secondary mechanical hyperalgesia. *PLoS One*, *9*(11), e112325. https://doi.org/10.1371/journal.pone.0112325

Rempe, T., Wolff, S., Riedel, C., Baron, R., Stroman, P. W., Jansen, O., & Gierthmuhlen, J. (2015). Spinal and supraspinal processing of thermal stimuli: an fMRI study. *J Magn Reson Imaging*, *41*(4), 1046-1055. https://doi.org/10.1002/jmri.24627

Rhee, J. M., Heflin, J. A., Hamasaki, T., & Freedman, B. (2009). Prevalence of physical signs in cervical myelopathy: a prospective, controlled study. *Spine (Phila Pa 1976)*, *34*(9), 890-895. https://doi.org/10.1097/BRS.0b013e31819c944b

Rhee, J. M., Shamji, M. F., Erwin, W. M., Bransford, R. J., Yoon, S. T., Smith, J. S., Kim, H. J., Ely, C. G., Dettori, J. R., Patel, A. A., & Kalsi-Ryan, S. (2013). Nonoperative management of cervical myelopathy: a systematic review. *Spine (Phila Pa 1976)*, *38*(22 Suppl 1), S55-67. https://doi.org/10.1097/BRS.0b013e3182a7f41d

Rocca, M. A., Absinta, M., Valsasina, P., Copetti, M., Caputo, D., Comi, G., & Filippi, M. (2012). Abnormal cervical cord function contributes to fatigue in multiple sclerosis. *Mult Scler*, *18*(11), 1552-1559. https://doi.org/10.1177/1352458512440516

Salamon, N., Ellingson, B. M., Nagarajan, R., Gebara, N., Thomas, A., & Holly, L. T. (2013). Proton magnetic resonance spectroscopy of human cervical spondylosis at 3T. *Spinal Cord*, *51*(7), 558-563. https://doi.org/10.1038/sc.2013.31

Sampath, P., Bendebba, M., Davis, J. D., & Ducker, T. B. (2000). Outcome of patients treated for cervical myelopathy. A prospective, multicenter study with independent clinical review. *Spine (Phila Pa 1976)*, *25*(6), 670-676. https://doi.org/10.1097/00007632-200003150-00004

San Emeterio Nateras, O., Yu, F., Muir, E. R., Bazan, C., 3rd, Franklin, C. G., Li, W., Li, J., Lancaster, J. L., & Duong, T. Q. (2016). Intrinsic resting-state functional connectivity in the human spinal cord at 3.0 T. *Radiology*, *279*(1), 262-268. https://doi.org/10.1148/radiol.2015150768

Santillan, A., Nacarino, V., Greenberg, E., Riina, H. A., Gobin, Y. P., & Patsalides, A. (2012). Vascular anatomy of the spinal cord. *J Neurointerv Surg*, *4*(1), 67-74. https://doi.org/10.1136/neurintsurg-2011-010018

Schafer, K., Blankenburg, F., Kupers, R., Gruner, J. M., Law, I., Lauritzen, M., & Larsson, H. B. (2012). Negative BOLD signal changes in ipsilateral primary somatosensory cortex are

associated with perfusion decreases and behavioral evidence for functional inhibition. *Neuroimage*, *59*(4), 3119-3127. https://doi.org/10.1016/j.neuroimage.2011.11.085

Seitzman, B. A., Snyder, A. Z., Leuthardt, E. C., & Shimony, J. S. (2019). The state of resting state networks. *Top Magn Reson Imaging*, *28*(4), 189-196. https://doi.org/10.1097/RMR.0000000000000214

Sharma, S., Sial, A., Sima, S., & Diwan, A. (2025). Clinical signs and symptoms for degenerative cervical myelopathy: a scoping review of case-control studies to facilitate early diagnosis among healthcare professionals with stakeholder engagement. *Spinal Cord*. https://doi.org/10.1038/s41393-025-01065-1

Sherman, J. L., Nassaux, P. Y., & Citrin, C. M. (1990). Measurements of the normal cervical spinal cord on MR imaging. *AJNR Am J Neuroradiol*, *11*(2), 369-372. https://www.ncbi.nlm.nih.gov/pubmed/2107721

Smith, S. D., & Kornelsen, J. (2011). Emotion-dependent responses in spinal cord neurons: a spinal fMRI study. *Neuroimage*, *58*(1), 269-274. https://doi.org/10.1016/j.neuroimage.2011.06.004

Smith, S. M., & Brady, J. M. (1997). SUSAN - A new approach to low level image processing. *International Journal of Computer Vision*, *23*(1), 45-78. https://doi.org/Doi 10.1023/A:1007963824710

Smith, Z. A., Barry, A. J., Paliwal, M., Hopkins, B. S., Cantrell, D., & Dhaher, Y. (2019). Assessing hand dysfunction in cervical spondylotic myelopathy. *PLoS One*, *14*(10), e0223009. https://doi.org/10.1371/journal.pone.0223009

Smith, Z. A., Weber, K. A., 2nd, Paliwal, M., Hopkins, B. S., Barry, A. J., Cantrell, D., Ganju, A., Koski, T. R., Parrish, T. B., & Dhaher, Y. (2020). Magnetic Resonance Imaging

Atlas-Based Volumetric Mapping of the Cervical Cord Gray Matter in Cervical Canal Stenosis. *World Neurosurg*, *134*, e497-e504. https://doi.org/10.1016/j.wneu.2019.10.109

Soda, C., Squintani, G., Teli, M., Marchesini, N., Ricci, U. M., D'Amico, A., Basaldella, F., Concon, E., Tramontano, V., Romito, S., Tommasi, N., Pinna, G., & Sala, F. (2022). Degenerative cervical myelopathy: Neuroradiological, neurophysiological and clinical correlations in 27 consecutive cases. *Brain Spine*, *2*, 100909. https://doi.org/10.1016/j.bas.2022.100909

Sofroniew, M. V. (2018). Dissecting spinal cord regeneration. *Nature*, *557*(7705), 343-350. https://doi.org/10.1038/s41586-018-0068-4

Soufi, K. H., Perez, T. M., Umoye, A. O., Yang, J., Burgos, M., & Martin, A. R. (2022). How Is Spinal Cord Function Measured in Degenerative Cervical Myelopathy? A Systematic Review. *J Clin Med*, *11*(5). https://doi.org/10.3390/jcm11051441

Sparacia, G., Parla, G., Cannella, R., Perri, A., Lo Re, V., Mamone, G., Miraglia, R., Torregrossa, F., & Grasso, G. (2019). Resting-state functional magnetic resonance imaging for brain tumor surgical planning: feasibility in clinical setting. *World Neurosurg*, *131*, 356-363. https://doi.org/10.1016/j.wneu.2019.07.022

Sprenger, C., Finsterbusch, J., & Buchel, C. (2015). Spinal cord-midbrain functional connectivity is related to perceived pain intensity: a combined spino-cortical FMRI study. *J Neurosci*, *35*(10), 4248-4257. https://doi.org/10.1523/JNEUROSCI.4897-14.2015

Staud, R., Boissoneault, J., Lai, S., Mejia, M. S., Ramanlal, R., Godfrey, M. M., & Stroman, P. W. (2021). Spinal cord neural activity of patients with fibromyalgia and healthy controls during temporal summation of pain: an fMRI study. *J Neurophysiol*, *126*(3), 946-956. https://doi.org/10.1152/jn.00276.2021

Stracke, C. P., Pettersson, L. G., Schoth, F., Moller-Hartmann, W., & Krings, T. (2005). Interneuronal systems of the cervical spinal cord assessed with BOLD imaging at 1.5 T. *Neuroradiology*, *47*(2), 127-133. https://doi.org/10.1007/s00234-004-1318-8

Stroman, P. W. (2006). Discrimination of errors from neuronal activity in functional MRI of the human spinal cord by means of general linear model analysis. *Magn Reson Med*, *56*(2), 452-456. https://doi.org/10.1002/mrm.20966

Stroman, P. W. (2009). Spinal fMRI investigation of human spinal cord function over a range of innocuous thermal sensory stimuli and study-related emotional influences. *Magn Reson Imaging*, *27*(10), 1333-1346. https://doi.org/10.1016/j.mri.2009.05.038

Stroman, P. W., Kornelsen, J., Bergman, A., Krause, V., Ethans, K., Malisza, K. L., & Tomanek, B. (2004). Noninvasive assessment of the injured human spinal cord by means of functional magnetic resonance imaging. *Spinal Cord*, *42*(2), 59-66. https://doi.org/10.1038/sj.sc.3101559

Stroman, P. W., Krause, V., Frankenstein, U. N., Malisza, K. L., & Tomanek, B. (2001). Spin-echo versus gradient-echo fMRI with short echo times. *Magn Reson Imaging*, *19*(6), 827-831. https://doi.org/10.1016/s0730-725x(01)00392-7

Stroman, P. W., Krause, V., Malisza, K. L., Frankenstein, U. N., & Tomanek, B. (2001). Characterization of contrast changes in functional MRI of the human spinal cord at 1.5 T. *Magn Reson Imaging*, *19*(6), 833-838. https://doi.org/10.1016/s0730-725x(01)00409-x

Stroman, P. W., Krause, V., Malisza, K. L., Frankenstein, U. N., & Tomanek, B. (2002a). Extravascular proton-density changes as a non-BOLD component of contrast in fMRI of the human spinal cord. *Magn Reson Med*, *48*(1), 122-127. https://doi.org/10.1002/mrm.10178

Stroman, P. W., Krause, V., Malisza, K. L., Frankenstein, U. N., & Tomanek, B. (2002b). Functional magnetic resonance imaging of the human cervical spinal cord with stimulation of different sensory dermatomes. *Magn Reson Imaging*, *20*(1), 1-6. https://doi.org/10.1016/s0730-725x(02)00468-x

Stroman, P. W., Nance, P. W., & Ryner, L. N. (1999). BOLD MRI of the human cervical spinal cord at 3 tesla. *Magn Reson Med*, *42*(3), 571-576. https://doi.org/10.1002/(sici)1522-2594(199909)42:3<571::Aid-mrm20>3.0.Co;2-n

Stroman, P. W., & Ryner, L. N. (2001). Functional MRI of motor and sensory activation in the human spinal cord. *Magn Reson Imaging*, *19*(1), 27-32. https://doi.org/10.1016/s0730-725x(01)00226-0

Stroman, P. W., Tomanek, B., Krause, V., Frankenstein, U. N., & Malisza, K. L. (2002). Mapping of neuronal function in the healthy and injured human spinal cord with spinal fMRI. *Neuroimage*, *17*(4), 1854-1860. https://doi.org/10.1006/nimg.2002.1305

Stroman, P. W., Wheeler-Kingshott, C., Bacon, M., Schwab, J. M., Bosma, R., Brooks, J., Cadotte, D., Carlstedt, T., Ciccarelli, O., Cohen-Adad, J., Curt, A., Evangelou, N., Fehlings, M. G., Filippi, M., Kelley, B. J., Kollias, S., Mackay, A., Porro, C. A., Smith, S., . . . Tracey, I. (2014). The current state-of-the-art of spinal cord imaging: methods. *Neuroimage*, *84*, 1070-1081. https://doi.org/10.1016/j.neuroimage.2013.04.124

Suleiman, L. I., Weber, K. A., 2nd, Rosenthal, B. D., Bhatt, S. A., Savage, J. W., Hsu, W. K., Patel, A. A., & Parrish, T. B. (2018). High-resolution magnetization transfer MRI in patients with cervical spondylotic myelopathy. *J Clin Neurosci*, *51*, 57-61. https://doi.org/10.1016/j.jocn.2018.02.023

Tafti, D., Ehsan, M., & Xixis, K. L. (2022). Multiple Sclerosis. In *StatPearls [Internet]*. StatPearls Publishing. https://www.ncbi.nlm.nih.gov/books/NBK499849/

Tejus, M. N., Singh, V., Ramesh, A., Kumar, V. R., Maurya, V. P., & Madhugiri, V. S. (2015). An evaluation of the finger flexion, Hoffman's and plantar reflexes as markers of cervical spinal cord compression - A comparative clinical study. *Clin Neurol Neurosurg*, *134*, 12-16. https://doi.org/10.1016/j.clineuro.2015.04.009

Tetreault, L., Kopjar, B., Cote, P., Arnold, P., & Fehlings, M. G. (2015). A Clinical Prediction Rule for Functional Outcomes in Patients Undergoing Surgery for Degenerative Cervical Myelopathy: Analysis of an International Prospective Multicenter Data Set of 757 Subjects. *J Bone Joint Surg Am*, *97*(24), 2038-2046. https://doi.org/10.2106/JBJS.O.00189

Tetreault, L., Kopjar, B., Nouri, A., Arnold, P., Barbagallo, G., Bartels, R., Qiang, Z., Singh, A., Zileli, M., Vaccaro, A., & Fehlings, M. G. (2017). The modified Japanese Orthopaedic Association scale: establishing criteria for mild, moderate and severe impairment in patients with degenerative cervical myelopathy. *Eur Spine J*, *26*(1), 78-84. https://doi.org/10.1007/s00586-016-4660-8

Tetreault, L., Wilson, J. R., Kotter, M. R. N., Cote, P., Nouri, A., Kopjar, B., Arnold, P. M., & Fehlings, M. G. (2019). Is Preoperative Duration of Symptoms a Significant Predictor of Functional Outcomes in Patients Undergoing Surgery for the Treatment of Degenerative Cervical Myelopathy? *Neurosurgery*, *85*(5), 642-647. https://doi.org/10.1093/neuros/nyy474

Tetreault, L. A., Karpova, A., & Fehlings, M. G. (2015). Predictors of outcome in patients with degenerative cervical spondylotic myelopathy undergoing surgical treatment: results of a

systematic review. *Eur Spine J*, *24 Suppl 2*, 236-251. https://doi.org/10.1007/s00586-013-2658-z

Tetreault, L. A., Nouri, A., Singh, A., Fawcett, M., & Fehlings, M. G. (2014). Predictors of outcome in patients with cervical spondylotic myelopathy undergoing surgical treatment: a survey of members from AOSpine International. *World Neurosurg*, *81*(3-4), 623-633. https://doi.org/10.1016/j.wneu.2013.09.023

Tinnermann, A., Sprenger, C., & Buchel, C. (2022). Opioid analgesia alters corticospinal coupling along the descending pain system in healthy participants. *Elife*, *11*. https://doi.org/10.7554/eLife.74293

Tognarelli, J. M., Dawood, M., Shariff, M. I., Grover, V. P., Crossey, M. M., Cox, I. J., Taylor-Robinson, S. D., & McPhail, M. J. (2015). Magnetic Resonance Spectroscopy: Principles and Techniques: Lessons for Clinicians. *J Clin Exp Hepatol*, *5*(4), 320-328. https://doi.org/10.1016/j.jceh.2015.10.006

Tu, J., Vargas Castillo, J., Das, A., & Diwan, A. D. (2021). Degenerative Cervical Myelopathy: Insights into Its Pathobiology and Molecular Mechanisms. *J Clin Med*, *10*(6). https://doi.org/10.3390/jcm10061214

Tuchman, A., Tan, L. A., Shillingford, J. N., Li, X. J., & Riew, K. D. (2019). Dynamic changes in the reflex exam of patients with sub-axial cervical stenosis. *J Clin Neurosci*, *60*, 84-87. https://doi.org/10.1016/j.jocn.2018.09.032

Ullmann, E., Pelletier Paquette, J. F., Thong, W. E., & Cohen-Adad, J. (2014). Automatic labeling of vertebral levels using a robust template-based approach. *Int J Biomed Imaging*, *2014*, 719520. https://doi.org/10.1155/2014/719520

Vallotton, K., David, G., Hupp, M., Pfender, N., Cohen-Adad, J., Fehlings, M. G., Samson, R. S., Wheeler-Kingshott, C., Curt, A., Freund, P., & Seif, M. (2021). Tracking White and Gray Matter Degeneration along the Spinal Cord Axis in Degenerative Cervical Myelopathy. *J Neurotrauma*, *38*(21), 2978-2987. https://doi.org/10.1089/neu.2021.0148

Valosek, J., Labounek, R., Horak, T., Horakova, M., Bednarik, P., Kerkovsky, M., Kocica, J., Rohan, T., Lenglet, C., Cohen-Adad, J., Hlustik, P., Vlckova, E., Kadanka, Z., Jr., Bednarik, J., & Svatkova, A. (2021). Diffusion magnetic resonance imaging reveals tract-specific microstructural correlates of electrophysiological impairments in non-myelopathic and myelopathic spinal cord compression. *Eur J Neurol*, *28*(11), 3784-3797. https://doi.org/10.1111/ene.15027

Valsasina, P., Agosta, F., Absinta, M., Sala, S., Caputo, D., & Filippi, M. (2010). Cervical cord functional MRI changes in relapse-onset MS patients. *J Neurol Neurosurg Psychiatry*, *81*(4), 405-408. https://doi.org/10.1136/jnnp.2009.187526

Valsasina, P., Agosta, F., Caputo, D., Stroman, P. W., & Filippi, M. (2008). Spinal fMRI during proprioceptive and tactile tasks in healthy subjects: Activity detected using cross-correlation, general linear model and independent component analysis. *Neuroradiology*, *50*(10), 895-902. https://doi.org/10.1007/s00234-008-0420-8

Valsasina, P., Rocca, M. A., Absinta, M., Agosta, F., Caputo, D., Comi, G., & Filippi, M. (2012). Cervical cord FMRI abnormalities differ between the progressive forms of multiple sclerosis. *Hum Brain Mapp*, *33*(9), 2072-2080. https://doi.org/10.1002/hbm.21346

Vernon, H., & Mior, S. (1991). The Neck Disability Index: a study of reliability and validity. *J Manipulative Physiol Ther*, *14*(7), 409-415. https://www.ncbi.nlm.nih.gov/pubmed/1834753

Weber, K. A., 2nd, Chen, Y., Paliwal, M., Law, C. S., Hopkins, B. S., Mackey, S., Dhaher, Y., Parrish, T. B., & Smith, Z. A. (2020). Assessing the spatial distribution of cervical spinal cord activity during tactile stimulation of the upper extremity in humans with functional magnetic resonance imaging. *Neuroimage*, *217*, 116905. https://doi.org/10.1016/j.neuroimage.2020.116905

Weber, K. A., 2nd, Chen, Y., Wang, X., Kahnt, T., & Parrish, T. B. (2016a). Functional magnetic resonance imaging of the cervical spinal cord during thermal stimulation across consecutive runs. *Neuroimage*, *143*, 267-279. https://doi.org/10.1016/j.neuroimage.2016.09.015

Weber, K. A., 2nd, Chen, Y., Wang, X., Kahnt, T., & Parrish, T. B. (2016b). Lateralization of cervical spinal cord activity during an isometric upper extremity motor task with functional magnetic resonance imaging. *Neuroimage*, *125*, 233-243. https://doi.org/10.1016/j.neuroimage.2015.10.014

Weber, K. A., 2nd, Sentis, A. I., Bernadel-Huey, O. N., Chen, Y., Wang, X., Parrish, T. B., & Mackey, S. (2018). Thermal stimulation alters cervical spinal cord functional connectivity in humans. *Neuroscience*, *369*, 40-50. https://doi.org/10.1016/j.neuroscience.2017.10.035

Wei, P., Li, J., Gao, F., Ye, D., Zhong, Q., & Liu, S. (2010). Resting state networks in human cervical spinal cord observed with fMRI. *Eur J Appl Physiol*, *108*(2), 265-271. https://doi.org/10.1007/s00421-009-1205-4

Wepking, K. N., Mohamed, A., Kurd, M. F., Lee, J. K., Ahmadinia, K., & An, H. S. (2013). The Prevalence of Cervical Radiculopathy in Patients with Cervical Myelopathy. NASS 28th Annual Meeting, New Orleans, LA.

Wilmink, J. T., Backes, W. H., & Mess, W. H. (2003). Functional MRI of the spinal cord: will it solve the puzzle of pain? *JBR-BTR*, *86*(5), 293-294. https://www.ncbi.nlm.nih.gov/pubmed/14651086

Wong, T. M., Leung, H. B., & Wong, W. C. (2004). Correlation between magnetic resonance imaging and radiographic measurement of cervical spine in cervical myelopathic patients. *J Orthop Surg (Hong Kong)*, *12*(2), 239-242. https://doi.org/10.1177/230949900401200220

Woolrich, M. W., Behrens, T. E., Beckmann, C. F., Jenkinson, M., & Smith, S. M. (2004). Multilevel linear modelling for FMRI group analysis using Bayesian inference. *Neuroimage*, *21*(4), 1732-1747. https://doi.org/10.1016/j.neuroimage.2003.12.023

Woolrich, M. W., Ripley, B. D., Brady, M., & Smith, S. M. (2001). Temporal autocorrelation in univariate linear modeling of FMRI data. *Neuroimage*, *14*(6), 1370-1386. https://doi.org/10.1006/nimg.2001.0931

Xie, C. H., Kong, K. M., Guan, J. T., Chen, Y. X., & Wu, R. H. (2007). Functional MR imaging of the cervical spinal cord by use of 20Hz functional electrical stimulation to median nerve. *Annu Int Conf IEEE Eng Med Biol Soc*, *2007*, 3392-3395. https://doi.org/10.1109/IEMBS.2007.4353059

Xie, G., Piche, M., Khoshnejad, M., Perlbarg, V., Chen, J. I., Hoge, R. D., Benali, H., Rossignol, S., Rainville, P., & Cohen-Adad, J. (2012). Reduction of physiological noise with independent component analysis improves the detection of nociceptive responses with fMRI of the human spinal cord. *Neuroimage*, *63*(1), 245-252. https://doi.org/10.1016/j.neuroimage.2012.06.057

Yonenobu, K., Abumi, K., Nagata, K., Taketomi, E., & Ueyama, K. (2001). Interobserver and intraobserver reliability of the japanese orthopaedic association scoring system for evaluation of cervical compression myelopathy. *Spine (Phila Pa 1976)*, *26*(17), 1890-1894; discussion 1895. https://doi.org/10.1097/00007632-200109010-00014

Yonenobu, K., Okada, K., Fuji, T., Fujiwara, K., Yamashita, K., & Ono, K. (1986). Causes of neurologic deterioration following surgical treatment of cervical myelopathy. *Spine (Phila Pa 1976)*, *11*(8), 818-823. https://doi.org/10.1097/00007632-198610000-00016

Yoo, D., Kang, K. C., Lee, J. H., Lee, K. Y., & Hwang, I. U. (2021). Diagnostic usefulness of 10-step tandem gait test for the patient with degenerative cervical myelopathy. *Sci Rep*, *11*(1), 17212. https://doi.org/10.1038/s41598-021-96725-6

Yoshizawa, T., Nose, T., Moore, G. J., & Sillerud, L. O. (1996). Functional magnetic resonance imaging of motor activation in the human cervical spinal cord. *Neuroimage*, *4*(3 Pt 1), 174-182. https://doi.org/10.1006/nimg.1996.0068

Yuan, W., Zhu, Y., Zhu, H., Cui, C., Pei, L., & Huang, Z. (2017). Preoperative cervical sagittal alignment parameters and their impacts on myelopathy in patients with cervical spondylotic myelopathy: a retrospective study. *PeerJ*, *5*, e4027. https://doi.org/10.7717/peerj.4027

Yukawa, Y., Kato, F., Ito, K., Horie, Y., Nakashima, H., Masaaki, M., Ito, Z. Y., & Wakao, N. (2009). "Ten second step test" as a new quantifiable parameter of cervical myelopathy. *Spine (Phila Pa 1976)*, *34*(1), 82-86. https://doi.org/10.1097/BRS.0b013e31818e2b19

Zdunczyk, A., Schwarzer, V., Mikhailov, M., Bagley, B., Rosenstock, T., Picht, T., & Vajkoczy, P. (2018). The Corticospinal Reserve Capacity: Reorganization of Motor Area and

Excitability As a Novel Pathophysiological Concept in Cervical Myelopathy. *Neurosurgery*, *83*(4), 810-818. https://doi.org/10.1093/neuros/nyx437

Zhang, C., Das, S. K., Yang, D. J., & Yang, H. F. (2014). Application of magnetic resonance imaging in cervical spondylotic myelopathy. *World J Radiol*, *6*(10), 826-832. https://doi.org/10.4329/wjr.v6.i10.826

Zhang, J. T., Wang, L. F., Wang, S., Li, J., & Shen, Y. (2016). Risk factors for poor outcome of surgery for cervical spondylotic myelopathy. *Spinal Cord*, *54*(12), 1127-1131. https://doi.org/10.1038/sc.2016.64

Zhang, R. J., Shen, C. L., Zhang, J. X., Zhang, X. J., Dong, F. L., Tao, H., Song, P. W., Ge, P., Xu, P., & Zhang, H. Q. (2018). Clinical features and surgical outcomes of cervical spondylotic myelopathy in patients of different ages: a retrospective study. *Spinal Cord*, *56*(1), 7-13. https://doi.org/10.1038/sc.2017.91

Zhong, X. P., Chen, Y. X., Li, Z. Y., Shen, Z. W., Kong, K. M., & Wu, R. H. (2017). Cervical spinal functional magnetic resonance imaging of the spinal cord injured patient during electrical stimulation. *Eur Spine J*, *26*(1), 71-77. https://doi.org/10.1007/s00586-016-4646-6

APPENDIX

A. Supplemental Figures Accompanying "Tract-specific magnetization transfer ratio provides insights into the severity of degenerative cervical myelopathy"

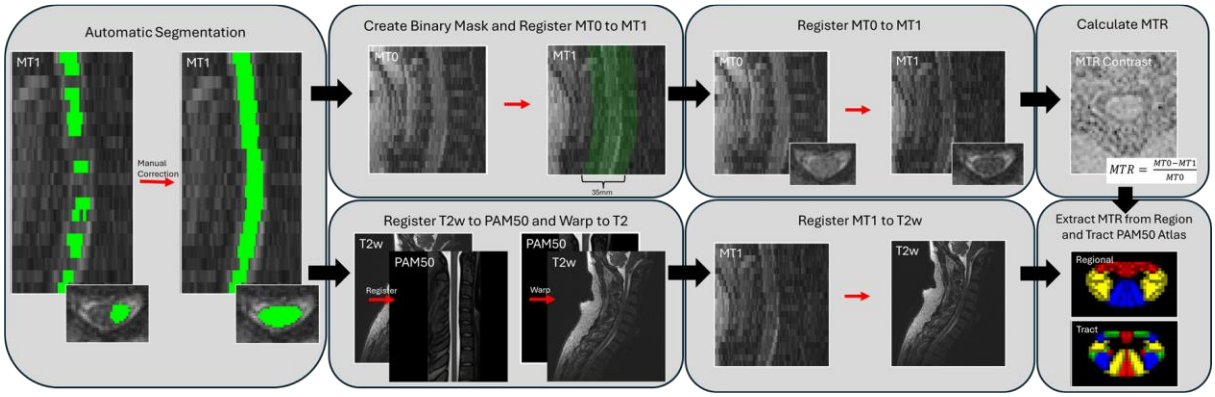

Supplemental Figure A.1: A visual description of magnetization transfer ratio (MTR) preprocessing and extraction employed in this study. After automatic segmentation is manual corrected on the MT image containing a saturation pulse (MT1), a binary mask is created to help with registration of the MT image not containing a saturation pulse (MT0), which is used to calculate MTR. Simultaneously, a T2w image is registered to the PAM50 template, which is then warped to the T2w native space. The MT1 is then registered to the T2w, which allows for the PAM50 atlas to be used to extract regional- and tract-specific MTR values from the maximum level of compression.

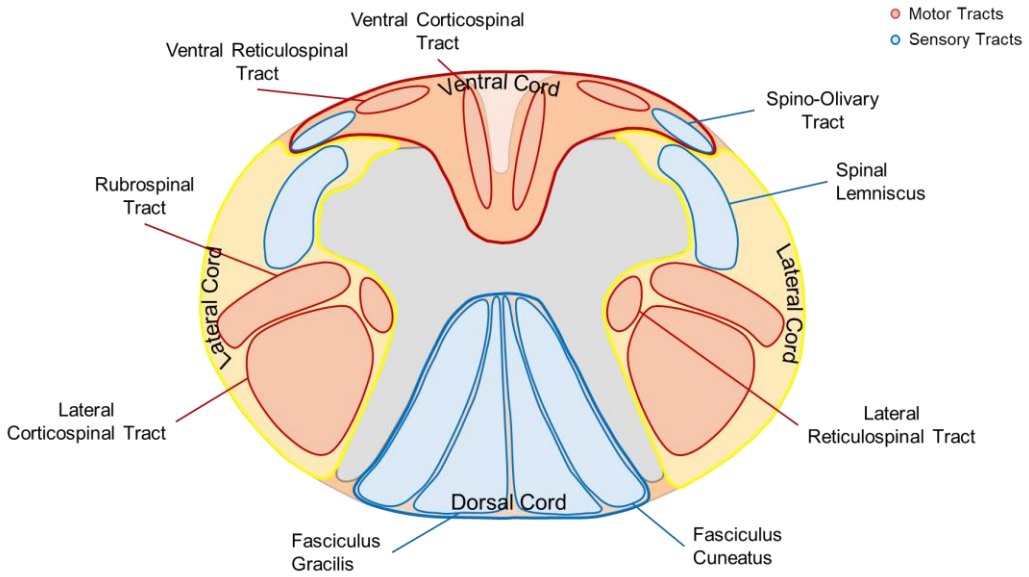

Supplemental Figure A.2: Regions and tracts that MTR values were extracted from. Regions include the dorsal, ventral, and lateral cords. Tracts include the ventral corticospinal, ventral reticulospinal, rubrospinal, lateral corticospinal, lateral reticulospinal, spinal lemniscus, spino-olivary, fasciculus cuneatus, and fasciculus gracilis tracts. The PAM50 white matter atlas was used to extract MTR values.

B. Supplemental Figures Accompanying "Task-Based Spinal fMRI using a Median Nerve Stimulation Reveals Functional Alterations in Degenerative Cervical Myelopathy"

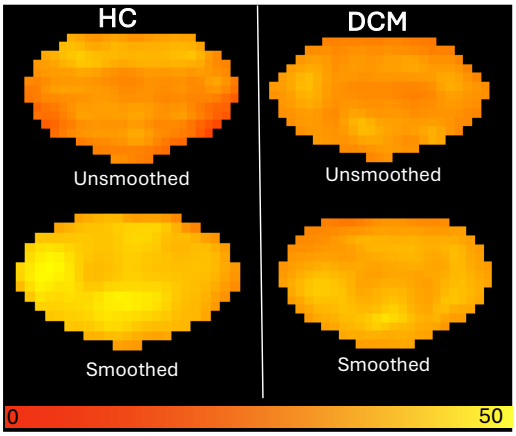

Supplemental Figure B.1: Average spinal cord temporal signal-to-noise ratio (TSNR) maps from a representative healthy control (HC, left) and degenerative myelopathy (DCM, right) subject at C5 vertebral level.

Supplemental Figure B.2: Axial slices over the C4-C7 vertebra displaying activation (red) and deactivation (blue) in healthy controls (HC, top) and degenerative myelopathy (DCM, bottom) groups.

C. Reuse License for "The current state of spinal cord fMRI and its

application in clinical research”

JOHN WILEY AND SONS LICENSE TERMS AND CONDITIONS

Dec 04, 2025

This Agreement between Grace Haynes ("You") and John Wiley and Sons ("John Wiley and Sons") consists of your license details and the terms and conditions provided by John Wiley and Sons and Copyright Clearance Center.

License Number	6160940323651
License date	Dec 02, 2025
Licensed Content Publisher	John Wiley and Sons
Licensed Content Publication	Journal of Neuroimaging
Licensed Content Title	The current state of spinal cord functional magnetic resonance imaging and its application in clinical research
Licensed Content Author	Grace Haynes, Fauziyya Muhammad, Ali F. Khan, et al
Licensed Content Date	Sep 23, 2023
Licensed Content Volume	33
Licensed Content Issue	6
Licensed Content Pages	12
Type of Use	Dissertation/Thesis
Requestor type	Author of this Wiley article
Format	Electronic
Portion	Full article
Will you be translating?	No
Title of new work	Anatomical and Functional Neuroimaging Biomarkers for Spinal Cord Alterations in Degenerative Cervical Myelopathy
Institution name	University of Oklahoma
Expected presentation date	Dec 2025
The Requesting Person / Organization to Appear on the License	Grace Haynes
Requestor Location	Ms. Grace Haynes 173 Felgar St RM 101 Norman, OK 73019 United States
Publisher Tax ID	EU826007151

Total **0.00 USD**

Terms and Conditions

TERMS AND CONDITIONS

This copyrighted material is owned by or exclusively licensed to John Wiley & Sons, Inc. or one of its group companies (each a "Wiley Company") or handled on behalf of a society with which a Wiley Company has exclusive publishing rights in relation to a particular work (collectively "WILEY"). By clicking "accept" in connection with completing this licensing transaction, you agree that the following terms and conditions apply to this transaction (along with the billing and payment terms and conditions established by the Copyright Clearance Center Inc., ("CCC's Billing and Payment terms and conditions"), at the time that you opened your RightsLink account (these are available at any time at http://myaccount.copyright.com).

Terms and Conditions

- The materials you have requested permission to reproduce or reuse (the "Wiley Materials") are protected by copyright.

- You are hereby granted a personal, non-exclusive, non-sub licensable (on a stand-alone basis), non-transferable, worldwide, limited license to reproduce the Wiley Materials for the purpose specified in the licensing process. This license, **and any CONTENT (PDF or image file) purchased as part of your order,** is for a one-time use only and limited to any maximum distribution number specified in the license. The first instance of republication or reuse granted by this license must be completed within two years of the date of the grant of this license (although copies prepared before the end date may be distributed thereafter). The Wiley Materials shall not be used in any other manner or for any other purpose, beyond what is granted in the license. Permission is granted subject to an appropriate acknowledgement given to the author, title of the material/book/journal and the publisher. You shall also duplicate the copyright notice that appears in the Wiley publication in your use of the Wiley Material. Permission is also granted on the understanding that nowhere in the text is a previously published source acknowledged for all or part of this Wiley Material. Any third party content is expressly excluded from this permission.

- With respect to the Wiley Materials, all rights are reserved. Except as expressly granted by the terms of the license, no part of the Wiley Materials may be copied, modified, adapted (except for minor reformatting required by the new Publication), translated, reproduced, transferred or distributed, in any form or by any means, and no derivative works may be made based on the Wiley Materials without the prior permission of the respective copyright owner.**For STM Signatory Publishers clearing permission under the terms of the STM Permissions Guidelines only, the terms of the license are extended to include subsequent editions and for editions in other languages, provided such editions are for the work as a whole in situ and does not involve the separate exploitation of the permitted figures or extracts,** You may not alter, remove or suppress in any manner any copyright, trademark or other notices displayed by the Wiley Materials. You may not license, rent, sell, loan, lease, pledge, offer as security, transfer or assign the Wiley Materials on a stand-alone basis, or any of the rights granted to you hereunder to any other person.

- The Wiley Materials and all of the intellectual property rights therein shall at all times remain the exclusive property of John Wiley & Sons Inc, the Wiley Companies, or their respective licensors, and your interest therein is only that of having possession of and the right to reproduce the Wiley Materials pursuant to Section 2 herein during the continuance of this Agreement. You agree that you own no right, title or interest in or to the Wiley Materials or any of the intellectual property rights therein. You shall have no rights hereunder other than the license as provided for above in Section 2. No right, license or interest to any trademark, trade name, service mark or other branding ("Marks") of WILEY or its licensors is granted hereunder, and you agree that you shall not assert any such right, license or interest with respect thereto

- NEITHER WILEY NOR ITS LICENSORS MAKES ANY WARRANTY OR REPRESENTATION OF ANY KIND TO YOU OR ANY THIRD PARTY, EXPRESS, IMPLIED OR STATUTORY, WITH RESPECT TO THE MATERIALS OR THE ACCURACY OF ANY INFORMATION CONTAINED IN THE MATERIALS, INCLUDING, WITHOUT LIMITATION, ANY IMPLIED WARRANTY OF MERCHANTABILITY, ACCURACY, SATISFACTORY QUALITY, FITNESS FOR A PARTICULAR

PURPOSE, USABILITY, INTEGRATION OR NON-INFRINGEMENT AND ALL SUCH WARRANTIES ARE HEREBY EXCLUDED BY WILEY AND ITS LICENSORS AND WAIVED BY YOU.

- WILEY shall have the right to terminate this Agreement immediately upon breach of this Agreement by you.

- You shall indemnify, defend and hold harmless WILEY, its Licensors and their respective directors, officers, agents and employees, from and against any actual or threatened claims, demands, causes of action or proceedings arising from any breach of this Agreement by you.

- IN NO EVENT SHALL WILEY OR ITS LICENSORS BE LIABLE TO YOU OR ANY OTHER PARTY OR ANY OTHER PERSON OR ENTITY FOR ANY SPECIAL, CONSEQUENTIAL, INCIDENTAL, INDIRECT, EXEMPLARY OR PUNITIVE DAMAGES, HOWEVER CAUSED, ARISING OUT OF OR IN CONNECTION WITH THE DOWNLOADING, PROVISIONING, VIEWING OR USE OF THE MATERIALS REGARDLESS OF THE FORM OF ACTION, WHETHER FOR BREACH OF CONTRACT, BREACH OF WARRANTY, TORT, NEGLIGENCE, INFRINGEMENT OR OTHERWISE (INCLUDING, WITHOUT LIMITATION, DAMAGES BASED ON LOSS OF PROFITS, DATA, FILES, USE, BUSINESS OPPORTUNITY OR CLAIMS OF THIRD PARTIES), AND WHETHER OR NOT THE PARTY HAS BEEN ADVISED OF THE POSSIBILITY OF SUCH DAMAGES. THIS LIMITATION SHALL APPLY NOTWITHSTANDING ANY FAILURE OF ESSENTIAL PURPOSE OF ANY LIMITED REMEDY PROVIDED HEREIN.

- Should any provision of this Agreement be held by a court of competent jurisdiction to be illegal, invalid, or unenforceable, that provision shall be deemed amended to achieve as nearly as possible the same economic effect as the original provision, and the legality, validity and enforceability of the remaining provisions of this Agreement shall not be affected or impaired thereby.

- The failure of either party to enforce any term or condition of this Agreement shall not constitute a waiver of either party's right to enforce each and every term and condition of this Agreement. No breach under this agreement shall be deemed waived or excused by either party unless such waiver or consent is in writing signed by the party granting such waiver or consent. The waiver by or consent of a party to a breach of any provision of this Agreement shall not operate or be construed as a waiver of or consent to any other or subsequent breach by such other party.

- This Agreement may not be assigned (including by operation of law or otherwise) by you without WILEY's prior written consent.

- Any fee required for this permission shall be non-refundable after thirty (30) days from receipt by the CCC.

- These terms and conditions together with CCC's Billing and Payment terms and conditions (which are incorporated herein) form the entire agreement between you and WILEY concerning this licensing transaction and (in the absence of fraud) supersedes all prior agreements and representations of the parties, oral or written. This Agreement may not be amended except in writing signed by both parties. This Agreement shall be binding upon and inure to the benefit of the parties' successors, legal representatives, and authorized assigns.

- In the event of any conflict between your obligations established by these terms and conditions and those established by CCC's Billing and Payment terms and conditions, these terms and conditions shall prevail.

- WILEY expressly reserves all rights not specifically granted in the combination of (i) the license details provided by you and accepted in the course of this licensing transaction, (ii) these terms and conditions and (iii) CCC's Billing and Payment terms and conditions.

- This Agreement will be void if the Type of Use, Format, Circulation, or Requestor Type was misrepresented during the licensing process.

- This Agreement shall be governed by and construed in accordance with the laws of the State of New York, USA, without regards to such state's conflict of law rules. Any legal action, suit or proceeding arising out of or relating to these Terms and Conditions or the breach thereof shall be instituted in a court of competent jurisdiction in New York County in the State of New York in the United States of America and each party hereby consents and submits to the personal jurisdiction of such court, waives any objection to venue in such court and consents to service of process by registered or certified mail, return receipt requested, at the last known address of such party.

WILEY OPEN ACCESS TERMS AND CONDITIONS
Wiley Publishes Open Access Articles in fully Open Access Journals and in Subscription journals offering Online Open. Although most of the fully Open Access journals publish open access articles under the terms of the Creative Commons Attribution (CC BY) License only, the subscription journals and a few of the Open Access Journals offer a choice of Creative Commons Licenses. The license type is clearly identified on the article.
The Creative Commons Attribution License
The Creative Commons Attribution License (CC-BY) allows users to copy, distribute and transmit an article, adapt the article and make commercial use of the article. The CC-BY license permits commercial and non-
Creative Commons Attribution Non-Commercial License
The Creative Commons Attribution Non-Commercial (CC-BY-NC)License permits use, distribution and reproduction in any medium, provided the original work is properly cited and is not used for commercial purposes.(see below)

Creative Commons Attribution-Non-Commercial-NoDerivs License
The Creative Commons Attribution Non-Commercial-NoDerivs License (CC-BY-NC-ND) permits use, distribution and reproduction in any medium, provided the original work is properly cited, is not used for commercial purposes and no modifications or adaptations are made. (see below)
Use by commercial "for-profit" organizations
Use of Wiley Open Access articles for commercial, promotional, or marketing purposes requires further explicit permission from Wiley and will be subject to a fee.
Further details can be found on Wiley Online Library http://olabout.wiley.com/WileyCDA/Section/id-410895.html

Other Terms and Conditions:

v1.10 Last updated September 2015

Questions? E-mail us at customercare@copyright.com.

D. Reuse Permissions for "Tract-specific magnetization transfer ratio provides insights into the severity of degenerative cervical myelopathy"

Springer Nature Reuse Conditions

Ownership of copyright in original research articles remains with the Author, and provided that, when reproducing the contribution or extracts from it or from the Supplementary Information, the Author acknowledges first and reference publication in the Journal, the Author retains the following non-exclusive rights:

To reproduce the contribution in whole or in part in any printed volume (book or thesis) of which they are the author(s).

The author and any academic institution, where they work, at the time may reproduce the contribution for the purpose of course teaching.

To reuse figures or tables created by the Author and contained in the Contribution in oral presentations and other works created by them.

To post a copy of the contribution as accepted for publication after peer review (in locked Word processing file, of a PDF version thereof) on the Author's own web site, or the Author's institutional repository, or the Author's funding body's archive, six months after publication of the printed or online edition of the Journal, provided that they also link to the contribution on the publisher’s website.

Authors wishing to use the published version of their article for promotional use or on a web site must request in the normal way.

If you require further assistance please read Springer Nature's online author reuse guidelines.

For full paper portion: Authors of original research papers published by Springer Nature are encouraged to submit the author's version of the accepted, peer-reviewed manuscript to their relevant funding body's archive, for release six months after publication. In addition, authors are

encouraged to archive their version of the manuscript in their institution's repositories (as well as their personal Web sites), also six months after original publication.

v1.0

E. Reuse Permissions for "Increased Involuntary Motor Threshold Stimulation in Patients with Degenerative Cervical Myelopathy"

IEEE Reuse Conditions

Below are the instructions for reuse in a dissertation. You cannot use the paper until after the conference is held. You would need to create a citation saying the proceedings are "in Press" if your dissertation is published before the proceedings are included in Xplore.

The IEEE does not require individuals working on a dissertation/thesis to obtain a formal reuse license however, you must follow the requirements listed below:

Textual Material

Using short quotes or referring to the work within these papers) users must give full credit to the original source (author, paper, publication) followed by the IEEE copyright line © [Year of publication] IEEE.

In the case of illustrations, figures, or tabular material, we require that the copyright line © [Year of original publication] IEEE appears prominently with each reprinted figure and/or table.

If a substantial portion of the original paper is to be used, and if you are not the senior author (lead researcher/writer), also obtain the senior author's approval.

Full-Text Article

If you are using the entire IEEE copyright owned article, the following IEEE copyright/ credit notice should be placed prominently in the references: © [year of original publication] IEEE. Reprinted, with permission, from [author names, paper title, IEEE publication title, and month/year of publication]

Only the **accepted** version of an IEEE copyrighted paper can be used when posting the paper or your thesis on-line. You may not use the **final published** version

In placing the thesis on the author's university website, please display the following message in a prominent place on the website: In reference to IEEE copyrighted material which is used with permission in this thesis, the IEEE does not endorse any of [university/educational entity's name goes here]'s products or services. Internal or personal use of this material is permitted.

If interested in reprinting/republishing IEEE copyrighted material for advertising or promotional purposes or for creating new collective works for resale or redistribution, please go to

http://www.ieee.org/publications_standards/publications/rights/rights_link.html

to learn how to obtain a License from RightsLink.